Benefits of supersymmetry: from scattering amplitudes to higher-spin gravity

by

Cheng Peng

A dissertation submitted in partial fulfillment
of the requirements for the degree of
Doctor of Philosophy
(Physics)
in The University of Michigan
2013

Doctoral Committee:

Associate Professor Henriette Elvang, Chair
Professor Gordon Kane
Professor Finn Larsen
Professor Yongbin Ruan
Professor Bing Zhou

For all the people

ACKNOWLEDGEMENTS

First and foremost, I would like to express my deepest gratitude to my adviser, Prof Henriette Elvang, for her continuous and patient guidance in my research and career development. It would not have been possible for me to finish this thesis without the knowledge she teaches me, the time she spends in reading the draft and her critical comments on my work. She also makes me realise the importance of communication with people and shares with me many useful skills to clearly present my work to others. Furthermore, she provides me financial support which allows me to put more effort on my research.

I owe Gordon Kane, Finn Larsen, and James Wells for several useful courses and the vast amount knowledge they have willingly and enthusiastically shared with me. I also would like to thank all other great teachers during my graduate study at the University of Michigan: Ratindranath Akhoury, Luming Duan, Leopoldo Pando-Zayas, Yongbin Ruan, Leonard Sander, Joel Smoller, and Bing Zhou.

I am also indebted to fellow graduate students and postdocs-both those at Michigan and colleagues from afar-from whom I learned countless knowledge and invaluable experience to maintain a good status in my graduate study. Let me thank Kentaro Hanaki and Yu-tin Huang in particular for their advices and very nice examples of how to conduct independent research as a graduate student and a junior researcher, and also David McGady for helpful discussions and collaboration.

Last, but not the least, I would also like to thank my friends and family, especially Zhixian Zhu, for their constant support and encouragement.

TABLE OF CONTENTS

LIST OF FIGURES

Figure

ABSTRACT

Benefits of supersymmetry:
from scattering amplitudes to higher-spin gravity

by

Cheng Peng

Chair: Prof. Henriette Elvang

In this dissertation, we study two topics related to supersymmetry. One topic is the computation of scattering amplitudes in supersymmetric Yang-Mills (SYM) theory via on-shell methods. We develop a formalism to compute the SYM scattering amplitudes with $\mathcal{N} < 4$ supersymmetries and examine various properties of the results. In particular, with the help of the generalized unitarity method, we identify the origin of the 1-loop UV divergence of the $\mathcal{N} < 4$ SYM amplitudes. The second topic is on higher-spin gravity in 3-dimensional anti-de Sitter spacetime. We find a noval generalization of higher-spin gravity that includes supersymmetry in the framework of the gauge/gravity correspondence. By explicit computation, we match the asymptotic symmetry of the higher-spin supergravity with the chiral symmetry of the 't Hooft limit of the $\mathbb{C}\mathrm{P}^n$ model, which is the proposed dual 2-dimensional conformal field theory (CFT). In addition, we consider the special case of spin-3 supergravity and find 3 distinct vacua. We find renormalization group (RG) flows connecting two of them to the third vacuum. Thus a new duality between the two ultraviolet (UV)

theories emerges in the sense that the two theories flow to the same infrared (IR) theory. We also match this with a similar duality structure in the dual CFT, which comes from the Hamiltonian reductions of the 2-dimensional Wess-Zumino-Witten (WZW) model.

CHAPTER I

Introduction

The past century has witnessed remarkable progress in understanding the microscopic foundations of the world we live in. A major part of this progress is the development of successful relativistic quantum theories of fields, which in turn helps us further explore the unknown features of nature.

A fundamental principle of quantum mechanics is the wave-particle duality, which is inspired by the statistic explanation of black body radiation and the photoelectric effect. This principle states that matter admits two equivalent descriptions, either as waves or as particles. The quantitative relation is provided by Louis de Broglie in terms of the following proposed identities

$$E = h\nu\,, \qquad \vec{p} = h\vec{k}\,, \tag{1.1}$$

where on the left-hand-side the $E, \vec{p}$ are the energy and momentum of the particle, on the right-hand-side, the $\nu, \vec{k}$ are the frequency and wave vector in the wave description.

The wave equation describing a non-relativistic quantum system is

$$i\hbar\frac{\partial}{\partial t}\Psi(\vec{r},t) = \hat{H}\Psi(\vec{r},t)\,, \tag{1.2}$$

where t is the time coordinate, $\vec{r} = (x, y, z)$ represents the three spatial coordinates,

$\hbar = h/(2\pi)$ and $\hat{H}$ is the Hamiltonian operator that admits a canonical form

$$\hat{H} = \frac{-\hbar^2}{2m}\nabla^2 + V(\vec{r}, t)\,, \tag{1.3}$$

for a single particle with mass m moving in a non-trivial background with time-dependent potential $V(\vec{r}, t)$. Equation (1.2) is called the (time-dependent) Schrödinger equation and it is the master equation in non-relativistic quantum mechanics.

As mentioned above, this equation is limited to describe a system that is moving slowly enough that the relativistic effects can be ignored. This fact can be justified by noting that the Schrödinger equation (1.2) is not Lorentz invariant, which indicates that (1.2) is not compatible with special relativity.

Special relativity assumes the 3+1 dimensional spacetime we live in has the local geometry of Minkowski spacetime, a pseudo-Riemannian manifolds with metric $\eta_{\mu\nu} = diag(-1, 1, 1, 1)$ with $\mu = 0, 1, 2, 3$. The local isometry group of this pseudo-Riemannian manifold (also known as the Lorentzian manifold) is the Lorentz group, which has the vector representation in terms of 4×4 matrices Λ such that

$$\Lambda_\alpha{}^\mu \Lambda_\beta{}^\nu \eta_{\mu\nu} = \eta_{\alpha\beta}\,. \tag{1.4}$$

Equation (1.4) simply tells that the metric $\eta_{\mu\nu}$ is an invariant tensor of the Lorentz group, and we can construct Lorentz scalars, which is crucial in constructing a theory that is compatible with special relativety, with this bilinear invariant tensor. One example of a Lorentz scalar is the length of a spacetime vector $x^\mu \equiv (x^0, x^1, x^2, x^3) = (ct, x, y, z)$

$$l^2 = x^\mu x^\nu \eta_{\mu\nu}\,. \tag{1.5}$$

Notice that we have written out explicitly the factor of c in front of the time coordinate t so that all four components have the same unit. In the following, we set $c = 1$ most of

the time for brevity of notation. Another example of a Lorentz scalar is the invariant mass of any actual/real particle with energy E and spacetime momentum $\vec{p}$

$$m^2 = -p^\mu p^\nu \eta_{\mu\nu} = E^2 - \vec{p}^2 \,, \tag{1.6}$$

where we have used the $p^\mu = (E, \vec{p})$ to denote the momentum vector. Starting with this equation, the wave-particle duality (1.1) gives

$$m^2 = h^2(\nu^2 - \vec{k}^2) \,. \tag{1.7}$$

To promote this into an operator equation rather than an numeric identity, we can do an inverse Fourier transformation back to the configuration space

$$f(t, \vec{x}) = \frac{1}{2\pi} \int d^4k e^{i(t\nu - \vec{r}\cdot\vec{k})} \tilde{f}(\nu, \vec{k}) \,, \tag{1.8}$$

where we have used the symbol k to represent the Lorentz-covariant wave vector $k^\mu = (\nu, \vec{k})$. Then in configuration space the equation (1.9) reads

$$m^2 = \big(i\hbar \frac{\partial}{\partial t}\big)^2 - \big(-i\hbar\vec{\nabla}\big)^2 \,. \tag{1.9}$$

In the following, we will again for simplicity set $\hbar = 1$. The $\hbar$ has the unit of ML^2/T, where M is the unit of mass and we have identified $L \sim T$, therefore setting $\hbar = 1$ has the effect of identifying (appropriate rescaled) M with L^{-1} and T^{-1}.

In this unit system, we can rewrite (1.9) as

$$0 = -\frac{\partial^2}{\partial t^2} + \vec{\nabla}^2 + m^2 \equiv \Box^2 + m^2 \,. \tag{1.10}$$

Expressing this operator equation in the more convenient form gives the famous Klein-

Gordon equation

$$(\Box^2 + m^2)\Phi(w) = 0\,. \tag{1.11}$$

Another master equation that is compatible with the special relativity is the Dirac equation

$$(i\gamma^\mu \partial_\mu - m)\Psi = 0\,, \tag{1.12}$$

where $\partial_\mu = (\frac{\partial}{\partial t}, \frac{\partial}{\partial \vec{x}})$ is a Lorentz contra-variant vector of spacetime derivatives. The γ^μ are 4×4 matrices that furnish the spin 1/2 representation of the Lorentz group. This equation is used to describe the motion of spin-1/2 particles, which are fermions.

The two relativistic wave-equations (1.11) and (1.12) form the foundations of the relativistic quantum wave mechanics. They are profound equations and lead to fruitful results in understanding the quantum world. However, there are problems of relativistic quantum mechanics. First, there is the problem of negative energy solutions of the Dirac equation and Klein-Gordon equation. For example, for each solution to the wave equation (1.12) describing the motion of an electron with $E = \sqrt{m^2 + \vec{p}^2}$, there must be another solution with $E = -\sqrt{m^2 + \vec{p}^2}$. What makes the situation worse is that due to the electromagnetic radiation, or through the interaction with the photons in the particle point of view, the positive energy state can involve continuously to the negative energy states, which means the energy is not bounded from below and thus a state can emit as much energy as it wants.

Another problem that is more relevant to this thesis is the physical process of colliding or scattering: the number of particles in a certain system is fixed in quantum mechanics. Thus some processes like one particle decaying to several other particles cannot be included in quantum mechanics.

The cure of these problems is the development of quantum field theory. Unlike in quantum mechanics, where the fundamental objects we study are particles, the fundamental objects we study are quantum fields and the particles are treated as

excitations of the corresponding fields. This idea is realized by the process of "second quantization", which promotes the wave functions in quantum mechanics to operators that are able to extract particles out of vacuum states of the corresponding fields and thus the total number of particles in the system can change. [1]

A useful way to characterize a scattering process is to compare the initial "in-coming" states with the final "out-going" states. In general, given any set of in-coming states, there are many possible final states and/or different kinematics of the final states. By studying the final states and their kinematics, we can learn the properties of the interactions among particles.

The quantitative observable that can be measured in experiments is the cross-section or decay rate whose dependence on dynamics of a certain theory is entirely encoded in the S-matrix, whose entries are transition amplitudes of observing a certain initial state scatter to a certain final state.

The computation of the S-matrix could be very complicated, especially when we compute higher-point amplituds or when we take into account of the higher order corrections in the perturbative computation. To simplify the computation, Feynman invented a diagrammatic method known as the "Feynman rules" and "Feynman diagrams". The basic idea is to represent each external particle that is involved in the scattering process by a point on the peripheral area, represent each interaction term as a vertex and use a line to connect two different vertices or a vertex with an external point. Then the Feynman rules say that each line connecting two vertices carries a Feynman propagator, each vertex carries a coupling and each line connecting a vertex with an external point carries a wavefunction factor. By taking the product of all factors of a diagram and then integrating over the spacetime points, we get the contribution of a diagram to a scattering process. Then the scattering amplitude is the

[1] Here we have adopted the point of view of the canonical quantization approach. There are other quantization approaches, for example the Path Integral approach, which we will not discuss in this thesis.

Figure 1.1: Two examples of the Feynman diagram. The solid lines represent fermions and the wavy lines represent gauge bosons. Each vertex in the diagram represents a 3-point interaction between two fermions and a gauge boson. The diagram on the left is an example of tree-level amplitude, and the diagram on the right illustrates a 1-loop amplitude, which means there is one closed loop in the diagram. When considering the time direction to go from left to right, these diagrams can be used to describe the physical process where an electron and a positron annihilate into a virtual photon which then decays to a pair of muon and anti-muon.

sum of contributions from all possible diagrams. In principle, there can be infinitely many different Feynman diagrams contributing to a general scattering process, since we can put in as many internal vertices as we want. However, in the perturbative regime, in which the coupling constants are small, the computation of the scattering amplitudes organizes to a loop expansion in terms of the Feynman diagrams; higher loop contributions are suppressed by higher powers of the coupling constants. Two examples of Feynman diagrams are shown in Fig. 1.1, where the left diagram is a "tree-level" diagram and the diagram on the right represent a "1-loop" diagram.

Feynman's diagrammatic method of computing scattering amplitude can get very involved when we try to compute general scattering amplitudes. One complication comes from the case of many-particle scattering. We will use the word "n-point amplitude" to represent a scattering process that involves n particles. It is not hard to imagine that as the total number of particles in a process grows, the number of contributing Feynman diagrams increases very quickly and each Feynman becomes much more complicated.

Another type of complication arises when we compute scattering amplitudes in

gauge theories, for example electromagnetism or Yang-Mills theory. Gauge theory describes the dynamics of massless particles that transform in the 4-dimensional vector representations of the Lorentz group. We use A_μ to represent the corresponding quantum field. This type of particle falls into the spin-1 representation of the spatial rotations [1].

Massless spin-1 particles are labeled by the *helicity* $h = \pm 1$. Under a Lorentz transformation $U(\Lambda)$, the A_μ field transforms as

$$A_\mu(x) \to U(\Lambda) A_\mu(x) U(\Lambda)^{-1} = \Lambda_\mu{}^\nu A_\nu(x) + \frac{\partial}{\partial x^\mu}\Omega(x)\,. \tag{1.13}$$

Thus, to render the A_μ formally Lorentz covariant, we can introduce a compensating "gauge transformation"

$$A_\mu(x) \to A_\mu(x) - \frac{\partial}{\partial x^\mu}\Omega(x)\,. \tag{1.14}$$

Since this transformation is introduced to restore Lorentz covariance, all fields A_μ that are related by this type of transformation correspond to the same set of physical states. Therefore, we can use the A_μ field to describe the massless vector particles but the theory we construct, for example the Lagrangian density, should be invariant under both the Lorentz transformation and the gauge transformation (1.14). Gauge theory describe the dynamics of massless vector fields with the extra "gauge transformation" (1.14), hence also referred to as the "gauge fields". We can generalize this to "non-abelian" gauge theories where both the gauge field $A_\mu(x)$ and the gauge transformation parameters $\Omega(x)$ are matrix valued. If the $A_\mu(x)$ and $\Omega(x)$ fall into some representation of a group G, namely $A_\mu = \sum_a A_\mu^a T_{\rm R}^a$ with $T_{\rm R}^a$ being the generators of G in some representation R, then we will call G the "gauge group" of this non-abelian gauge theory. The 4-dimensional non-abelian gauge theory is the well-known Yang-Mills theory [2].

The non-abelian gauge theory plays an important role in building the "Standard Model" of particle physics. In the Standard Model, the fundamental interactions of our world, except for gravity, are unified into a non-abelian gauge theory with gauge group $SU(3) \times SU(2) \times U(1)$. The $SU(3)$ factor corresponds to the strong interaction and the $SU(2) \times U(1)$ corresponds to the electroweak interaction. We know that gauge theory describes massless gauge fields, while the weak interaction is observed to be a short-range force in experiment, which means that the gauge bosons of the weak interaction should be massive. The way to give mass to those gauge bosons (and other matter fields) is the well-known "Higgs mechanism", where two complex scalars that couple to the electroweak gauge fields are introduced to the Standard model and a non-trival vacuum-expectation-value of the Higgs fields gives masses to the gauge bosons. Theoretically, the Higgs mechanism predicts the existence of a massive scalar, known as the "Higgs boson". Thus searching for this Higgs boson becomes one of the most important experiments to test the Standard Model. Quite recently, the experiments at the Large Hadron Collider by the ATLAS and the CMS collaborations have discovered this Higgs boson [3, 4], which is another milestone of particle physics.

Theoretically, the necessity of the "gauge transformation" reflects a redundancy in our Lorentz covariant "off-shell" formulation of the quantum field theory of vector massless particles. Here the term "off-shell" is in opposite to the concept "on-shell", which is the requirement that the equation of motion and other constraints are satisfied so that an "on-shell" state is really a physical state that can be observed in experiment. For example the scattering amplitudes, or the S-matrix elements, are on-shell quantities and are gauge invariant. However, due to the redundancy (1.14) the quantum field A_μ cannot be an on-shell state since we have infinitely many equivalent representations of the same physical field. However, when we compute gauge theory scattering amplitudes in the Feynman approach, the internal propagators we used are

for the off-shell gauge field, which means we have also included the contribution from the gauge degree of freedom $\Omega(x)$. But these are redundant and should not be taken into account, so we have to do extra work to separate out the contribution from these pure gauge degrees of freedom. This introduces another type of complication.

In the first two chapters of this thesis, we study an "on-shell" approach to compute scattering amplitudes, especially amplitudes in 4-dimensional non-abelian gauge theories. The key ingredient of the on-shell approach is recursion relations that express higher-point on-shell amplitudes as sums of products of lower-point on-shell amplitudes under some mild conditions. Since the lower-point on-shell amplitudes are physical observables, they only carry on-shell information and the gauge redundancies are all eliminated; this significantly simplifies the computation of the amplitudes. In the on-shell approach, we still need to sum over many different channels, each corresponding to a partition of the external states into subsets to form the lower-point building blocks. But the contributing channels in the on-shell approach are much fewer than the number of Feynman diagrams in the off-shell approach.

Another really powerful concept that makes the on-shell method more efficient is supersymmetry. Supersymmetry is a revolutionary concept and it has innumerable significant effects in particle physics, therefore we will give a brief introduction here.

As we have seen from the previous discussion, symmetry, especially the spacetime Lorentz symmetry has played an important role since the invariance/covariance of the physical quantities under this symmetry impose strong constraints on the theory. A simple generalization of the Lorentz group is to also include the spacetime translations so that the resulting symmetry group becomes the Poincaré group.

The Poincaré group turns out the be the largest spacetime symmetry group of the S-matrix of a 4-dimensional unitary quantum field theory. This was proven by Coleman and Mandula [5] subject to the following assumptions

1. The S-matrix is non-trivial and is an analytic function of the momentum of

external particles in the elastic scattering regime.

2. For a given mass M, there are only a finite number of different particles with mass smaller than M.

3. The symmetry group is continuous and can be obtained from the exponential map of a Lie algebra at least locally.

Note that this "no-go" theorem of Coleman and Mandula has no constraint on the internal symmetries, which by definition are the symmetry transformations that commute with the Poincaré group.

This celebrated Coleman-Mandula theorem can be understood in another way in that it tells us what assumptions should be relaxed if we want to have larger spacetime symmetries. Supersymmetry is one such example of enlarged symmetry by relaxing the last assumption in the above list. We can consider the Lie *super*algebra instead of the Lie algebra. The supersymmetry we mostly refer to nowadays is a $\mathbb{Z}_2$ graded Lie superalgebra that is generated by a set of "bosonic" generators, which have grade 0 (*mod* 2), as well as a set of "fermionic" generators with grade 1 (*mod* 2).

Due to the existence of the fermionic symmetry generators, there are fermionic states in the spectrum. These fermionic states come from acting the fermionic generators on the bosonic states. Thus supersymmetry relates bosons with fermions and vice versa. By definition, the fermionic generators of any Lie superalgebra, which are also called "supercharges", fall into finite representations of the bosonic subalgebra. In the case that we are interested in, the bosonic subgroup is the Poincaré group, so the fermionic generators are representations of the Poincaré group. It can be shown [6] that the fermionic generators can only be in the left- or right-handed Weyl spinor representations. We say that a 4-dimensional quantum field theory has $\mathcal{N}$-fold supersymmetry if there are $\mathcal{N}$ pairs of the left- and right-handed Weyl spinor supercharges. From a simple group theory analysis, we see that the maximal number

of supersymmetry is $\mathcal{N} = 4$, since otherwise the theory has gauge fields with spin $s > 1$. Thus $\mathcal{N} = 4$ super-Yang-Mills theory (SYM) is the maximally supersymmetric Yang-Mills theory. This $\mathcal{N} = 4$ theory is unique.

With SUSY, we can collect all the states that are related by supersymmetry into a compact on-shell superfield. Then in terms of these superfields, amplitudes with different external states can be grouped into very simple and compact forms which are known as superamplitudes. These superamplitudes can also be regarded as the generating functions of all the component physical amplitudes, which can be extracted out by applying simple projections to the superamplitudes. Furthermore, the recursion relations of these superamplitudes are also much simpler. These nice properties of the on-shell methods were initially explored in the 4-dimensional supersymmetric Yang-Mills theory with maximally extended $\mathcal{N} = 4$ supersymmetries [7, 8, 9, 10, 11, 12, 13, 14, 15, 16, 17, 18, 19].

In Chapter II, we focus on 4-dimensional Yang-Mills theory with $\mathcal{N} < 4$ extended supersymmetries. In general, the more supersymmetries a theory has, the simpler the theory is, since each symmetry effectively imposes some constraints on the theory. Therefore, in $\mathcal{N} < 4$ SYM the amplitudes we study is expected to be more complicated compared to maximal $\mathcal{N} = 4$ theory. Thus the main motivation of our work is to check with less supersymmetries which of the good properties of $\mathcal{N} = 4$ theory remain and which do not. This can help us understand the role played by supersymmetry in scattering amplitudes. Moreover, no strong evidence of supersymmetry has been found in all the experiments that people have performed. This suggests that the supersymmetry, if really exists, has to be broken at the relative low energy level that we have searched for.[2] Therefore, our generalization to the $\mathcal{N} < 4$ theories is a first step trying to connect the beautiful structure of the $\mathcal{N} = 4$ theory with the real-world

[2]Notice that throughout this thesis, we do not consider any kind of supersymmetry breaking. A further study of these topics in the future with broken supersymmetry is interesting since it makes connections with the real-world physics that can be tested by experiments.

physics that can be tested in experiments.

In detail, we find two different representations of the on-shell superfield in $\mathcal{N} < 4$ SYM theory, each of which is good to build superamplitudes independently. We derive the supersymmetric Ward identity, which is the concrete realization of the constraints imposed by supersymmetry. We study the properties of one type of on-shell recursion relations, namely the super-Britto-Cachazo-Feng-Witten (super-BCFW) recursion relation. The BCFW recursion relation states that if we introduce a complex shift z of two of the external momenta, then there will be poles on the z-plane in general. Approaching each pole corresponds to sending an internal propagator "on-shell" (the propagator diverges). The residue at each pole is naturally a product of two sub-amplitudes separated by the propagator. Then the amplitudes is a sum of all the residues on the z-plane provided that the infinity on the z-plane is not a pole. This recursion relation was studied in the case of $\mathcal{N} = 0, 4$ in the literature. We discuss the BCFW recursion relations for $\mathcal{N} < 4$ SYM, study various properties of the recursion relations, especially the "large-z" behavior, and apply the recursion relations to study the 1-loop structure of scattering amplitudes. This chapter is based on the paper [20] with Henriette Elvang and Yu-tin Huang (currently a postdoc fellow at University of Michigan).

In Chapter III, we extend the study of the UV divergence structure of one-loop amplitudes, which is briefly studied at the end of Chapter II, with the help of the generalized unitarity method and the integral reduction techniques. By definition, each Feynman diagram contributing to a 1-loop amplitude contains a closed loop, one example is shown in the diagram on the right in Fig. 1.1. Because the momentum running in the loop can be arbitrarily large, the one-loop diagrams are often divergent. We will use the term "Ultraviolet (UV) divergence" to represent the divergence of the amplitudes coming from the large loop momentum. In the presence of supersymmetry, more particles run in the loop. Moreover, the coupling constants of certain types of

interactions are related to each other. As a result, there can be non-trivial cancellation between different diagrams and the divergence is often milder than the theory with no supersymmetry.

In four spacetime dimensions, integral reduction techniques [21, 22, 23] allow one to express one-loop gauge theory amplitudes in terms of rational functions and a basis of scalar integrals that includes boxes I_4, triangles I_3 and bubbles I_2 [22, 24]:

$$A^{1-\text{loop}} = \sum_i C_4^i I_4^i + \sum_j C_3^j I_3^j + \sum_k C_2^k I_2^k + \text{rationals} \ . \tag{1.15}$$

Here the index i (j or k) labels the distinct integrals categorized by the set of momenta flowing into each corner of the box (triangle, or bubble). In this basis, the scalar bubble integrals, I_2^i, are the only ultraviolet divergent integrals in four dimensions. Moreover, in the dimensional regularization scheme, namely take $D = 4 - 2\epsilon$, the UV divergences of the bubble integrals take the universal form:

$$I_2^i = \frac{1}{(4\pi)^2} \frac{1}{\epsilon} + \mathcal{O}(1) \tag{1.16}$$

for all i. Thus the *sum of bubble coefficients* C_2^k contains information about the ultraviolet behavior of the theory at one-loop. Thus the UV divergence purely comes from the sum of the coefficients $\sum_k C_2^k$. Following [25, 13], we extract the bubble coefficient by identifying it as the contribution from the "pole at infinity" in the complex z-plane of a BCFW-deformation [26, 27] of the two internal momenta in the two-particle cut, where the complex deformation is introduced on the internal momenta. Furthermore, we find a systematic cancellation between the contribution from each channels to the bubble coefficient, which helps us to identify the UV divergence from two channels of the same type and give a physical explanation of why this type of channel contribute to the UV divergence. As a byproduct, we compute the UV divergence very efficiently using this result, which agrees with the known results and demonstrate the

change of it with respect to the change of number of supersymmetries. This chapter is based on the work [28] with Yu-tin Huang and David McGady (a graduate student at Princeton University).

The second half of this thesis is about another way to go around the Coleman-Mandula "no-go" theorem. Now we consider a theory on anti-de-Sitter space with an infinite tower of massless gauge fields of integer (and half integer) spin. Because there is no well-defined S-matrix in anti-de-Sitter spacetime, together with the fact that an infinite tower of massless fields violates the second condition we listed about the Coleman-Mandula theorem, it is possible that the theory has a larger spacetime symmetry group than the ordinary Poincaré group. One example of this type of theory is known as higher-spin theories with an infinite dimensional higher spin symmetry [29, 30, 31, 32].

The higher-spin theory is interesting on its own right due to its connection with gravity and string theory. The higher-spin theory describes a tower of massless fields including spin-2 gravitons. So the higher-spin theory is an extension of the usual gravity theory described by general relativity.

On the other hand, the higher-spin theory is also conjectured to be the tensionless limit of string theory. String theory is a framework for unifying all the known fundamental interactions. The basic idea is to consider a 1-dimensional extended object, the string, as the fundamental building block of the world instead of the conventional point-like particles. String theory has succeeded in many aspects, for example, it gives a quantum theory that includes the gravity sector as a built-in part, it is shown to be an ultraviolet finite theory, it has different types of extended object except for the fundamental strings such as D-branes which can be used to provide microscopic constructions of various low energy effective theories, it also possesses a rich family of dualities that can be used to explain the known duality relations of the corresponding low energy quantum field theories.

In terms of string theory, different particles are understood as different quantum vibration modes of the fundamental string. Because there can be infinitely many different vibration modes, the spectrum of string theory contains a tower of states with arbitrary quantized, integer or half-integer spin. We can further compute the masses of these states and they are all proportional to a fundamental quantum $1/\alpha'$ which has a physical interpretation as the tension of the string. So we can imagine to consider a tensionless limit of string theory so that the tower of states are all massless in this limit. We then notice that this recovers the spectrum of the higher-spin theory we are interested in. Then the above conjecture that the higher-spin theory is a tensionless limit of string theory follows naturally from the fact that string theory is the only known consistent theory that has an infinite tower of states with arbitrary spin.

Higher-spin theory turns out also to be a very interesting and useful example in the context of the gauge/gravity correspondence. The gauge/gravity correspondence is a conjectured equivalence between a quantum gravity theory and a (conformal) field theory. Conformal field theory is a special type of quantum field theory in which the Poincaré group is extended to the (global) conformal symmetry. One well studied example is the duality between the type IIB string theory on the spacetime background of $AdS_5 \times S^5$ and $\mathcal{N} = 4$ SYM theory on the 4-dimensional boundary of AdS_5 [33]. Here the AdS_5 stands for "anti-de Sitter" space, which is the maximal symmetric homogeneous space with a negative cosmological constant and S^5 is a 5-dimensional sphere. Another example is the duality between Chern-Simons theory on $AdS_3 \times S^3$ and the 2-dimensional Wess-Zumino-Witten (WZW) model [34]. However, it is hard to do actual computations in the full quantum string theory, so it is convenient to take a limit $\alpha' \to 0$. In this limit, the full string theory reduces to a weakly coupled gravity theory on an AdS background and hence we can do perturbative computations. On the other hand, if we consider the $1/\alpha' \to 0$, ie $\alpha' \to \infty$, limit of the string,

we should get the higher-spin theory as conjectured. Therefore, higher-spin gravity theory provides a different angle to understand the gauge/gravity correspondence and it may thus provide further evidence of it.

In this thesis, we focus on one type of higher-spin theory, namely the Vasiliev higher-spin theory. A long-term effort of Fronsdal, Fradkin, Vasiliev and collaborators has succeeded in constructing gravitational theories with spin $s > 2$ gauge fields in arbitrary dimensions [29, 35, 35, 36, 37]. These higher-spin theories fit in the context of holography very well. In particular, there are two types, namely A-type and B-type, of parity invariant higher-spin theories in AdS_4 spacetime. Klebanov and Polyakov conjectured a duality between the A-type minimal bosonic higher-spin theory in AdS_4 spacetime and the 3d $O(N)$ vector model [31]. Sezgin and Sundell proposed a duality between the B-type minimal bosonic higher-spin theory in AdS_4 spacetime and the 3d Gross-Neveu model [32]. In the same paper [32], the $\mathcal{N} = 1$ supersymmetric versions of these dualities were also conjectured. One exciting feature of higher-spin theory is its potential link with the tensionless limit of string theory, as speculated for a long time since [38, 39, 40]. Recently, the authors of [41, 42] proposed a generalized duality between parity violating higher-spin theory and the (supersymmetric) Chern-Simons matter theory based on the study of correlation functions in [43], which builds a direct connection to the type IIA string theory. Significant progress has been made on higher-spin holography. For example, exact or slightly broken higher-spin symmetry were shown to impose strong constraints on the CFT by Maldacena and Zhiboedov [44, 45]. Aharony, Gur-Ari and Yacoby clarified the interpolation between the A-type higher-spin theory and the B-type theory [46, 47]. Different attempts to understand the physical origin of the higher-spin holography have been carried out in [48, 49, 50, 51, 52]. A de-Sitter/CFT higher-spin holography is also conjectured in [53, 54, 55]. For a recent review, see [56] and the references therein.

At one-dimension lower, higher-spin theories have also been studied intensively in

the context of AdS_3/CFT_2 duality. Gaberdiel and Gupakumar proposed a duality between bosonic higher-spin gravity in AdS_3 and 2-dimensional W_N minimal models [57]. This duality was refined later in [58, 59] and extended to even-spin higher-spin theory [60]. The supersymmetric generalizations have been carried out by Creutzig, Hikida and Ronne [61, 62] and refined by Candu and Gaberdiel [63, 64]. This duality has been studied and checked intensively, including the match of the partition functions [65, 61, 62], the asymptotic symmetries [66, 67, 68, 69, 70, 71, 72], and the correlation functions [73, 74]. Classical solutions such as conical singularities [75, 76] and black holes with higher spin charges [77, 31, 78, 79, 80, 81, 82] are also constructed. A further extension to higher-spin supergravity based on the $D(2,1;\alpha)$ Lie superalgebra is constructed and is considered to be related to IIB string theory on an $AdS_3 \times S^3 \times S^3 \times S^1$ background [83]. For recent reviews, see [84, 85] and the references therein.

In Chapter IV, we study higher-spin supergravity theory in AdS_3 spacetime in the framework of gauge/gravity duality. It has been proposed [61] that this higher-spin theory is dual to a 2-dimensional conformal field theory, the $\mathbb{C}P^n$ model in the 't Hooft limit. We provide further evidence on this proposed duality. We analyze the asymptotic symmetry of the supergravity theory supersymmetrically coupled to an infinite tower of higher-spin fields, and match it with the chiral algebra of the $\mathbb{C}P^n$ CFT model in the 't Hooft limit. We also show that the degenerate representations on gravity side can be mapped to the degenerate representations of the $\mathbb{C}P^n$ model and vice versa. Our work is a generalization of a similar study of the bosonic higher-spin theory [66]. The new ingredient of supersymmetry makes it possible to match the symmetry explicitly, which is not possible in the purely bosonic case. The work in this chapter is based on [70] with Kentaro Hanaki (a former graduate student at University of Michigan).

Another interesting phenomenon observed in [86] is that $sl(3,\mathbb{R})$ higher-spin grav-

ity, which contains spin-3 states in addition to the gravitons, admits two distinct AdS_3 vacua with different asymptotic symmetries. The two vacua are obtained from different $sl(2,\mathbb{R})$ embeddings into $sl(3,\mathbb{R})$. A holographic RG flow triggered by a finite chemical potential connects the vacuum corresponding to the diagonal embedding in the UV and the principal embedding vacuum in the IR. A detailed relation between the operators in the UV theory and the operators in the IR theory is obtained by perturbing the RG flow and solving the linearized equation of motion. An extension of this work to the thermodynamic properties of higher-spin black holes was carried out in [87].

In Chapter V, we consider the supersymmetric extension of the above phenomenon. The supersymmetric extension of 3D general relativity can be written as a Chern-Simons theory with $sl(2|1)$ gauge fields. Its simplest higher-spin generalization is the 3d spin-3 supergravity that can be described as a Chern-Simons theory with $sl(3|2)$ gauge fields. The vacuum of this theory contains only an empty AdS_3, in other words finding the vacuum is equivalent of finding the pure gravity sector of the higher-spin theory. Mathematically, this translates to finding an embedding of $sl(2|1)$ into $sl(3|2)$. We carry our this analysis and find three different embeddings, hence three different vacua, with interesting relations among the vacua found. Further, we identify a similar structure in the dual conformal field theory from the know literature. In addition, we find another duality between different vacua, in the sense that there are two distinct vacua at high energy level that will flow to the same vacuum at low energy level. This new duality is also brought to us by supersymmetry, since we can track the origin of the two high energy vacua, one of them is seen in the pure bosonic theory while the other is only present when supersymmetry is considered. This chapter is based on the work [88].

CHAPTER II

On-shell superamplitudes in $\mathcal{N} < 4$ SYM

2.1 Introduction and summary of results

The study of on-shell scattering amplitudes has in recent years revealed many surprising structures and completely new ways to evaluate amplitudes at both tree and loop level. Particularly remarkable results have been found in the planar sector of massless $\mathcal{N} = 4$ SYM theory. It is obviously of considerable practical and theoretical interest to generalize the results of this very special integrable sector to theories with less symmetry. In this chapter we take a step towards this goal by studying basic properties of scattering amplitudes in pure $\mathcal{N} = 1$ and $\mathcal{N} = 2$ SYM.

A cornerstone in the recent developments in $\mathcal{N} = 4$ SYM has been the on-shell superfield formalism which encodes amplitudes related by supersymmetry into *superamplitudes* and the connection to the *twister space*[89, 7, 8, 90, 91, 9, 92, 10, 11]. In this formalism, the CPT self-conjugate supermultiplet of on-shell states is collected into a superfield, or *superwavefunction*,

$$\Omega_i = G_i^+ + \eta_{ia}\,\lambda_i^a - \frac{1}{2!}\eta_{ia}\eta_b\,S_i^{ab} - \frac{1}{3!}\eta_{ia}\eta_{ib}\eta_{ic}\,\lambda_i^{abc} + \eta_{i1}\eta_{i2}\eta_{i3}\eta_{i4}\,G_i^- \,. \tag{2.1}$$

The Grassmann variables η_{ia} are labeled by particle number i and $SU(4)$ R-symmetry index $a = 1, 2, 3, 4$, and the components are on-shell states — gluons G, gluinos λ,

and scalars S — with momentum p_i. The superamplitude $\mathcal{A}_n(\Omega_1, \Omega_2, \ldots, \Omega_n)$ is a polynomial in the η_{ia}-variables and each coefficient is an on-shell scattering amplitude. To project out a particular scattering amplitude from $\mathcal{A}_n$ we act with the unique set of Grassmann derivatives that project out the desired set of external states from the superwavefunctions Ω_i. Thus superamplitudes are generating functions for the component amplitudes.

The purpose of the present chapter is to develop on-shell superfield formalisms for pure $\mathcal{N} < 4$ SYM theory (and we will briefly comment on $\mathcal{N} < 8$ supergravity). While the spectrum of $\mathcal{N} = 4$ SYM is CPT self-conjugate, this is not the case for SYM theory with less supersymmetry. Thus two superfields are needed to encode the spectrum of pure[1] $\mathcal{N} < 4$ SYM theory: one superfield for the 'positive helicity sector' and one for the 'negative helicity sector'. For example, for $\mathcal{N} = 1$ SYM we use

$$\Phi = G^+ + \eta_i \, \lambda^+ \, , \;\; \Phi^\dagger = G^- + \bar{\eta}_i \, \lambda^- \, . \tag{2.2}$$

Note that Φ is simply the truncation $\eta_{i2}, \eta_{i3}, \eta_{i4} \to 0$ of the $\mathcal{N} = 4$ superfield (2.1) while $\Phi^\dagger$ can be obtained from (2.1) by carrying out a Fourier transformation of the Grassmann variables and then taking $\bar{\eta}_{i2}, \bar{\eta}_{i3}, \bar{\eta}_{i4} \to 0$. Clearly this procedure can be exploited to systematically truncate $\mathcal{N} = 4$ SYM superamplitudes at *tree level* to $\mathcal{N} = 1$ SYM, and more generally to $\mathcal{N} = 0, 1, 2, 3$ SYM. This works because $\mathcal{N} = 0, 1, 2$ SYM form closed subsectors of the $\mathcal{N} = 4$ theory at tree level. The $\mathcal{N} = 3$ formulation provides a non-chiral[2] but otherwise equivalent on-shell superspace formulation of the $\mathcal{N} = 4$ theory.

N^{K}MHV superamplitudes in $\mathcal{N} < 4$ SYM involve $(K+2)$ $\Phi^\dagger$ superwavefunctions and $(n-K-2)$ Φ's. Since the amplitudes are color-ordered and $\mathcal{N} < 4$ SUSY does not mix the states of the 'positive' and 'negative helicity sectors', there are now

[1] Unless otherwise stated, we use $\mathcal{N} < 4$ SYM to refer to *pure* $\mathcal{N} < 4$ SYM.

[2] We use "chiral" to denote on-shell superspace with only η-Grassmann variables; thus "non-chiral" means that both η and $\bar{\eta}$ are used.

superamplitudes for each arrangement of the $\Phi^\dagger$ and Φ states. For example, the MHV superamplitudes $\mathcal{A}_{n;12}(\Phi_1^\dagger\Phi_2^\dagger\Phi_3\ldots\Phi_n)$ and $\mathcal{A}_{n;13}(\Phi_1^\dagger\Phi_2\Phi_3^\dagger\Phi_4\ldots\Phi_n)$ are distinct. The formalism is discussed in **section 2.2**.

The non-chiral Φ-$\Phi^\dagger$ formulation (2.2) of $\mathcal{N}<4$ SYM turns out to be somewhat impractical for explicit calculations, and it is convenient to replace $\Phi^\dagger$ by its Fourier transform $\Psi=\lambda^-+\eta G^-$. We introduce the chiral Φ-Ψ formalism in **section 2.3** and apply it in subsequent sections. In this formalism, the tree-level MHV amplitudes in pure SYM with $0\leq\mathcal{N}\leq 4$ can be written compactly as (see also [93])

$$\mathcal{F}^{\mathcal{N}}_{n,ij} \;=\; (-1)^{\frac{1}{2}\mathcal{N}(\mathcal{N}-1)}\;\frac{\langle ij\rangle^{4-\mathcal{N}}\;\delta^{(2\mathcal{N})}\big(\sum|k\rangle\eta_k\big)}{\langle 12\rangle\langle 23\rangle\cdot\cdot\langle n\,1\rangle}\,, \tag{2.3}$$

where the Grassmann delta-function expresses conservation of the $\mathcal{N}$ supermomenta; the standard momentum delta-function is implicit. We derive similar explicit $0\leq\mathcal{N}\leq 4$ formulas for the NMHV superamplitudes and discuss the general truncation procedure beyond NMHV. The resulting formalism should be straightforward to incorporate into numerical programs such as the Mathematica packages presented recently in [94, 95].

As applications of the $\mathcal{N}<4$ superamplitude formalism we study:[3]

- ▷ **Section 2.4: Super-BCFW recursion relations.** We formulate super-BCFW shift in $\mathcal{N}<4$ SYM, and show that the large-z behavior can be derived by a simple Grassmann integral argument. The tree-level superamplitudes in $\mathcal{N}=4$ SYM have large-z falloff under any super-BCFW shift. In $\mathcal{N}<4$ SYM, the shifts $[\Psi,\Psi\rangle$, $[\Psi,\Phi\rangle$, $[\Phi,\Phi\rangle$ give similar large-z falloffs and the associated super-BCFW recursion relations are therefore valid. However, under a $[\Phi,\Psi\rangle$-shift, the $\mathcal{N}$-fold superamplitudes behave as $z^{3-\mathcal{N}}$ (adjacent; $z^{2-\mathcal{N}}$ for

[3] Dual superconformal symmetry is not on the list of properties we explore in $\mathcal{N}<4$ SYM simply because in general it is not a property of the amplitudes.

non-adjacent) for large z; we study the consequences at loop level.[4]

- ▷ **Section 2.5: Solution to the SUSY Ward identities in $\mathcal{N}=1$ SYM.** The SUSY Ward identities in $\mathcal{N}=1$ SYM are even simpler to solve than in $\mathcal{N}=4$ SYM. A total of $\binom{n-4}{K}$ algebraically independent basis amplitudes determine the N^KMHV superamplitudes for each arrangement of external states Φ and Ψ. For $n=6$ and NMHV ($K=1$) the counting of 2 basis-amplitudes agrees with the only previous solution [97, 9, 98] for $\mathcal{N}=1$ SYM.

We end our story with two short sections: in **section 2.6** we outline the superfield formalism for superamplitudes of $\mathcal{N}<8$ supergravity, and in the Outlook, **section 2.7**, we briefly discuss the coupling of matter multiplets to the $\mathcal{N}=1,2$ SYM theories.

2.2 On-shell formalism for pure SYM: Φ-$\Phi^\dagger$ formalism

To set the stage for $\mathcal{N}<4$ SYM, we begin with a brief review of the relevant on-shell framework in $\mathcal{N}=4$ SYM.

2.2.1 On-shell superfields and MHV superamplitudes in $\mathcal{N}=4$ SYM

The on-shell supermultiplet of $\mathcal{N}=4$ SYM consists of 16 massless particles:

$$\text{two gluons } G^{\pm}\text{, four gluinos pairs } \lambda^a \text{ and } \lambda^{abc}\text{, and six scalars } S^{ab}\,. \tag{2.4}$$

The indices $a,b,\cdots=1,2,3,4$ are $SU(4)$ R-symmetry labels. The helicity $h=\pm1,\pm\frac{1}{2},0$ states transform as r-index anti-symmetric representations of $SU(4)$ with $r=2-2h$. We collect the 16 states into an $\mathcal{N}=4$ on-shell chiral superfield

$$\Omega = G^+ + \eta_a\lambda^a - \frac{1}{2!}\eta_a\eta_b S^{ab} - \frac{1}{3!}\eta_a\eta_b\eta_c\lambda^{abc} + \eta_1\eta_2\eta_3\eta_4\, G^-\,, \tag{2.5}$$

[4] Our work on super-BCFW shifts and their consequences for 1-loop amplitudes has a certain overlap with the work of [96].

where the four η_a's are Grassmann variables labeled by the $SU(4)$ index $a = 1, 2, 3, 4$. These variables were first introduced by Ferber [89] as the superpartners to the bosonic twistor variables. The relative signs are chosen such that the Grassmann differential operators

$$\mathcal{N} = 4 \text{ SYM:} \quad \begin{array}{c|c|c|c|c|c} \text{particle} & G^+ & \lambda^a & S^{ab} & \lambda^{abc} & G^{1234} \\ \hline \text{operator} & 1 & \partial_i^a & \partial_i^a \partial_i^b & \partial_i^a \partial_i^b \partial_i^c & \partial_i^1 \partial_i^2 \partial_i^3 \partial_i^4 \end{array} \tag{2.6}$$

exactly select the associated state from Ω.

All 16 states of the multiplet are related by supersymmetry. In the on-shell formalism the supercharges are

$$q^a \equiv q^{a\,\alpha}\,\epsilon_\alpha = -[p\,\epsilon]\,\frac{\partial}{\partial \eta_a}\,, \qquad \tilde{q}_a \equiv \tilde{\epsilon}_{\dot{\alpha}}\,\tilde{q}_a^{\dot{\alpha}} = \langle \epsilon\, p\rangle\,\eta_a\,, \tag{2.7}$$

with $|p\rangle$ and $|p]$ the spinors associated with the null momentum p of the particle. ϵ is an arbitrary Grassmann spinor. The supercharges satisfy the anticommutation relation

$$\{q^{a\,\alpha}, \tilde{q}_b^{\dot{\beta}}\} = \delta_b^a\,|p\rangle^{\dot{\beta}}[p|^\alpha = \delta_b^a\,p^{\dot{\beta}\alpha} \tag{2.8}$$

of the Poincare supersymmetry algebra.

The supercharges (2.7) act on the spectrum by shifting states right or left in Ω. For example, if we compare Ω with

$$\tilde{q}_1\,\Omega \;\; = \;\; -\Big(\eta_1\langle\epsilon p\rangle G^+ - \eta_1\eta_a\langle\epsilon p\rangle\lambda^1 - \frac{1}{2}\eta_1\eta_a\eta_b\,\langle\epsilon p\rangle S^{ab} + \eta_1\eta_2\eta_3\eta_4\langle\epsilon p\rangle\lambda^{234}\Big) \tag{2.9}$$

order by order in η's to extract the action of $\tilde{q}_1$ on the individual states, we find[5]

$$\left[\tilde{q}_a, G^+\right] = 0\,,\ \left[\tilde{q}_a, \lambda^b\right] = \langle \epsilon\, p\rangle\, \delta_a^b\, G^+\,,\ \left[\tilde{q}_a, S^{bc}\right] = \langle \epsilon\, p\rangle\, 2!\, \delta_a^{[b}\, \lambda^{c]}\,,$$
$$\left[\tilde{q}_a, \lambda^{bcd}\right] = \langle \epsilon\, p\rangle\, 3!\, \delta_a^{[b} S^{cd]}\,,\ \left[\tilde{q}_a, G^{bcde}\right] = \langle \epsilon\, p\rangle\, 4!\, \delta_a^{[b} \lambda^{cde]}\,. \tag{2.10}$$

Similar relations are found for q^a. Note that the action of $\tilde{q}_a$ on operators in (2.6) is identical to (2.10). However, in this chiral representation, the q^a's commute with all the Grassmann differential operators in (2.6).

Superfields Ω can be regarded as *superwavefunctions* for the external lines of superamplitudes $\mathcal{A}_n(\Omega_1, \Omega_2, \ldots, \Omega_n)$. The N^KMHV superamplitudes of $\mathcal{N} = 4$ SYM are degree $4(K+2)$ polynomials in the n sets of Grassmann variables η_{ia}. The individual amplitudes are coefficients of this polynomial. One extracts an amplitude by applying the operators (2.6) to $\mathcal{A}_n$ to project out each of the desired states from the superwavefunctions Ω_i.

The tree-level MHV superamplitude [7] is simply given by

$$\mathcal{A}_n^{\mathrm{MHV}} = \frac{\delta^{(8)}(\tilde{Q})}{\langle 12\rangle\langle 23\rangle \ldots \langle n1\rangle}\,, \tag{2.11}$$

where the Grassmann delta-function is defined as

$$\delta^{(8)}(\tilde{Q}) \equiv \frac{1}{2^4} \prod_{a=1}^{4} \sum_{i,j=1}^{n} \langle ij\rangle \eta_{ia}\eta_{ja}\,. \tag{2.12}$$

The sums of supercharges (2.7)

$$\tilde{Q}_a^{\dot{\alpha}} = \sum_{i=1}^{n} |i\rangle^{\dot{\alpha}}\, \eta_{ia}\,, \qquad Q_\alpha^a = \sum_{i=1}^{n} |i]_\alpha\, \frac{\partial}{\partial \eta_{ia}} \tag{2.13}$$

both annihilate $\delta^{(8)}(\tilde{Q})$, so the MHV superamplitude $\mathcal{A}_n^{\mathrm{MHV}}$ is manifestly supersym-

[5] We drop an overall sign in (2.9).

metric. There are known tree-level expressions for all N^{K}MHV amplitudes of $\mathcal{N}=4$ SYM [12]. In this section we only consider MHV superamplitudes, but we go beyond MHV in section 2.3.

We have used a superfield Ω chiral in η_a to encode the states of $\mathcal{N}=4$ SYM. The conjugate superfield $\Omega^\dagger$ encodes exactly the same information as Ω, since the $\mathcal{N}=4$ SYM multiplet is CPT self-conjugate. The equivalence of the fields are easily seen by a Grassmann Fourier transformation; indeed one finds

$$\begin{aligned}\Omega^\dagger &= \int d\eta_1 d\eta_2 d\eta_3 d\eta_4 \; e^{\eta_a \overline{\eta}^a} \; \Omega \\ &= G^- + \frac{1}{3!}\epsilon_{abcd}\overline{\eta}^a \lambda^{bcd} + \frac{1}{2!}\frac{1}{2!}\epsilon_{abcd}\overline{\eta}^a\overline{\eta}^b \, S^{cd} + \frac{1}{3!}\epsilon_{abcd}\overline{\eta}^a\overline{\eta}^b\overline{\eta}^c \, \lambda^d + \overline{\eta}^1\overline{\eta}^2\overline{\eta}^3\overline{\eta}^4 \, G^+ \end{aligned} \tag{2.14}$$

Comparing with the directly conjugated field, we have identified $(G^+)^\dagger = G^-$, including the anti-self-conjugacy condition $\bar{S}_{ab} = -\frac{1}{2!}\epsilon_{abcd}S^{cd}$ for the scalars.

Since the two wavefunctions Ω and $\Omega^\dagger$ encode the exact same information, we are free to use either formulation in the superamplitudes. This will be useful in the following.

2.2.2 $\mathcal{N}=1$ SYM on-shell superfields Φ and $\Phi^\dagger$ and MHV superamplitude

The $\mathcal{N}=1$ SYM supermultiplet consists of a gluon, G^+, with helicity $+1$ and a gluino, λ^+, with helicity $+1/2$, and in addition the CPT conjugate gluon G^- and gluino λ^- with negative helicities. Classically, pure $\mathcal{N}=1$ SYM theory has a $U(1)_R$ global symmetry, under which the particles have the R-charges

	G^+	λ^+	λ^-	G^-
R-charge	0	1	-1	0

(2.15)

It is natural to encode the $\mathcal{N}=1$ states into two conjugate on-shell superfields

$$\Phi = G^+ + \eta\,\lambda^+\,, \qquad \Phi^\dagger = G^- + \overline{\eta}\,\lambda^-\,. \tag{2.16}$$

The $\mathcal{N}=1$ theory forms a closed subsector of the $\mathcal{N}=4$ theory, and the $\mathcal{N}=1$ wavefunctions Φ and $\Phi^\dagger$ in (2.16) can be obtained from the $\mathcal{N}=4$ superfields (2.5) and (2.14) by a truncation

$$\eta_{2,3,4} \to 0\,, \qquad \overline{\eta}_{2,3,4} \to 0 \tag{2.17}$$

with the identification $\lambda^+ = \lambda^1$ and $\lambda^- = \lambda^{234}$.

Let us now use this to obtain the MHV tree superamplitudes in $\mathcal{N}=1$ SYM. If we perform the truncation (2.17) directly on the $\mathcal{N}=4$ MHV superamplitude (2.11), it clearly vanishes. This is not surprising because it would correspond to an amplitude with external states only from the positive helicity sector of $\mathcal{N}=1$ SYM, and this is forbidden by supersymmetry.

We recall that the MHV sector in $\mathcal{N}=1$ SYM consists of n-point amplitudes with two states from the negative helicity sector $\Phi^\dagger$ and $n-2$ from the positive helicity sector Φ. It is therefore natural that $\mathcal{N}=1$ SYM superamplitudes in the MHV sector take the form

$$\mathcal{A}^{\mathcal{N}=1}_{n,ij} = \mathcal{A}^{\mathcal{N}=1}_{n}(\Phi_1\Phi_2\ldots\Phi^\dagger_i\,\Phi_{i+1}\ldots\Phi^\dagger_j\,\Phi_{j+1}\ldots\Phi_n)\,. \tag{2.18}$$

The subscript ij on $\mathcal{A}^{\mathcal{N}=1}_{n,ij}$ indicate the states in the $\Phi^\dagger$ sector.

The equivalence between the description of the $\mathcal{N}=4$ supermultiplet in the Ω or $\Omega^\dagger$ superfields can now be exploited to obtain the $\mathcal{N}=1$ SYM MHV superamplitudes $\mathcal{A}^{\mathcal{N}=1}_{n,ij}$ in two easy steps. The first step is to perform a Grassmann Fourier transform of the η-variables of lines i and j in the $\mathcal{N}=4$ superamplitude (2.11). This con-

$\mathcal{N} = 1$ SYM

particle	operator Φ-$\Phi^\dagger$	operator Φ-Ψ
G^+	1	1
λ^+	∂_i	∂_i
λ^-	$\overline{\partial}_i$	1
G^-	$\overline{1}$	∂_i

Table 2.1: Map from states to Grassmann derivatives for $\mathcal{N} = 1$ SYM. We present two different formalisms, one with on-shell superfields Φ-$\Phi^\dagger$ and conjugate Grassmann variables η_{ia} and $\bar{\eta}_i^a$ (section 2.2.2), and the other with superfields Φ-Ψ chiral in Grassmann variables η_{ia} (section 2.3).

verts Φ_i and Φ_j to $\Phi_i^\dagger$ and $\Phi_j^\dagger$, and thus yields the equally valid $\mathcal{N} = 4$ SYM MHV superamplitude[6]

$$\begin{aligned}\mathcal{A}_{n,ij}^{\mathcal{N}=4,\mathrm{MHV}}(\ldots\Phi_i^\dagger\ldots\Phi_j^\dagger\ldots) &= \int d^4\eta_i\, d^4\eta_j\; e^{\eta_{ib}\overline{\eta}_i^b}\; e^{\eta_{jc}\overline{\eta}_j^c}\; \mathcal{A}_n^{\mathrm{MHV}}(\Phi_1\Phi_2\ldots\Phi_n) \\ &= \frac{1}{\langle 12\rangle\langle 23\rangle\ldots\langle n1\rangle}\prod_{a=1}^{4}\Big(\langle ij\rangle + \langle ik\rangle\,\overline{\eta}_j^a\,\eta_{ka} - \langle jk\rangle\,\overline{\eta}_i^a\,\eta_{ka} - \frac{1}{2}\langle kl\rangle\,\overline{\eta}_i^a\,\overline{\eta}_j^a\,\eta_{ka}\,\eta_{la}\Big)\end{aligned} \tag{2.19}$$

There is an implicit sum over repeated indices $k, l = 1, 2, \ldots, n$ with $k, l \neq i, j$. The second step is to apply the truncation (2.17) to (2.19) to find the $\mathcal{N} = 1$ MHV superamplitudes:

$$\mathrm{MHV}:\;\; \mathcal{A}_{n,ij}^{\mathcal{N}=1} \;=\; \frac{\langle ij\rangle^3}{\langle 12\rangle\langle 23\rangle\ldots\langle n1\rangle}\Big(\langle ij\rangle + \langle ik\rangle\,\overline{\eta}_j\,\eta_k - \langle jk\rangle\,\overline{\eta}_i\,\eta_k - \frac{1}{2}\langle kl\rangle\,\overline{\eta}_i\,\overline{\eta}_j\,\eta_k\,\eta_l\Big)\,. \tag{2.20}$$

The choice of $\Phi^\dagger$ states i and j necessarily breaks the cyclic symmetry of the original $\mathcal{N} = 4$ superamplitude.

Explicit amplitudes are projected out by acting on $\mathcal{A}_{n,ij}^{\mathcal{N}=1}$ with Grassmann derivatives that select the requested external states from the superfields (2.16) *and* then set any remaining η-variables to zero. (Equivalently, we can convert the Grassman-

[6] We define $d^4\eta_i \equiv \prod_{a=1}^4 d\eta_{ia}$.

n differentiations to integrals.) The map between states and Grassmann derivative operators is summarized in table 2.1. We list three simple examples:

$$\begin{aligned}
\big\langle --+++\!+\big\rangle &= \mathcal{A}_{6,12}\big|_{\eta\to 0} = \frac{\langle 12\rangle^4}{\langle 12\rangle\langle 23\rangle\ldots\langle 61\rangle}\,, \\
\big\langle -\lambda^-\lambda^+++\!+\big\rangle &= \overline{\partial}_2\,\partial_3\,\mathcal{A}_{6,12}\big|_{\eta\to 0} = -\frac{\langle 12\rangle^3\langle 13\rangle}{\langle 12\rangle\langle 23\rangle\ldots\langle 61\rangle}\,, \\
\big\langle \lambda^-\lambda^-\lambda^+\lambda^+++\!+\big\rangle &= \overline{\partial}_1\,\overline{\partial}_2\,\partial_3\,\partial_4\,\mathcal{A}_{6,12}\big|_{\eta\to 0} = -\frac{\langle 12\rangle^3\langle 34\rangle}{\langle 12\rangle\langle 23\rangle\ldots\langle 61\rangle}\,.
\end{aligned} \tag{2.21}$$

The equivalent calculations in the $\mathcal{N}=4$ formalism yield the same results.

An alternative form of the $\mathcal{N}=1$ SYM generating function is

$$\mathcal{A}^{\rm MHV}_{n,ij} = \frac{\langle ij\rangle^3}{{\rm cyc}(1\ldots n)}\tilde{\delta}({\rm ext})\,\overline{\eta}_i\,\overline{\eta}_j\,, \tag{2.22}$$

where

$$\tilde{\delta}({\rm ext}) = \tilde{\delta}\Big(\sum_{k=1}^n |i\rangle\xi_i\Big) = \frac{1}{2}\sum_{k,l=1}^n \langle kl\rangle\xi_k\xi_l,\ \ \xi_k = \begin{cases} \eta_k & \text{if } \Phi_k \\ -\bar{\partial}_k & \text{if } \Phi_k^\dagger \end{cases}. \tag{2.23}$$

This representation is homogeneous in the ξ_i's, and it is easier to use in calculations.

One can formulate super-BCFW recursion relations in the Φ-$\Phi^\dagger$ formalism and use it to derive N^{K}MHV superamplitudes for $\mathcal{N}=1$ SYM. We have solved these relations explicitly at the NMHV level as a healthy exercise, and the result is similar to that of $\mathcal{N}=4$ SYM [12]. We spare the reader for details since we will shortly introduce a more convenient formalism.

2.2.3 MHV vertex expansion

The simple scaling argument given in [99] proves that the MHV vertex expansion is valid for all tree amplitudes in $\mathcal{N}=1$ SYM. In the superamplitude formalism, the MHV vertex diagrams consist of MHV superamplitudes 'glued' together with propagators $1/P_I^2$ and a sum over possible states of the internal line. This sum is

carried out in $\mathcal{N}=4$ SYM as the simple fourth order Grassmann differentiation (or, equivalently, integration) $\prod_{a=1}^{4}\frac{\partial}{\partial\eta_{Pa}}$ of the η_{Pa}'s associated with the internal line. This automatically takes care of the internal sum. For $\mathcal{N}=1$ SYM we reverse-engineer the equivalent sum as follows.

Consider a simple diagram with two MHV vertices:

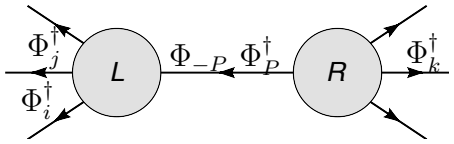

(2.24)

We assume that the external lines i,j,k are in the $\Phi^\dagger$-sector and all other lines are Φ's, as appropriate for an NMHV amplitude. Since we label both MHV superamplitudes in terms of outgoing particles, the internal line P_I propagates a $\Phi^\dagger$-state to a Φ state (and vice versa): if the left subamplitude has a positive helicity gluon on the internal line, it will be a negative helicity gluon on the right subamplitude. Similarly for the gluinos. There are no other possibilities in pure $\mathcal{N}=1$ SYM, so the rule for the internal line is

$$\text{internal sum} = (1+\partial_P\bar\partial_P)\ \mathcal{A}_L(\Phi_i^\dagger\dots\Phi_j^\dagger\dots\Phi_{-P}\dots)\ \mathcal{A}_R(\dots\Phi_P^\dagger\dots\Phi_k^\dagger)\Big|_{\eta_P,\bar\eta_P\to 0} \tag{2.25}$$

The first term "1" encodes the internal gluon state and the second term $\partial_P\bar\partial_P$ the internal gluino. The expression can be rewritten as $\int d\eta_P d\bar\eta_P(1+\bar\eta_P\eta_P)\mathcal{A}_L\mathcal{A}_R$. Promoting the prefactor to an exponential we find

$$\text{internal sum} = \int d\eta_P d\bar\eta_P\ e^{\bar\eta_P\eta_P}\ \mathcal{A}_L(\Phi_i^\dagger\dots\Phi_j^\dagger\dots\Phi_{-P}\dots)\ \mathcal{A}_R(\dots\Phi_P^\dagger\dots\Phi_k^\dagger) \tag{2.26}$$

$\mathcal{A}_L$ is independent of $\bar\eta_P$, so we can move the exponential and the $\bar\eta_P$-integral to act only on $\mathcal{A}_R$, where it becomes the inverse Fourier transform of the state $\Phi_P^\dagger$. We note

that

$$\int d\bar{\eta}\; e^{\bar{\eta}\eta}\; \Phi^\dagger \;=\; \lambda^- + \eta\, G^- \;\equiv\; \Psi\,, \tag{2.27}$$

and hence we can write

$$\text{internal sum} = \int d\eta_P\; \mathcal{A}_L(\dots \Phi_{-P} \dots)\; \mathcal{A}_R(\dots \Psi_P \dots)\,. \tag{2.28}$$

This is the simple $\mathcal{N} = 1$ SYM analogous of the $\mathcal{N} = 4$ internal line Grassmann integral.

We can convert all $\Phi^\dagger$'s in the superamplitudes to Ψ's by a inverse Fourier transformation. The resulting Φ-Ψ formalism only depends on η's and not $\overline{\eta}$'s, and this is more convenient for practical calculations than the perhaps more intuitive $\Phi, \Phi^\dagger$ formalism.

2.3 Pure $\mathcal{N} = 0, 1, 2, 3, 4$ SYM: Φ-Ψ formalism

It was observed in [93] that the unitarity cuts of pure $\mathcal{N} < 4$ SYM are subsets of the $\mathcal{N} = 4$ cuts. In particular, when the $\mathcal{N} = 4$ η-integrals are converted into index diagrams [93], the $\mathcal{N} < 4$ super-sum corresponds to the subset of diagrams where the $4 - \mathcal{N}$ index lines are grouped together. This can be understood as the embedding of the on-shell states of the $4 - \mathcal{N}$ theories in the maximal multiplet. Thus one can obtain the $\mathcal{N} < 4$ amplitudes from the maximally SUSY ones by simply separating out the needed $\mathcal{N}$ η's. This is implemented by either integrating out, or setting to zero, the remaining $4-\mathcal{N}$ η's. This gives the Φ-Ψ formalism which we now study in detail.

Let us first recall that $\Phi = G^+ + \lambda^+\eta$ was obtained from the $\mathcal{N} = 4$ superfield Φ of (2.5) by setting $\eta_{2,3,4} \to 0$, and dropping the subscript 1. We can obtain $\Psi = \lambda^- + \eta\, G^-$

from (2.5) by integrating over $\eta_{2,3,4}$. (This gives the same result as (2.27).) The higher-$\mathcal{N}$ generalizations should be clear, and we find that the on-shell states of the pure SYM theories are nicely packaged as

$$\begin{aligned}
&\Phi_{\mathcal{N}=1} = \Phi|_{\eta_2,\eta_3,\eta_4\to 0} \qquad \Psi_{\mathcal{N}=1} = \int d\eta_2\, d\eta_3\, d\eta_4\ \Phi\,, \\
&\Phi_{\mathcal{N}=2} = \Phi|_{\eta_3,\eta_4\to 0} \qquad \Psi_{\mathcal{N}=2} = \int d\eta_3\, d\eta_4\ \Phi\,, \\
&\Phi_{\mathcal{N}=3} = \Phi|_{\eta_4\to 0} \qquad \Psi_{\mathcal{N}=3} = \int d\eta_4\ \Phi\,.
\end{aligned} \tag{2.29}$$

Explicitly, we have

$$\begin{aligned}
\mathcal{N}=1 \ \to \quad & \Phi_{\mathcal{N}=1} = G^+ + \eta\lambda^+ \\
& \Psi_{\mathcal{N}=1} = \lambda^- + \eta\, G^- \qquad (\lambda^+=\lambda^1\,,\ \lambda^-=\lambda^{234}) \\
\mathcal{N}=2 \ \to \quad & \Phi_{\mathcal{N}=2} = G^+ + \eta_a\,\lambda^{a+} - \eta_1\eta_2\, S \\
& \Psi_{\mathcal{N}=2} = \bar{S} + \eta_a\,\lambda^{a-} - \eta_1\eta_2\, G^- \qquad (\bar{S}=S^{34}\,,\ \lambda^{a-}=\lambda^{a34}) \\
\mathcal{N}=3 \ \to \quad & \Phi_{\mathcal{N}=3} = G^+ + \eta_a\,\lambda^a - \eta_a\eta_b\, S^{ab} - \eta_1\eta_2\eta_3\,\lambda^{123} \\
& \Psi_{\mathcal{N}=3} = \lambda^4 + \eta_a\, S^{a4} + \tfrac{1}{2!}\eta_a\eta_b\,\lambda_c^{ab4} - \eta_1\eta_2\eta_3\, G^-
\end{aligned} \tag{2.30}$$

The Grassmann operators associated with each state can be read-off from the superfields, just as we did in the $\mathcal{N}=4$ case. For example, a negative helicity gluon is projected out from $\Psi_{\mathcal{N}=1}$ by ∂, from $\Psi_{\mathcal{N}=2}$ by $+\partial^1\partial^2$ and from $\Psi_{\mathcal{N}=3}$ by $+\partial^1\partial^2\partial^3$.

Equivalence of $\mathcal{N}=3$ and $\mathcal{N}=4$ SYM:

Let us compare the $\mathcal{N}=3$ superfields in (2.30) with the $\mathcal{N}=4$ self-conjugate superfield (2.5) with η_4 separated out:

$$\begin{aligned}
\Omega \ = \ & G^+ + \eta_a\lambda^{+a} - \frac{1}{2!}\eta_a\eta_b S^{ab} - \frac{1}{3!}\eta_a\eta_b\eta_c\lambda^{abc} \\
& + \eta_4\left(\lambda^4 + \eta_a S^{a4} + \frac{1}{2!}\eta_a\eta_b\lambda^{ab4} - \eta_1\eta_2\eta_3\, G^-\right),
\end{aligned} \tag{2.31}$$

with $a, b, c = 1, 2, 3$. We immediately recognize that $\Omega = \Phi_{\mathcal{N}=3} + \eta_4 \Psi_{\mathcal{N}=3}$, i.e. the field content of the $\mathcal{N} = 3$ superfields (2.30) is equivalent to that of $\mathcal{N} = 4$ SYM. This is no surprise since $\mathcal{N} = 3$ SYM is equivalent to $\mathcal{N} = 4$ SYM. When we apply the on-shell formalism for $\mathcal{N} < 4$ SYM in the following, we will occasionally compare the results of the $\mathcal{N} = 3$ formulation with that of $\mathcal{N} = 4$.

2.3.1 MHV superamplitudes for $0 \leq \mathcal{N} \leq 4$

Consider the $\mathcal{N} = 1$ MHV amplitude. Choosing the ith and jth particles to be in the Ψ sector, one derives the $\mathcal{N} = 1$ amplitude by integrating away $3\eta_i$'s and $3\eta_j$'s from the $\mathcal{N} = 4$ result:

$$\mathcal{F}_{n,ij}^{\mathcal{N}=1} \;=\; \int d^3\eta_i d^3\eta_j \frac{\delta^{(8)}\big(\sum |k\rangle\eta_k\big)}{\langle 12\rangle\langle 23\rangle\cdots\langle n\,1\rangle}\bigg|_{\eta_{k,\{2,3,4\}}\to 0} \;=\; \frac{\langle ij\rangle^3\;\delta^{(2)}\big(\sum |k\rangle\eta_k\big)}{\langle 12\rangle\langle 23\rangle\cdots\langle n\,1\rangle}\,. \qquad (2.32)$$

Here we have used $d^3\eta_i d^3\eta_j = d\eta_{i2}d\eta_{i3}d\eta_{i4}d\eta_{j2}d\eta_{j3}d\eta_{j4} = -d\eta_{i2}d\eta_{j2}d\eta_{i3}d\eta_{j3}d\eta_{i4}d\eta_{j4}$. Each $d\eta_{ia}d\eta_{ja}$ projects out $-\langle ij\rangle$, so all in all we get $-(-\langle ij\rangle)^3 = \langle ij\rangle^3$.

Similar, one finds the $\mathcal{N} = 0, 1, 2, 3, 4$ MHV superamplitude to be

$$\mathcal{F}_{n,ij}^{\mathcal{N}} \;=\; (-1)^{\frac{1}{2}\mathcal{N}(\mathcal{N}-1)}\;\frac{\langle ij\rangle^{4-\mathcal{N}}\;\delta^{(2\mathcal{N})}\big(\sum |k\rangle\eta_k\big)}{\langle 12\rangle\langle 23\rangle\cdots\langle n\,1\rangle}\,. \qquad (2.33)$$

Note that $\mathcal{N} = 3$ encodes $\mathcal{N} = 4$ processes in which the particles on lines i and j have been chosen to always carry $SU(4)$ index 4 while particles on all other lines never carry index 4. Thus the $\binom{n}{2}$ different superamplitudes $\mathcal{F}_{n,ij}^{\mathcal{N}=3}$ encode exactly the same processes as the $\mathcal{N} = 4$ superamplitude.

To obtain component amplitudes from the superamplitudes $\mathcal{F}_{n,ij}^{\mathcal{N}}$, one selects the superamplitude with superfields arranged according to the desired external states. For example, the $\mathcal{N} = 1$ SYM amplitude $\langle -\lambda^-\lambda^+ + +\rangle$ is projected out from the MHV superamplitude $\mathcal{F}_{6,12}^{\mathcal{N}=1}$. The only tricky part is to keep track of the overall sign of the amplitude. To illustrate the issue, consider how to obtain the following three

$\mathcal{N}=1$ amplitudes from the $\mathcal{N}=4$ constructions:

$$\begin{aligned}\langle + - - + + \rangle &= (\partial_2^1\partial_2^2\partial_2^3\partial_2^4)(\partial_3^1\partial_3^2\partial_3^3\partial_3^4)\mathcal{A}_5^{\mathcal{N}=4} = -\partial_2^1\partial_3^1\big[(\partial_2^2\partial_2^3\partial_2^4)(\partial_3^2\partial_3^3\partial_3^4)\mathcal{A}_5^{\mathcal{N}=4}\big] \\ &= -\partial_2^1\partial_3^1\,\mathcal{F}_{5,23}^{\mathcal{N}=1}\,, \qquad (2.34)\end{aligned}$$

$$\begin{aligned}\langle + \lambda^- - \lambda^+ + \rangle &= (\partial_2^2\partial_2^3\partial_2^4)(\partial_3^1\partial_3^2\partial_3^3\partial_3^4)\partial_4^1\mathcal{A}_5^{\mathcal{N}=4} = -\partial_3^1\partial_4^1\big[(\partial_2^2\partial_2^3\partial_2^4)(\partial_3^2\partial_3^3\partial_3^4)\mathcal{A}_5^{\mathcal{N}=4}\big] \\ &= -\partial_3^1\partial_4^1\,\mathcal{F}_{5,23}^{\mathcal{N}=1}\,, \qquad (2.35)\end{aligned}$$

$$\begin{aligned}\langle + - \lambda^- \lambda^+ + \rangle &= (\partial_2^1\partial_2^2\partial_2^3\partial_2^4)(\partial_3^2\partial_3^3\partial_3^4)\partial_4^1\mathcal{A}_5^{\mathcal{N}=4} = \partial_2^1\partial_4^1\big[(\partial_2^2\partial_2^3\partial_2^4)(\partial_3^2\partial_3^3\partial_3^4)\mathcal{A}_5^{\mathcal{N}=4}\big] \\ &= +\partial_2^1\partial_4^1\,\mathcal{F}_{5,23}^{\mathcal{N}=1}\,. \qquad (2.36)\end{aligned}$$

Recall that the $\mathcal{N}=1$ projection rules are

$$\Phi\colon\ G^+ \leftrightarrow 1\,,\ \lambda^+ \leftrightarrow \partial_i^1\,,\ \Psi\colon\ G^- \leftrightarrow \partial_i^1\,,\ \lambda^- \leftrightarrow 1\,. \qquad (2.37)$$

The first two cases (2.34)-(2.35) require a minus sign in addition to the projection rules (2.37). This arises from anti-commuting $\partial^{2,3,4}$'s all the way to the right. We can take this into account by the

Sign Rule: in the Φ-Ψ *formalism for* $\mathcal{N}=1,3$ *SYM one must include a minus sign everytime a Grassmann derivative moves past a* Ψ*-state.*

In the example (2.34), ∂_3^1 has to move past Ψ_2 to hit Ψ_3, and the Sign Rule tells us to include the overall minus sign. In the second example, (2.35), ∂_4^1 moves past both Ψ_2 and Ψ_3 while ∂_3^1 has to move past Ψ_2; this gives an overall minus sign. In the final case (2.36), the Grassmann derivatives move past an even number of Ψ's, so the Sign Rule gives "+".

For $\mathcal{N}=2$ SYM, let us for example consider the 6-point amplitudes $\langle\lambda_1^-\lambda_2^-\lambda^{+1}\lambda^{+2}+ +\rangle$. and $\langle\lambda_1^-\lambda_2^- + S + +\rangle$. These come from the MHV superamplitude $\mathcal{F}_{6,12}^{\mathcal{N}=2}$ in (2.33).

We apply the operators corresponding to the external states and find

$$\begin{aligned}\langle\lambda^{1-}\lambda^{2-}\lambda^{1+}\lambda^{2+}++\rangle &= (\partial_1^1)\,(\partial_2^2)\,(\partial_3^1)\,(\partial_4^2)\,\mathcal{F}_{6,12}^{\mathcal{N}=2} = \frac{\langle 12\rangle^2\langle 13\rangle\langle 24\rangle}{\langle 12\rangle\langle 23\rangle\cdot\cdot\langle 61\rangle}\\ \langle\lambda^{1-}\lambda^{2-}+S++\rangle &= (\partial_1^1)\,(\partial_2^2)\,(\partial_4^1\partial_4^2)\,\mathcal{F}_{6,12}^{\mathcal{N}=2} = \frac{\langle 12\rangle^2\langle 14\rangle\langle 24\rangle}{\langle 12\rangle\langle 23\rangle\cdot\cdot\langle 61\rangle}\end{aligned}$$

These can be seen to agree with the equivalent amplitudes obtained in the $\mathcal{N}=4$ formalism.

2.3.2 NMHV superamplitudes for $0 \leq \mathcal{N} \leq 4$

We start with the dual superconformal form of the $\mathcal{N}=4$ NMHV amplitude derived in [12]. It is expressed in terms of variables $x_i^{\alpha\dot\alpha}$, $|i\rangle^\alpha$, η_i^a, where the 'region variables' $x_i^{\alpha\dot\alpha}$ are related to the momenta via

$$x_i^{\alpha\dot\alpha} - x_{i+1}^{\alpha\dot\alpha} = p_i^{\alpha\dot\alpha}\,. \tag{2.38}$$

The $\mathcal{N}=4$ NMHV superamplitude is given as

$$\mathcal{N}=4: \quad \mathcal{A}_n^{\rm NMHV} = \frac{\delta^{(8)}(\sum|k\rangle\eta_k)}{\langle 12\rangle\langle 23\rangle\cdot\cdot\langle n\ 1\rangle}\sum_{2\leq s<t\leq n-1} R_{nst}\,, \tag{2.39}$$

where

$$R_{nst} = \frac{\langle s\ s-1\rangle\langle t\ t-1\rangle\ \prod_{a=1}^4\Xi_{nst,a}}{x_{st}^2\langle n|x_{ns}x_{st}|t\rangle\langle n|x_{ns}x_{st}|t-1\rangle\langle n|x_{nt}x_{ts}|s\rangle\langle n|x_{nt}x_{ts}|s-1\rangle}\,, \tag{2.40}$$

and the Grassmann odd function $\Xi_{nst,a}$ is defined as

$$\Xi_{nst,a} \equiv \sum_{i=t}^{n-1}\langle n|x_{ns}x_{st}|i\rangle\eta_{ia} + \sum_{i=s}^{n-1}\langle n|x_{nt}x_{ts}|i\rangle\eta_{ia}\,. \tag{2.41}$$

To derive superamplitudes for $\mathcal{N}<4$ SYM, we simply perform the integrals

$\int d^{4-\mathcal{N}}\eta$ of $\mathcal{A}_n^{\rm NMHV}$ for the three Ψ-states which we choose to be i, j, n. The details of the derivation are omitted, here we simply state the result valid for $\mathcal{N} = 0, 1, 2, 3, 4$:

$$\mathcal{F}^{\mathcal{N}}_{n,ijn} = (-1)^{\frac{1}{2}\mathcal{N}(\mathcal{N}+1)}\,\mathcal{F}^{\mathcal{N}}_{n,ij}\times \tag{2.42}$$
$$\Bigg[\sum_{i<s\leq j<t\leq n-1}\left(\frac{\langle in\rangle\langle n|x_{nt}x_{ts}|j\rangle}{\langle ij\rangle}\right)^{4-\mathcal{N}} R^{\mathcal{N}}_{nst} + \sum_{i<s<t\leq j\leq n-1}\left(\frac{\langle ni\rangle\langle nj\rangle x_{st}^2}{\langle ij\rangle}\right)^{4-\mathcal{N}} R^{\mathcal{N}}_{nst}$$
$$+\sum_{2\leq s\leq i<j<t\leq n-1}\Big(\langle n|x_{nt}x_{ts}|n\rangle\Big)^{4-\mathcal{N}} R^{\mathcal{N}}_{nst} + \sum_{2\leq s\leq i<t\leq j}\left(\frac{\langle jn\rangle\langle n|x_{ns}x_{st}|i\rangle}{\langle ij\rangle}\right)^{4-\mathcal{N}} R^{\mathcal{N}}_{nst}\Bigg],$$

where

$$R^{\mathcal{N}}_{nst} = \frac{\langle s\ s-1\rangle\langle t\ t-1\rangle\prod_{a=1}^{\mathcal{N}}\Xi_{nst,a}}{x_{st}^2\langle n|x_{ns}x_{st}|t\rangle\langle n|x_{ns}x_{st}|t-1\rangle\langle n|x_{nt}x_{ts}|s\rangle\langle n|x_{nt}x_{ts}|s-1\rangle}\,. \tag{2.43}$$

For $\mathcal{N} = 0$ SYM, the product in (2.43) is set to 1, and one then recovers the result presented recently in [94].

2.3.3 On the range of $\mathcal{N}$ in SYM

We have derived MHV and NMHV superamplitudes $\mathcal{F}^{\mathcal{N}}_{n,ij}$ and $\mathcal{F}^{\mathcal{N}}_{n,ijk}$ in which the number of supersymmetries $\mathcal{N}$ appeared as a parameter. We know the interpretation of these superamplitudes for $\mathcal{N} = 0, 1, 2, 3, 4$, but what if $\mathcal{N}$ takes other (integer) values? Clearly, $\delta^{(2\mathcal{N})}$ makes sense only for $\mathcal{N} \geq 0$. For $\mathcal{N} > 4$, $\mathcal{F}^{\mathcal{N}}_{n,ij\ldots}$ is not a physical object. To see this, let us just consider $\mathcal{N} = 5$.

For $\mathcal{N} = 5$, the tree level MHV superamplitude $\mathcal{F}^{\mathcal{N}=5}_{n,ij}$ in (2.33) includes an amplitude

$$\langle A\ldots\rangle = \frac{\langle ij\rangle^{-1}\langle ab\rangle^5}{\langle 12\rangle\ldots\langle n1\rangle} \tag{2.44}$$

where $a, b \neq i$. Under a little group scaling of line i, the amplitude (2.44) scales as

t^{-3}, so this immediately tells us that line i is a particle with helicity 3/2. This should already raise suspicion since it is also easy to see that there are no spin 2 particles possible within the same superamplitude. Now if lines i and j are non-adjacent, (2.44) has a pole in the ij-momentum channel. This is unphysical because the amplitude is color-ordered. If the ij are adjacent, then (2.44) $\langle ij\rangle$ already appears in the cyclic product of angle brackets, and hence there is a double-pole in the ij-momentum channel; this is also unphysical. We conclude that $\mathcal{F}_{n,ij}^{\mathcal{N}=5}$ (or $\mathcal{F}_{n,ij}^{\mathcal{N}>4}$) does not encode sensible tree amplitudes of a local non-gravitational field theory.

In supergravity, $\mathcal{N}$ can take a larger range of values; we will discuss briefly the $0 \leq \mathcal{N} \leq 8$ supergravity superamplitudes in section 2.6.

2.4 Super-BCFW

The super-BCFW shift, introduced for the maximally supersymmetric theories $\mathcal{N} = 4$ SYM (and $\mathcal{N} = 8$ supergravity) in [13, 100] is[7]

$$\begin{aligned} \mathcal{N} = 4 \text{ SYM:} \qquad & |\hat{I}] = |I] + z\,|J]\,, \qquad |\hat{J}\rangle = |J\rangle - z\,|I\rangle\,, \\ & \hat{\eta}_{Ia} = \eta_{Ia} + z\eta_{Ja} \text{ for } a = 1,2,3,4\,. \end{aligned} \tag{2.45}$$

Under this shift, the tree level $\mathcal{N} = 4$ superamplitudes behave as

$$\mathcal{A}_n^{\mathcal{N}=4} \sim 1/z \text{ as } z \to \infty \tag{2.46}$$

when lines I and J are adjacent, and as $1/z^2$ when they are non-adjacent.

The large-z falloff implies a set of valid recursion relations for superamplitudes. These recursion relations were solved in [12] to yield dual superconformal invariant expressions for any tree-level N^KMHV superamplitudes of $\mathcal{N} = 4$ SYM. This includes

[7] There is also a super-shift relevant for the MHV vertex expansion, see [101].

the $\mathcal{N}=4$ NMHV superamplitude expressions used in section 2.3.2.

In this section, we generalize the super-BCFW shift to $\mathcal{N}<4$ SYM and discuss its validity. When valid, the super-BCFW recursion relations can be solved just as in $\mathcal{N}=4$ SYM; however, as we have shown how to truncate the $\mathcal{N}=4$ SYM tree results to $\mathcal{N}<4$ SYM, there is no need to pursue this direction. The important outcome of this section therefore is to characterize when the super-BCFW shifts have large-z falloff and when that fails.

We work in the Φ-Ψ formalism. To be specific, we specialize to $\mathcal{N}=1$ SYM, but our discussion and results generalize directly to $\mathcal{N}=2$ and $\mathcal{N}=3$. Consider a $[I,J\rangle$ super-BCFW shift

$$|\hat{I}] = |I] + z\,|J]\,, \qquad |\hat{J}\rangle = |J\rangle - z\,|I\rangle\,, \qquad \hat{\eta}_I = \eta_I + z\eta_J\,. \tag{2.47}$$

All other spinors and η's are unshifted. By construction, the shift (2.47) leaves the Grassmann δ-function $\delta^{(2)}(\tilde{Q})$ invariant. It only takes a moment of inspection to realize that the MHV amplitude (2.32) behaves as

$$\begin{array}{cccc} [\Psi,\Psi\rangle & [\Phi,\Phi\rangle & [\Psi,\Phi\rangle & [\Phi,\Psi\rangle \\ 1/z & 1/z & 1/z & z^2 \end{array} \tag{2.48}$$

for large z under the adjacent super-BCFW shift (2.47). We have indicated to which sectors the two shifted lines belong. For shifts of non-adjacent lines, the falloff is a factor of $1/z$ better than in (2.48).[8]

The large-z behavior (2.48) is valid also for N^{K}MHV tree superamplitudes. To show this, consider a general N^{K}MHV superamplitude of $\mathcal{N}=1$ SYM; it has $(K+2)$ Ψ-lines and the $(n-K-2)$ Φ-lines. The $\mathcal{N}=1$ superamplitude $\mathcal{F}_n$ is obtained from

[8]Note that the behavior mimics that of gluon amplitudes under regular BCFW $[\pm,\pm\rangle$ and $[\mp,\pm\rangle$ shifts, with only a small improvement $z^3 \to z^2$ thanks to the $\mathcal{N}$=1 supershift.

that of $\mathcal{N}=4$ SYM as

$$\mathcal{F}_n \;=\; \Big[\int \Big(\prod_{a=2}^{4}\prod_{x\in\Psi} d\eta_{xa}\Big)\,\mathcal{A}_n^{\mathcal{N}=4}\Big]_{\eta_{y2},\eta_{y3},\eta_{y4}\to 0 \text{ for } y\in\Phi}\,. \tag{2.49}$$

The truncation rule $\eta_{y2},\eta_{y3},\eta_{y4}\to 0$ for $y\in\Phi$ can be converted an Grassmann integration by integrating over all $\eta_{2,3,4}$'s with a 'measure' containing the product of all η_{ya}'s for $a=2,3,4$:

$$\mathcal{F}_n \;=\; \int \Big(\prod_{a=2}^{4}\prod_{i=1}^{n} d\eta_{ia}\prod_{y\in\Phi}\eta_{ya}\Big)\,\mathcal{A}_n^{\mathcal{N}=4}\,. \tag{2.50}$$

When we apply the $\mathcal{N}=1$ supershift (2.47), it only acts on η_{I1} in $\mathcal{A}_n^{\mathcal{N}=4}$, i.e. the shifted superamplitude $\mathcal{A}_n^{\mathcal{N}=4}$ depends on $\hat{\eta}_{I1}=\eta_{I1}+z\eta_{J1}$ and on η_{Ia} for $a=2,3,4$. To use the result (2.46) for the large-z falloff of $\mathcal{A}_n^{\mathcal{N}=4}$, we need all four η_{Ia} to be shifted. To accomplish this, we redefine for $a=2,3,4$ the integration variables as

$$\eta_{Ia}\to\tilde{\eta}_{Ia}-z\tilde{\eta}_{Ja}\,,\ \text{and}\ \eta_{ia}\to\tilde{\eta}_{ia}\ \text{for all}\ i\neq I\,. \tag{2.51}$$

The Jacobian is 1, so we can write the shifted $\mathcal{N}=1$ superamplitude

$$\hat{\mathcal{F}}_n(z) \;=\; \int \Big(\prod_{a=2}^{4}\prod_{i=1}^{n} d\tilde{\eta}_{ia}\,\hat{m}_a\Big)\,\hat{\mathcal{A}}_n^{\mathcal{N}=4}(z)\,,\ \text{with}\ \hat{m}_a=\prod_{y\in\Phi}\eta_{ya}(\tilde{\eta}_{ia})\,. \tag{2.52}$$

Note that $\hat{}$ on $\mathcal{F}$ indicates the $\mathcal{N}=1$ supershift (2.47) while $\hat{}$ on $\hat{\mathcal{A}}_n^{\mathcal{N}=4}$ refers to a full $\mathcal{N}=4$ supershift (2.45), thanks to the coordinate transformation in the integral. We already know that for large z, $\hat{\mathcal{A}}_n^{\mathcal{N}=4}(z)$ goes as $1/z$ (or better), so the only way the large-z behavior of $\hat{\mathcal{F}}_n(z)$ can differ is if the 'measure'-factor $\hat{m}_a$ shifts. Let us go through the four different shifts and track the large-z behavior:

- $[\Psi,\Psi\rangle$ and $[\Psi,\Phi\rangle$: when $I\notin\Phi$, all $\eta_{ya}(\tilde{\eta}_{ia})=\tilde{\eta}_{ya}$; they are z-independent, so $\hat{m}_a\sim O(1)$ for large z.

- $[\Phi, \Phi\rangle$: when $I, J \in \Phi$, the factor $\hat{m}_a$ contains both η_{Ia} and η_{Ja}. Their product is $(\tilde{\eta}_{Ia} - z\tilde{\eta}_{Ja})\,\tilde{\eta}_{Ja} = \tilde{\eta}_{Ia}\,\tilde{\eta}_{Ja}$, so $\hat{m}_a \sim O(1)$ for large z.

- $[\Phi, \Psi\rangle$: in this case $I \in \Phi$, and hence $\hat{m}_a$ contains a factor of $\eta_{Ia} \to (\tilde{\eta}_{Ia} - z\tilde{\eta}_{Ja})$. But there is no factor of $\tilde{\eta}_{Ja}$ in $\hat{m}_a$ because $J \in \Psi$, so we conclude that $\hat{m}_a \sim z$ for large z. The three factors $a = 2, 3, 4$ of $\hat{m}_a$ thus give a large z behavior of z^3.

Together with the result (2.46) that $\hat{\mathcal{A}}_n^{\mathcal{N}=4}(z) \sim 1/z$ for large z for a shift of adjacent lines, we conclude that (2.48) indeed holds for all $\mathcal{N} = 1$ superamplitudes. The generalization of this result to $\mathcal{N} = 2, 3$ follows from a similar argument, but with $4 - \mathcal{N}$ factors in the Grassmann integration. The general result can be summarized as

$$\begin{array}{cccc} [\Psi, \Psi\rangle & [\Phi, \Phi\rangle & [\Psi, \Phi\rangle & [\Phi, \Psi\rangle \\ 1/z & 1/z & 1/z & z^{3-\mathcal{N}} \end{array} \tag{2.53}$$

This is valid for all pure SYM N^{K}MHV superamplitudes at the tree level with $\mathcal{N} = 0, 1, 2, 3, 4$.

2.5 Solution to the SUSY Ward identities in $\mathcal{N} < 4$ SYM

It has recently been shown [102] that the on-shell SUSY Ward identities in $\mathcal{N} = 4$ SYM have a simple solution which presents the N^{K}MHV superamplitude as a sum of SUSY and R-symmetry invariant Grassmann polynomials. Each invariant polynomial is multiplied by a basis amplitude; the number of algebraically independent basis amplitudes needed to determine an N^{K}MHV superamplitude is given by the dimension of the irrep of $SU(n-4)$ corresponding to the rectangular 4-by-K Young diagram. Moreover, the basis amplitudes are characterized precisely by the semi-standard tableaux of this Young diagram. The solutions to the SUSY Ward

identities in $\mathcal{N}=4$ SYM and $\mathcal{N}=8$ supergravity and their applications are reviewed [103]. In this section, we show that the solution from maximally supersymmetric Yang-Mills theory is easily generalized to $\mathcal{N}<4$ SYM.

At the level of superamplitudes, the SUSY Ward identities are equivalent to the statement that the SUSY charges (ϵ denote arbitrary Grassmann-odd spinors)

$$Q^a = \sum_{i=1}^{n} [\epsilon\, i] \frac{\partial}{\partial \eta_{ia}}\,, \;\; \tilde{Q}_a = \sum_{i=1}^{n} \langle \epsilon\, i \rangle\, \eta_{ia}\,, \;\; \text{for } a = 1, 2, \ldots, \mathcal{N} \tag{2.54}$$

annihilate the superamplitude, $Q^a \mathcal{F} = \tilde{Q}_a \mathcal{F} = 0$. Here we have specialized to the Φ-Ψ formulation of the on-shell superspace. Both constraints are solved by the $\delta^{(2\mathcal{N})}$-function, provided momentum conservation is enforced, so the MHV superamplitudes $\mathcal{F}^{\mathcal{N}}_{n,ij}$ in (2.33) are manifestly supersymmetric. The N^{K}MHV superamplitudes have Grassmann degree $\mathcal{N}(K+2)$, so if they are written with an overall factor of $\delta^{(2\mathcal{N})}$, then the $\tilde{Q}_a$ SUSY Ward identities are satisfied, and one must then just ensure that the order $\mathcal{N}K$ polynomial multiplying $\delta^{(2\mathcal{N})}$ is annihilated by Q^a.

Rather than deriving the most general solution, we simply illustrate the procedure in the simple case of the NMHV sector of $\mathcal{N}=1$ SYM. Let lines u, v and w be the Ψ-sector states. We then write the NMHV superamplitude of $\mathcal{N}=1$ SYM as

$$\mathcal{F}_{n,uvw} \;=\; \delta^{(2)}(\tilde{Q}) \sum_{i=1}^{n} f_i\, \eta_i \;=\; -\frac{1}{\langle vw \rangle} \delta^{(2)}(\tilde{Q}) \sum_{i \neq v,w} c_i\, \eta_i\,. \tag{2.55}$$

In the second equality we have used the δ-function to eliminate η_v and η_w from the sum and included a convenient normalization factor $-\langle vw \rangle^{-1}$. The coefficients c_i can be written in terms of the f_i, but their specific relationship is not needed in the following.

The requirement $Q^a \mathcal{F}_{n,uvw} = 0$ now turns into the condition

$$\sum_{i\neq v,w} [\epsilon\, i]\, c_i \;= 0 \;\longrightarrow\; \begin{cases} [r\, s]\, c_s + \sum_{i\neq v,w,r,s} [r\, i]\, c_i \;= 0 \\ [s\, r]\, c_r + \sum_{i\neq v,w,r,s} [s\, i]\, c_i \;= 0 \end{cases} \tag{2.56}$$

We have selected two lines $r, s \neq u, v, w$, and used $\epsilon = r, s$ to extract the two conditions that are now used to eliminate c_r and c_s from (2.55). The result is

$$\mathcal{F}_{n,uvw} \;=\; -\frac{1}{\langle vw\rangle [rs]} \delta^{(2)}(\tilde{Q}) \sum_{i\neq v,w} c_i\, m_{rsi} \tag{2.57}$$

where

$$m_{rsi} = [rs]\, \eta_i + [s\, i]\, \eta_r + [i\, r]\, \eta_s\,. \tag{2.58}$$

Note that $\tilde{Q}\, m_{rsi} = 0$ thanks to the Schouten identity. The polynomial m_{rsi} is familiar from the 3-point anti-MHV superamplitudes.

Now the final step is to identify the c_i as basis amplitudes for the superamplitude $\mathcal{F}_{n,uvw}$. Let us project out negative helicity gluons on lines v and w; this amounts to applying $-\partial_v \partial_w$ to $\mathcal{F}_{n,uvw}$. The derivatives only hit $\delta^{(2)}$ and the result is a factor $-\langle vw\rangle$ that cancels the same factor in the denominator in (2.57). We need to apply one more ∂ to extract a component amplitude. There are two options: 1) applying ∂_u is equivalent to taking state u to be a negative helicity gluon. The derivative produces a factor $[rs]$ from m_{rsu} so the result is

$$c_u \;\sim\; \langle \ldots -_u \ldots -_v \ldots -_w \ldots \rangle \tag{2.59}$$

where dots "$\ldots$" stand for positive helicity gluons. The other option is 2) applying ∂_k for $k \neq u, v, w, r, s$. This designates k as a positive helicity gluino and forces u to

be negative helicity gluino; hence

$$c_k \;\sim\; \langle \lambda_k^+ \ldots \lambda_u^- \ldots -_v \ldots -_w \ldots \rangle \text{ for } k \neq u, v, w, r, s \tag{2.60}$$

We use $\sim$ here to indicate that minus signs arise when the derivative ∂_k is required to move past an odd number of Ψ states. Also, the position of λ_k^+ is only indicated schematically and depends on the value of k relative to u, v, w.

With c_i's identified in (2.59) and (2.60), the result (2.57) is then our manifestly supersymmetric $\mathcal{N} = 1$ NMHV superamplitude. The basis amplitudes are the $n-5$ gluino amplitudes (2.60) and the pure gluon amplitude (2.59). This is a total of $n-4$ basis amplitudes. For $n = 6$ this is the familiar result of [9, 97] that 2 basis amplitudes are required to determine all amplitudes in each of the 3 NMHV sectors. Our basis here is different from that of [9, 97]; we made choices above that fixed our basis. For example, we selected to eliminate η_v and η_w and this fixed the states v and w to be negative helicity gluons. If we had chosen to eliminate the η of a Φ state instead, then that line would have been fixed to be a positive helicity gluino. The choices that lead to (2.57) are equivalent to those made in the $\mathcal{N} = 4$ SYM analysis of [102, 103], so indeed we could just have carried out the truncation procedure of the $\mathcal{N} = 4$ result. We found it useful to carry out the analysis here to illustrate it in the much simpler context of $\mathcal{N} = 1$ SYM.

Going beyond NMHV is easy in $\mathcal{N} = 1$ SYM. Now one needs a polynomial $\sum c_{\{i_k\}} \eta_{i_1} \ldots \eta_{i_K}$. The coefficients $c_{\{i_k\}}$ are fully anti-symmetric in the indices $\{i_k\}$. As above, $\tilde{Q}$-SUSY allow us to fix two Ψ states to be negative helicity gluons and Q-SUSY can fix two Φ-states to be positive helicity gluons. The remaining n–4 states are K Ψ states and $n-4-K$ Φ states. The algebraic basis consists of amplitudes with m pairs $\lambda^+\lambda^-$ on the $n-4$ unfixed lines. There are $\binom{K}{m}$ ways to choose the position of the m λ^-'s and $\binom{n-4-K}{m}$ ways to choose the position of the m λ^+'s. $m = 0$ is the

unique[9] pure gluon amplitude and we can maximally have K pairs $\lambda^+\lambda^-$; hence the total number of N^{K}MHV basis amplitudes is

$$\sum_{m=0}^{K} \binom{K}{m} \binom{n-4-K}{m} = \binom{n-4}{K} . \tag{2.61}$$

This number is also the dimension of the fully anti-symmetric irrep of $SU(n-4)$, whose Young diagram is rectangular 1-by-K.

For $\mathcal{N} = 2$ the analysis can be carried out similarly, now also incorporating the $SU(2)$ R-symmetry. For $\mathcal{N} = 3$ the analysis is completely analogue, and once all possible positions of the Ψ-states are considered the result should be equivalent to the $\mathcal{N} = 4$ SYM result.

2.6 Pure $\mathcal{N} < 8$ SG amplitudes

The formalism for non-maximal SYM can be straightforwardly extended to supergravity amplitudes. Here we outline the procedure for obtaining the $\mathcal{N} < 8$ supergravity MHV amplitudes in the Φ-Ψ formalism.

The on-shell states of the $\mathcal{N} < 8$ supergravity multiplet can be neatly packaged into two superfields Φ, Ψ, with the positive helicity graviton appearing as the leading component of Φ, and the negative helicity graviton at the top of Ψ. Similar to the discussion of embedding the $\mathcal{N} < 4$ SYM multiplets within the maximal one, the two superfields can be obtained from the maximal $\mathcal{N} = 8$ superfield $\Phi_{\mathcal{N}=8}$ as

$$\Phi_{\mathcal{N}<8} = \Phi_{\mathcal{N}=8}\Big|_{\eta_{\mathcal{N}+1},\ldots,\eta_8\to 0}, \quad \Psi_{\mathcal{N}<8} = \int \prod_{i=\mathcal{N}+1}^{8} d\eta_i \Phi_{\mathcal{N}=8} . \tag{2.62}$$

[9] Recall that the Ψ-states are fixed.

The MHV amplitude of the $\mathcal{N}=8$ theory can be conveniently written as

$$\mathcal{A}_n^{\rm MHV} = \frac{M_n(1^-2^-3^+\ldots n^+)}{\langle 12\rangle^8}\delta^{(16)}\left(\sum_{i=1}^n |i\rangle\eta_{ia}\right)$$
$$\text{with}\quad \delta^{(16)}\left(\sum_{i=1}^n |i\rangle\eta_{ia}\right) = \frac{1}{2^8}\prod_{a=1}^8\sum_{i,j}^n\langle ij\rangle\eta_{ia}\eta_{ja}\,, \tag{2.63}$$

where $M_n(1^-2^-3^+\ldots n^+)$ is the MHV graviton n-point amplitude; at tree level it is unaffected by any other fields. To obtain the MHV superamplitudes for the $\mathcal{N}<8$ theories, we choose the ith and jth particles to be in the Ψ multiplet and integrate the $8-\mathcal{N}$ η_i's and η_j's from the $\mathcal{N}=8$ MHV amplitude. Explicitly

$$\begin{aligned}\mathcal{F}^{\mathcal{N}}_{n,ij} &= \int d^{8-\mathcal{N}}\eta_i d^{8-\mathcal{N}}\eta_j \frac{M_n(1^+\ldots i^-\ldots j^-\ldots n^+)}{\langle ij\rangle^8}\,\delta^{(16)}\left(\sum_{k=1}^n |k\rangle\eta_{ka}\right)\Bigg|_{\eta_{\mathcal{N}+1},\ldots,\eta_8\to 0}\\ &= (-1)^{\frac{1}{2}\mathcal{N}(\mathcal{N}-1)}\frac{M_n(1^+\ldots i^-\ldots j^-\ldots n^+)}{\langle 12\rangle^{\mathcal{N}}}\,\delta^{(2\mathcal{N})}\left(\sum_{k=1}^n |k\rangle\eta_{ka}\right)\,.\end{aligned} \tag{2.64}$$

The $\binom{n}{2}$ different choices of i,j for $\mathcal{F}^{\mathcal{N}}_{n,ij}$ are related to each other by simple momentum relabeling.[10] The $\mathcal{N}=7$ formalism provides an alternative encoding of the $\mathcal{N}=8$ supergravity amplitudes; having non-manifest SUSY may be useful in some applications.

2.7 Outlook

We have presented a uniform approach to $\mathcal{N}<4$ SYM amplitudes in terms of a 4d on-shell superspace formulation that allow us to encode the amplitudes into superamplitudes. The tree superamplitudes are simply truncations of the $\mathcal{N}=4$ SYM tree superamplitudes, while at loop level one must take into account the different state sums, for example when evaluating unitarity cuts to reconstruct the loop amplitudes.

A truncation prescription from maximal SUSY to lower SUSY can also be applied

[10] This was not the case for the color-ordered SYM amplitudes.

in other dimensions. We have demonstrated this in 6 dimensions. An interesting by-product of the 6d analysis is the curious relationship between 4d amplitudes of different helicity structures, i.e. in different N^KMHV sectors. This could be interesting to explore further; one would benefit from knowledge of compact explicit expressions for $n>5$-point tree amplitudes in 6d.

An interesting direction is to explore renormalization using on-shell techniques. On general grounds, we might expect the sum of bubble coefficients, which capture the UV divergences, to be proportional to a tree amplitude. From a computational point of view this is not at all obvious, and for N^KMHV amplitudes, this becomes even more non-trivial since even the tree-level amplitudes take more complicated form. It will be interesting to explore if there is a simple on-shell mechanism that guarantees the sum of bubble coefficients to be proportional to a tree amplitude.

Another interesting, and phenomenologically relevant, generalization of our work is to couple matter multiplets to the $\mathcal{N}=1,2$ SYM theories. In that case, it is natural to include a set of Grassmann book-keeping variables for each of the matter multiplets; these can be labeled by the a flavor index A. As a fairly trivial example, consider $\mathcal{N}=4$ SYM as $\mathcal{N}=1$ SYM coupled to three chiral multiplets with $SU(3)$ flavor symmetry. Or as $\mathcal{N}=2$ SYM coupled to two hypermultiplets with $SU(2)$ flavor symmetry. In both cases, the original η's, which are fundamentals of the $SU(4)$ R-symmetry, now transforms under $SU(\mathcal{N})\times SU(4-\mathcal{N})$, i.e. $\mathcal{N}$ η's carry R-symmetry index while the $4-\mathcal{N}$ other ones carry flavor symmetry index. Thus by assigning the original R-index into the reduced R-symmetry index plus flavor indices, one obtains a superamplitude defined on the reduced on-shell superspace plus flavor space. This is of course a trivial rewriting of the $\mathcal{N}=4$ superamplitudes, but it may give a hint about what to expect for $\mathcal{N}=1,2$ SYM with matter. The work [96] together with our results here would be a useful starting point of obtaining explicit results for tree- and loop-level superamplitudes in $\mathcal{N}=1,2$ SYM with matter.

CHAPTER III

One-loop renormalization and the S-matrix

3.1 Introduction and summary of results

In field theory, renormalizability requires that the divergences of the theory at one-loop can be removed by inserting a finite number of counterterms to the corresponding tree diagrams for the same process. We can also understand this renormalizability from the amplitude point of view. In terms of amplitudes, renormalizability implies that the ultraviolet divergence at one-loop must be proportional to the tree-amplitude. As we will see in detail below, this proportionality between tree amplitudes and the bubble coefficients, which encapsulate UV behavior of the theory, in renormalizable theories is cleanly illustrated in pure-scalar QFTs. In ϕ^4 theory, the bubble coefficient of the 4-point one-loop amplitude evaluates to the 4-point tree amplitude 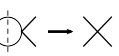 . However, in ϕ^5 theory, the bubble coefficient of the simplest 1-loop amplitude evaluates to a 6-point amplitude 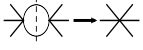 . Similarly, this new 6-point amplitude will generate higher-point amplitudes at higher loops, which is the trademark of a non-renormalizable theory. This observation connects renormalizability with the 1-loop bubble coefficient: in a renormalizable theory, the *sum of bubble coefficients* is

proportional to the tree amplitude

$$\mathcal{C}_2 \equiv \sum_i C_2^i \propto A^{\text{tree}} \,. \tag{3.1}$$

where the sum i runs over all distinct bubble cuts, and we use the calligraphic $\mathcal{C}_2$ to denote the *sum* of the bubble coefficients. This proportionality relation takes a very simple form in (super) Yang-Mills theory with all external lines being gluons [104, 105, 106, 107, 108, 13] (see [20] for detailed discussion)

$$\mathcal{C}_2 = -\beta_0 A_n^{\text{tree}} \,, \qquad \beta_0 = -\left(\frac{11}{3}n_v - \frac{2}{3}n_f - \frac{1}{6}n_s\right) . \tag{3.2}$$

where β_0 is the coefficient of the one-loop beta function and n_v, n_f, n_s are numbers of gauge bosons, fermions and scalars respectively. From the amplitude point of view, eq. (3.2) appears to be a miraculous result as each individual bubble coefficient is now a complicated rational function of Lorentz invariants. For example, it is shown in [20] that for the helicity amplitude $A_4(1^+2^-3^+4^-)$ in $\mathcal{N}$-fold superYang-Mills theory, the bubble coefficients of the two cuts are:

$$\begin{aligned} C_2^{(23,41)} &= -(\mathcal{N}-4)\frac{\langle 12\rangle\langle 34\rangle}{\langle 13\rangle\langle 24\rangle} A_4^{\text{tree}}(1^+2^-3^+4^-) \,, \text{ and} \\ C_2^{(12,34)} &= -(\mathcal{N}-4)\frac{\langle 14\rangle\langle 23\rangle}{\langle 13\rangle\langle 24\rangle} A_4^{\text{tree}}(1^+2^-3^+4^-) \,. \end{aligned}$$

However the sum of these two bubble coefficients is exactly proportional to the tree amplitude: $C_2^{(23,41)} + C_2^{(12,34)} = -(\mathcal{N}-4)A_4^{\text{tree}}(1^+2^-3^+4^-) = -\beta_0 A_4^{\text{tree}}(1^+2^-3^+4^-)$ by the Schouten identity. For an arbitrary n-point amplitude, eq. (3.2) implies cancellation among a large number of these rational functions, in the end yielding a simple constant multiplying A_n^{tree}. The fact that the proportionality in eq. (3.2) holds for any renormalizable theory, hints at possible hidden structures in the sum of the bubble coefficients. In this chapter, we seek to partially expose aspects of such structure.

Following [25, 13], we extract the bubble coefficient by identifying it as the contribution from the pole at infinity in the complex z-plane of a BCFW-deformation [26, 27] of the two internal momenta in the two-particle cut, where the complex deformation is introduced on the internal momenta. As above, we discuss scalar theories as a warm up: here the contributions to bubble coefficients are tractable using Feynman diagrams in the two-particle cut. However, Feynman diagrams become intractable in gauge theories and it is simpler to use helicity amplitudes in the cut. Our results are as follows:

- For scalar ϕ^n theories, we demonstrate that the bubble coefficient only receives contributions from one-loop diagrams that have exactly two loop-propagators. For each diagram, the contribution is proportional to a tree diagram with a new $2(n-2)$-point interaction vertex. Renormalizability requires $n = 2(n-2)$, so this implies the familiar result, $n = 4$.

- In (super) Yang-Mills theory, we study general MHV n-point amplitudes and find that for each 2-particle cut, the bubble coefficient can be separated into four separate terms. Each term stems from the four distinct singularities which appear as the loop momenta become collinear to one of the adjacent external legs, indicated in Fig. 3.1 (a). We show that these singularities localize the Lorentz invariant phase space (dLIPS-) integral to residues at four separate poles.

  Once given in this form, we find: *for each collinear residue in a generic cut, there is a residue in the adjacent cut that has the same form but with opposite sign.* When we sum over all channels, residues stemming from common collinear poles (CCP) in *adjacent* channels cancel pair-wise, as indicated in Fig. 3.1. The sum therefore "telescopes" to four unique terminal poles that come from two terminal cuts. A "terminal cut" contains a 4-point tree amplitude and an n-

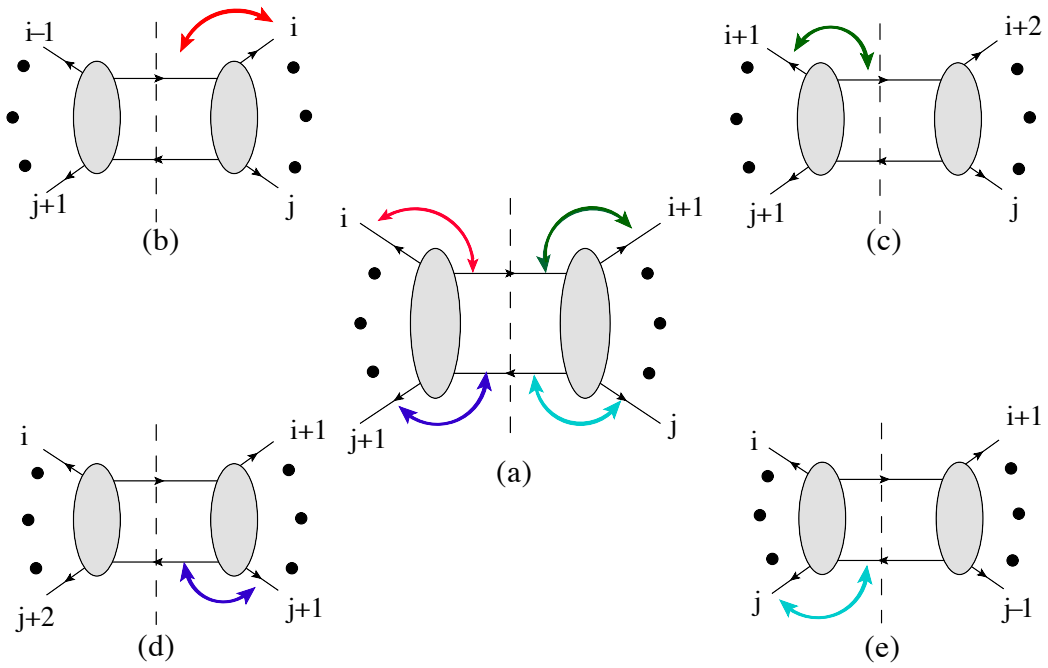

Figure 3.1: A schematic representation of the cancellation of common collinear poles (CCP). The bubble coefficient of the cut in figure (a), receives contributions from the four collinear poles indicated by colored arrows. Each collinear pole is also present in the corresponding adjacent cut indicated in figures (b), (c), (d), and (e) respectively. In the sum of bubble coefficients such contributions cancel in pairs.

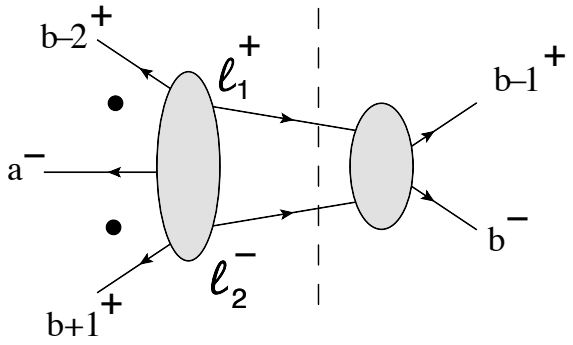

Figure 3.2: The terminal channels that gives non-trivial contribution to the sum of bubble coefficients. Note the helicity configurations of the loop legs of the n-point tree amplitude is identical with the two external legs on the 4-point tree amplitude in the cut.

point tree amplitude on opposite sides of the cut.

- Among these terminal contributions to MHV bubble coefficients further cancellation occurs and the only non-trivial parts come from terminal cuts where the helicity configuration is "preserved". More precisely, these are cuts where the loop helicity configuration is the same as the external lines on the 4-point tree amplitude as shown in Fig. 3.2. Contributions from these terminal cuts, which we call "terminal residues", correspond to a unique point in phase-space where the two on-shell loop momenta become collinear with the two external scattering states in the 4-point sub-amplitude.

  For MHV amplitudes in the Yang-Mills theory, we show that for a given internal helicity configuration of the loop legs, there is a unique terminal cut that has this property and explicit evaluation shows that the residue is $11/6A_n^{\text{tree}}$. Summing the two helicity configuration then gives the desired result, $\mathcal{C}_2 = 11/3A_n^{\text{tree}}$ for the pure Yang-Mills theory, in agreement with eq. (3.2). The relation (3.2) is also derived in the super Yang-Mills theory where $\mathcal{C}_2 = -(\mathcal{N}-4)\mathcal{A}_n^{\text{tree}}$ for $\mathcal{N} = 1, 2$.

- For general N^{k}MHV split-helicity amplitudes in pure Yang-Mills theory, we prove that for each of the two internal helicity configurations the double forward poles in the helicity conserving terminal cuts indeed give $11/6\, A_n^{\rm tree}$. We demonstrate this by using the CSW [109] representation for the N^{k}MHV tree amplitudes appearing in the two-particle cut. The fact that these terminal cuts give the correct proportionality factor indicates that these are indeed the only non-trivial contributions to the sum of bubble coefficients.

This chapter is organized as follows. In section 3.2, we compute the bubble coefficients for theories of self-interacting scalar fields, and rederive the well known renormalizability conditions. We proceed to analyze (super) Yang-Mills theories with emphasis on the cancellation of common collinear poles (CCP) in section 3.3. We will use super Yang-Mills MHV amplitudes as the simplest demonstration of such cancellation. Similar results occur for MHV amplitudes in Yang-Mills as well. In section 3.4, we give an argument for the cancelation of CCP for generic external helicity configurations by showing, using splitting functions of the tree amplitude in the cut, that the residue of collinear poles of the entire cut is indeed shared with an adjacent channel.

3.2 Bubble coefficients in scalar field theories

As a toy model, we consider scalar theories with single interaction vertex $\alpha_k \phi^k$ in this section. It was shown in [13], following previous work in [25], that the bubble coefficient for a given two-particle cut can be calculated as:

$$C_2^{(\mathrm{i,j})} = \frac{1}{(2\pi i)^2} \int d\mathrm{LIPS}[l_1, l_2] \int_{\mathcal{C}} \frac{dz}{z}\, \widehat{S}_n^{(\mathrm{i,j})} \tag{3.3}$$

where (i, j) indicates the momentum channel $P = p_{i+1} + \cdots + p_j$ of the cut as shown in Fig. 3.7, $\widehat{S}_n^{(\mathrm{i,j})} = \hat{A}_L^{\rm tree}(|\hat{l}_1\rangle, |\hat{l}_2]) \, \hat{A}_R^{\rm tree}(|\hat{l}_1\rangle, |\hat{l}_2])$, and $d\mathrm{LIPS}= d^4 l_1 d^4 l_2 \, \delta^{(+)}(l_1^2) \, \delta^{(+)}(l_2^2) \, \delta^4(l_1 +$

$l_2 - P$). Here $\hat{A}^{\text{tree}}_{L,R}$ in (3.3) are the amplitudes on either side of the cut; hats in (3.3) indicate a BCFW shift [26, 27] of the two cut loop momenta:

$$\widehat{l}_1(z) = l_1 + qz, \qquad \widehat{l}_2(z) = l_2 - qz\,, \qquad \text{with } q\cdot q = q\cdot l_1 = q\cdot l_2 = 0\,. \tag{3.4}$$

We integrate the shift parameter z along a contour $\mathcal{C}$ that goes around infinity, which evaluates to the residue at the $z=\infty$ pole of the integrand.[1]

In a scalar theory, the only z dependence in BCFW-shifted tree-amplitudes comes from propagators which depend on one of the two loop momenta. Under BCFW-deformations, propagators of this type scales as $\sim 1/z$ for large-z. Diagrams containing such propagators die-off as $1/z$ or faster. The only non-vanishing contribution to the bubble coefficient comes from diagrams with the two shifted lines on the same vertex [110]. In this case there is neither z-dependence nor dependence on l_1, or l_2 in the double-cut and (3.3) evaluates to

$$C_2^{(\text{i,j})} \;=\; -\frac{1}{2\pi i}\int d\text{LIPS}\; A_L^{\text{tree}} A_R^{\text{tree}} = A_L^{\text{tree}} A_R^{\text{tree}}\,, \tag{3.5}$$

where $A^{\text{tree}}_{L,R}$ are the unshifted amplitudes on either side of the cut as in Fig. 3.4, and we have used $\frac{1}{2\pi i}\int d\text{LIPS}(1) = -1$. The bubble coefficient (3.2) is a sum over all cuts.

Before the general n-point analysis, we first consider explicit examples at 4- and 6-points. For simplicity, we consider these examples with ***color-ordered amplitudes***, where the scalars transform under the *adjoint representation* of some gauge group. We will switch to the *non-color-ordered amplitudes* later for the general analysis.

[1] Simple degree of freedom counting tells us that the double-cut constraint still leaves two undetermined loop parameters. These parameters are neatly encoded within the complex BCFW deformation parameter, z. BCFW shifts of the two-particle cut, null, loop legs naturally allows one to explore all possible on-shell realizations of a double-cut at for a given set of kinematics. However, BCFW deformations of these amplitudes introduce finite-z_P poles within the integrand. These finite-z poles indicate contributions of triple- and quad- cuts of the loop amplitude. To isolate the contribution of the given double-cut, we must evaluate the large-z pole of the deformed double-cut. Hence the contour choice.

At 4-point, the tree amplitude is $A_4^{\rm tree} = \alpha_4$. There are two cuts of the 1-loop 4-point amplitudes, namely the s and t channels. Then (3.5) gives

$$\begin{aligned} \mathcal{C}_2 &= A_4^{\rm tree}(1,2,\hat{l}_1,\hat{l}_2) \times A_4^{\rm tree}(-\hat{l}_2,-\hat{l}_1,3,4) + A_4^{\rm tree}(4,1,\hat{l}_1,\hat{l}_2) \times A_4^{\rm tree}(-\hat{l}_2,-\hat{l}_1,2,3) \\ &= \alpha_4^2 + \alpha_4^2 = 2\alpha_4 A_4^{\rm tree}\,. \end{aligned} \tag{3.6}$$

At 6-point, the tree amplitudes is $A_6^{\rm tree} = \frac{1}{S_{123}} + \frac{1}{S_{612}} + \frac{1}{S_{561}}$. There are six cuts with two shifted lines sitting on one vertex, whose bubble coefficients are listed in the following table

Channel	$\frac{\alpha_4^2}{S_{123}}$	$\frac{\alpha_4^2}{S_{234}}$	$\frac{\alpha_4^2}{S_{345}}$	$\frac{\alpha_4^2}{S_{456}}$	$\frac{\alpha_4^2}{S_{561}}$	$\frac{\alpha_4^2}{S_{612}}$
(12|3456)			1	1		
(23|4561)				1	1	
(34|5612)					1	1
(45|6123)	1					1
(56|1234)	1	1				
(61|2345)		1	1			
$\mathcal{C}_2$	2	2	2	2	2	2

From this table, we see

$$\mathcal{C}_2 = 2\alpha_4^2\left(\frac{1}{S_{123}} + \frac{1}{S_{234}} + \frac{1}{S_{345}} + \frac{1}{S_{456}} + \frac{1}{S_{561}} + \frac{1}{S_{612}}\right) = 4\alpha_4 A_6^{\rm tree}\,. \tag{3.7}$$

For ***non-color-ordered amplitudes***,

$$\mathcal{C}_2 = \frac{3}{2}\alpha_4(n-2)A_n^{\rm tree} = \frac{(n-2)}{2}\beta_0 A_n^{\rm tree}\,, \qquad \beta_0 = 3\alpha_4\,. \tag{3.8}$$

The above result can also be understood by simply noting the fact that the contribution to the bubble coefficient of each one-loop diagram, is in fact proportional to a tree diagram. More precisely:

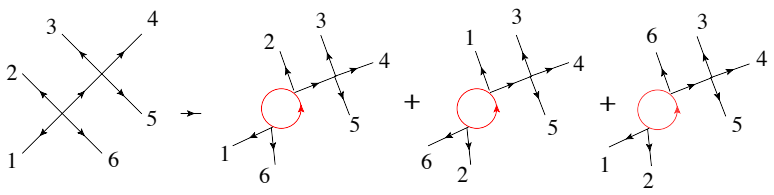

Figure 3.3: For any given tree-diagram in the ϕ^4 theory, each vertex can be blown up into 4-point one-loop subdiagrams in three distinct ways, while preserving the tree graph propagators. Each case contributes a factor of α_4 times the original tree diagram to the bubble coefficient. In this figure we show the example of 6-point amplitude.

- From (3.5), the bubble coefficient for each cut equals the product of the two cut amplitudes. This value coincides with the the tree diagram obtained by replacing the loop with a 4-point contact vertex multiplied by a factor of α_4.

- Reverse the above statement. Each 1-loop diagram with a non-zero bubble coefficient can be obtained by taking a tree diagram and "blowing up" one of the interaction vertices into a one-loop sub-diagram. Taking all distinct tree diagrams and "blowing up" one vertex at a time, produces all relevant one-loop diagrams.

- There are three different ways of "blowing up" each distinct interaction vertex, as indicated in Fig 3.3. Essentially these are the s, t, u channels for a given one-loop four-point amplitude. Each of these one-loop diagrams gives an identical contribution to the overall bubble coefficient.

In ϕ^4-theory, each n-point tree-diagram has $(n-2)/2$ vertices, hence there are $3(n-2)/2$ one-loop diagrams that contribute to the bubble coefficients. This gives $3 \times (n-2)/2$ copies of the original tree diagram. This proves (3.8).

Further, we can re-derive the standard renormalizability criterion for 4-dimensional scalar field theories. The result (3.5) is true for any $\alpha_k \phi^k$ interaction. It suggests that we can think of the bubble coefficient as shrinking the loop to generate a new $2(k-2)$

vertex, which is illustrated in Fig. 3.4. Thus we see that the sum of bubble coefficients for the n-point amplitude is a sum of n-point tree-diagrams that are constructed from the original k-point contact vertex as well as one $2(k-2)$-vertex. As discussed in the introduction, the renormalizability requires that the bubble coefficient is proportional to the tree amplitude. Since the tree-level amplitudes are built from k-point vertices only, the proportionality between bubble coefficient and tree amplitude (3.2) requires

$$2(k-2) = k \quad \rightarrow \quad k = 4\,. \tag{3.9}$$

This reproduces the known result of renormalizability from the power-counting arguments of local perturbative QFT in four dimensions.

Above we studied scalar theories with just a single real scalar field. It is useful to now considered a model with two real scalars ϕ_1 and ϕ_2 and an interaction $\phi_1^2\phi_2^2$. The sum of bubble coefficients for the 4-point amplitude $A_4(\phi_1, \phi_1, \phi_1, \phi_1)$ will be proportional to tree amplitudes with a single ϕ_1^4-vertex. Similarly for ϕ_2. So even if ϕ_1^4 and ϕ_2^4 were not part of the original theory, they were generated at loop-level. Since $A_4^{\text{tree}}(\phi_1, \phi_1, \phi_1, \phi_1)$ vanishes in the original theory, one might now object to the statement that for renormalizable theories (such as this one, of course) the sum of bubble coefficients $\mathcal{C}_2$ is proportional to the tree amplitude. However, the point here is whether the "new" interactions give rise to an infinite tower of other new interactions or not. The former would not be a renormalizable theory. An infinite tower would be generated in the case of ϕ^5 while for our example here, ϕ_1^4 and ϕ_2^4 do not generate any new interactions. So when we say that in a renormalizable theory, the sum of bubble coefficients $\mathcal{C}_2$ is proportional to the tree amplitude, then we regard the tree level theory as the renormalizable theory with generic couplings. In that case, the two-scalar theory does include ϕ_1^4 and ϕ_2^4 and we simply learn from the bubble coefficients that these couplings are renormalized.

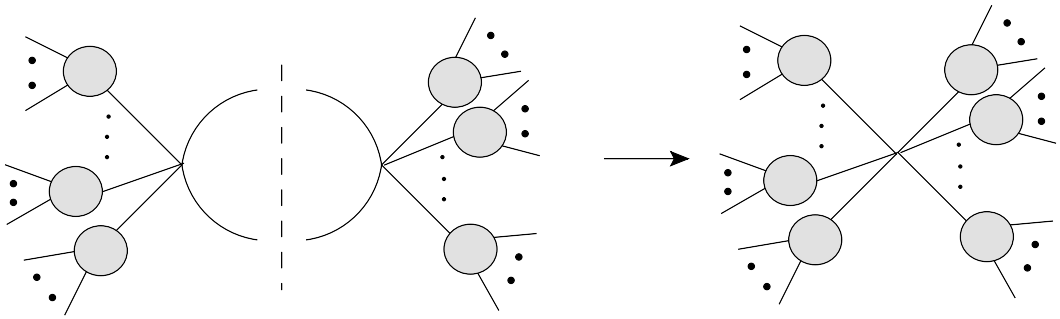

Figure 3.4: For pure ϕ^k theory, the only one-loop diagrams that gives non-trivial contribution to the bubble integrals are those with only two loop propagator. The contribution is simply the product of the tree diagrams on both side of the cut, connected by a new $2(k-2)$ vertex.

We can do a similar analysis to the Yukawa theory with complex scalars. For *pure scalar amplitudes*, Feynman diagrams are tractable and eq. (3.2) renormalizes the coupling constant of the $\phi^2\phi^{*2}$ interaction in the action. For *amplitudes with external fermions*, complications arise due to the z-dependence of external line factors of the fermions and we use helicity amplitudes. As an example we show that eq. (3.2) does not generate the non-renormalizable $\phi^2\psi^2$ or ψ^4 interaction terms, as expected.

3.3 Bubble coefficients for MHV (super) Yang-Mills amplitude

When we consider the (super) Yang-Mills theory, the proportionality between the sum of bubble coefficients and the tree amplitude becomes extremely non-trivial. Here, individual bubble coefficients are generically complicated rational functions of spinor inner products as illustrated for the $\langle\Phi_1\Psi_2\Phi_3\Psi_4\rangle$ case in the introduction. In general, only after summing all the bubble coefficients and repeated use of Schouten identities, will the result reduce to a simple constant times $\mathcal{A}_n^{\text{tree}}$. Thus from the amplitude point of view, this proportionality is a rather miraculous result.

In this section we show that the cancellation is in fact systematic. To see this,

we show that for MHV amplitudes, the dLIPS integration will be localized by the collinear poles of the tree amplitude on both sides of the two-particle cut. For a generic cut, there are four distinct collinear poles involving the loop legs, each of which is also present in an adjacent cut, as illustrated in Fig. 3.5. It can be shown that the residues of these two adjacent cuts on their common collinear pole, $\langle \lambda, i \rangle \to 0$, are exactly equal and with opposite sign. By separating the bubble coefficient into four different terms, corresponding to contributions from four different poles, the cancellation between common collinear poles (CCP) in the sum of bubble coefficients is manifest.

Cancellation stops at "terminal cuts" where a 4-point tree and an n-point tree appear on opposites sides of the cut. The uncanceled terms in these terminal cuts correspond to the residues of collinear poles where the two loop-momenta become collinear with the external momenta of the two external legs on the 4-point amplitude, as illustrated in Fig. 3.6. The sum of these "terminal pole" contributions give

$$-\beta_0 A_n^{\text{tree}}(1^+ \dots a^-, \dots, b^- \dots n^+) = \left(\frac{11}{3} n_v - \frac{2}{3} n_f - \frac{1}{6} n_s\right) \frac{\langle a, b\rangle^4}{\langle 1, 2\rangle \dots \langle i, i+1\rangle \dots \langle n, 1\rangle} \tag{3.10}$$

for MHV amplitudes with $n-2$ positive helicity gluons and negative helicity gluons a and b [111]. In the following, we will demonstrate this for n-point MHV amplitudes in $\mathcal{N} = 1, 2$ super Yang-Mills theory. This systematic cancellation is also present for pure Yang-Mills MHV amplitudes.

Before going further, we pause to note an important distinguishing feature between the bubble coefficients in scalar QFT and in (S)YM. Specifically, the proportionality constant in (super) Yang-Mills is independent of the number of external legs: it is just -β_0, the coefficient of the one-loop beta function. To see this note that for (super)Yang-Mills theory, there are diagrams with one-loop bubbles in the external legs. These massless bubbles do not appear in eq. (1.15), as they are set to zero in

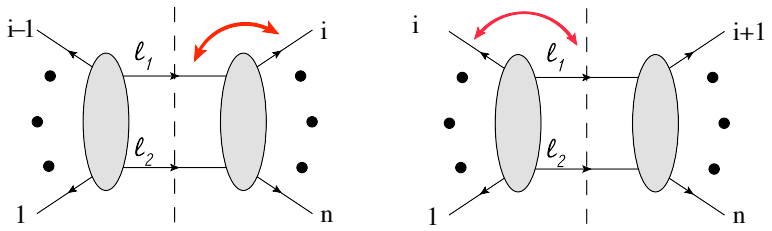

Figure 3.5: An illustration of the cancellation between adjacent channels. The contribution to the bubble coefficient coming from the dLIPS integral evaluated around the collinear pole $\langle l_1 i\rangle \to 0$, indicated by the (red) arrows, of the two diagrams cancels as indicated in eq. (3.28).

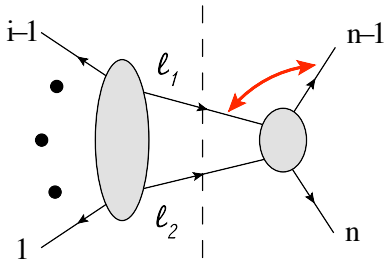

Figure 3.6: The "terminal" pole that contributes to the bubble coefficient. Such poles appear in the two particle cuts that have two legs on one side of the cut and one of the legs has to be a minus helicity. Note that, at this point in phase-space, $l_1 = -p_{n-1}$ and $l_2 = -p_n$.

dimensions regularization, reflecting the cancellation between collinear IR and UV divergences. However, when one is only considering the pure UV divergence of the amplitude, one must take into the account the existence of the UV divergences in the external bubble diagrams, which are simply the same as that of the infrared divergences in the external bubbles, but with a relative minus sign. Thus we have

$$\begin{aligned} A_n|_{\text{UV-div.}} &= \big(\sum C_{\text{bubble}} I_{\text{bubble}}\big)_{\text{UV}} + \text{UV}_{\text{ext. bubbles}} \\ &= \big(\sum C_{\text{bubble}} I_{\text{bubble}}\big)_{\text{UV}} - \text{IR}_{\text{ext. bubbles}} \,. \end{aligned} \tag{3.11}$$

For n-gluon 1-loop amplitudes, the collinear IR divergences take the form [104, 105, 106, 107]

$$\text{IR: } A^{\text{1-loop}}_{n,\text{collinear}} = -\frac{g^2}{(4\pi)^2}\frac{1}{\epsilon}\,\frac{n}{2}\,\beta_0 A^{\text{tree}}_n \,. \tag{3.12}$$

At leading order in $\epsilon \to 0$, the UV divergence is [104, 105, 106, 107]

$$\text{UV: } A^{\text{1-loop}}_{n,\text{UV}} = +\frac{g^2}{(4\pi)^2}\frac{1}{\epsilon}\left(\frac{n-2}{2}\right)\beta_0 A^{\text{tree}}_n \,. \tag{3.13}$$

Thus the bubble coefficients (total UV divergence) in *purely* gluonic one-loop amplitudes are

$$\sum_i C_2^i = A^{\text{1-loop}}_{n,\text{UV}} + A^{\text{1-loop}}_{n,\text{collinear}} = -\beta_0\, A^{\text{tree}}_n = \frac{11}{3}\, A^{\text{tree}}_n \,. \tag{3.14}$$

Scalar field theory lacks these collinear divergences on external legs, and no UV/IR mixing occurs, hence pure scalar bubble coefficients scale with $\frac{n-2}{2}$, the number of interaction vertices. As originally pointed out in [108], this UV/IR mixing continues to hold for YM theories with scalars and fermions. Specifically,

$$\mathcal{C}_2 = \left(\frac{11}{3}n_v - \frac{2}{3}n_f - \frac{1}{6}n_s\right) A^{\text{tree}}_n \,. \tag{3.15}$$

In the explicit on-shell calculations below, we reproduce this result for $\mathcal{N} = 1, 2$ SYM without reference to massless bubbles on external states.

3.3.1 Extracting bubble coefficients in ($\mathcal{N} = 0, 1, 2$ super) Yang-Mills

The bubble coefficient for a given two-particle cut of a one-loop (S)YM amplitude is computed in essentially the same way as for scalar field theory. However, as emphasized in the introduction, unlike the case for scalar QFT extracting this through Feynman diagrams is rather intractable. Roughly in YM this is because BCFW shifts of the two internal on-shell gluon lines in the double-cut introduces z-dependence in local interaction vertices *and* polarization vectors. These difficulties are only amplified in ($\mathcal{N} \neq 0$) SYM.

It is more efficient to directly express the LH- and RH- amplitudes as entire on-shell objects through use of the spinor-helicity formalism. Here the dLIPS integration over allowed on-shell momenta is conveniently converted into an integration over spinor variables which automatically solve the delta functions,

$$\int d^4l_1 d^4l_2\, \delta^{(+)}(l_1^2)\, \delta^{(+)}(l_2^2)\, \delta^4(l_1+l_2-P) g(|l_1\rangle, |l_2\rangle) = \int\limits_{\tilde{\lambda}=\bar{\lambda}} P^2 \frac{\langle \lambda, d\lambda\rangle [\tilde{\lambda}, d\tilde{\lambda}]}{\langle \lambda | P | \tilde{\lambda}]^2} g(|\lambda\rangle, P|\tilde{\lambda}])\,, \tag{3.16}$$

where we have identified $|l_1\rangle = |\lambda\rangle$, $|l_2\rangle = P|\tilde{\lambda}]$, and $\int_{\tilde{\lambda}=\bar{\lambda}}$ indicates we are integrating over the real contour (real momenta). The $\widehat{S}_n^{(\mathrm{i,j})}$ in (3.3) takes the form

$$\widehat{S}_n^{(i,j)} = \widehat{\mathcal{S}}_{n,0}^{(i,j)} \equiv \sum_{\text{state sum}} \hat{A}_L^{\text{tree}}(|\hat{l}_1\rangle, |\hat{l}_2]) \, \hat{A}_R^{\text{tree}}(|\hat{l}_1\rangle, |\hat{l}_2])\,, \tag{3.17}$$

in the Yang-Mills theory. Note that to fully integrate out the bubble coefficients' dependence on the internal lines, we sum over all possible states in the loop.

Further, extraction of simple bubble coefficients is aided by on-shell SUSY.[2] Here

[2]The calculations for the simplest bubble coefficients are simpler in $\mathcal{N} = 1, 2$ SYM than in YM. To see this, compare non-adjacent MHV bubble computations in SYM (subsection 3.3.2).

amplitudes and state sums are promoted to superamplitudes and Grassmann integrals

$$\widehat{S}_n^{(i,j)} = \hat{\mathcal{S}}_{n,\mathcal{N}}^{(i,j)} \equiv \sum_\sigma \int d^{\mathcal{N}}\eta_{l_1} d^{\mathcal{N}}\eta_{l_2}\, \hat{\mathcal{A}}^{\text{tree}}_{L\sigma}\, \hat{\mathcal{A}}^{\text{tree}}_{R\bar{\sigma}}\,, \qquad \mathcal{N} = 1, 2\,, \tag{3.18}$$

where σ labels the different pairs of multiplets that the loop legs, l_1 and l_2, belong to. Following [20], on-shell states are encoded into two separate on-shell superfields, Φ and Ψ, that contain states in the 'positive' and 'negative helicity' sectors. In this language, $\{\sigma\} = \{(\Phi,\Psi),(\Psi,\Phi),(\Phi,\Phi),(\Psi,\Psi)\}$. The $\bar{\sigma}$ is the conjugate configuration of σ.

Crucially, to preserve SUSY the *bosonic* BCFW shift (3.4) must be combined with a *fermionic* shift of the Grassmann variables η^a [89, 13]

$$|\widehat{l_1}(z)\rangle = |l_1\rangle + z|l_2\rangle, \qquad |\widehat{l_2}(z)] = |l_2] - z|l_1]\,, \tag{3.19a}$$

$$\hat{\eta}_{l_2 a} = \eta_{l_2 a} + z\eta_{l_1 a}, \qquad a = 1, \ldots, \mathcal{N} \tag{3.19b}$$

Note the bosonic shift (3.19a) is identical to the shift (3.4), when cast in terms of the spinor-helicty variables; it is referred to as an $[l_2,\, l_1\rangle$-shift.

Combined super-shifts (3.19), of any tree amplitude of the $\mathcal{N} = 4$ SYM fall-off as $1/z$ for large-z. In (S)YM theory with $\mathcal{N} = 0, 1, 2$ supersymmetry, it was shown [20] that the super-BCFW shifts $[\Phi,\Phi\rangle$, $[\Psi,\Phi\rangle$ and $[\Psi,\Psi\rangle$ fall off as $1/z$ at large z while the $[\Phi,\Psi\rangle$ super-shift grows as $z^{3-\mathcal{N}}$ for large-z. For $\mathcal{N} = 0$ pure Yang-Mills, this reduces to the familiar observation that for shifts $[-,-\rangle$, $[-,+\rangle$, and $[+,+\rangle$ the amplitudes fall off as $1/z$, while the $[+,-\rangle$ shifts grow as z^3 [26, 27, 112].

Carrying out the z integral gives

$$C_2^{(i,j)} \;=\; -\frac{1}{2\pi i}\int d\text{LIPS}[l_1, l_2]\, \left[\widehat{\mathcal{S}}_{n,\mathcal{N}}^{(i,j)}\right]_{O(1)\text{ as } z\to\infty}, \; \mathcal{N} = 0, 1, 2\,, \tag{3.20}$$

where $\left[\widehat{\mathcal{S}}_{n,\mathcal{N}}^{(i,j)}\right]_{O(1)\text{ as } z\to\infty}$ is the residue of $\widehat{\mathcal{S}}_{n,\mathcal{N}}^{(i,j)}$ at the $z\to\infty$ pole.

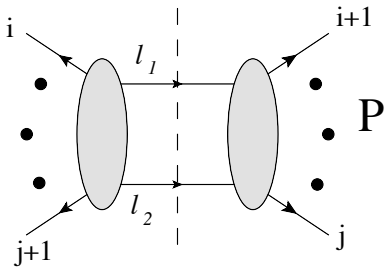

Figure 3.7: A two-particle cut for a generic n-point amplitude.

Double-cuts with internal states $\sigma \in \{(\Phi,\Phi),(\Psi,\Psi)\}$, shown in cut (a) of Fig. 3.8, scale as

$$\widehat{\mathcal{S}}^{[\text{Cut (a)}]}_{n,\mathcal{N}} \;\sim\; \frac{1}{z}\times\frac{1}{z} \;\sim\; \frac{1}{z^2} \text{ as } z\to\infty\,. \tag{3.21}$$

Cuts of this type do not contribute to the bubble coefficient. On the other hand, for $\sigma \in \{(\Phi,\Psi),(\Psi,\Phi)\}$, such as cut (b) in Fig. 3.8, always involve a shift that acts as $[\Psi,\Phi\rangle$ on one subamplitude and as $[\Phi,\Psi\rangle$ on the other. This gives

$$\widehat{\mathcal{S}}^{[\text{Cut (b)}]}_{n,\mathcal{N}} \;\sim\; \frac{1}{z}\times z^{3-\mathcal{N}} \;\sim\; z^{2-\mathcal{N}} \text{ as } z\to\infty\,. \tag{3.22}$$

Note immediately that there are no bubble contributions for $\mathcal{N}=4$, reflecting the UV-finiteness of $\mathcal{N}=4$ SYM. The large z-behavior indicates that there can be non-vanishing $O(1)$-terms and hence bubble contributions for $\mathcal{N}=0,1,2$ SYM. This is consistent with the known non-vanishing 1-loop β-functions in these theories.

3.3.2 MHV bubble coefficients in $\mathcal{N}=1,2$ super Yang-Mills theory

It was shown in ref. [20], that for the MHV amplitudes in $\mathcal{N}=1,2$ super Yang-Mills theory, the $\mathcal{O}(z^0)$ part of the BCFW-shifted two-particle cut $\widehat{\mathcal{S}}^{(i,j)}_{\{a,b\},\mathcal{N}}$ is given

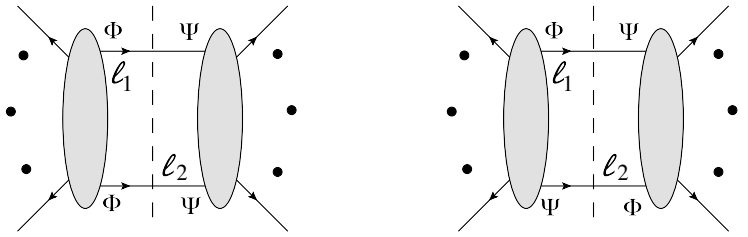

(a) Cuts with $\sigma \in \{(\Phi,\Phi),(\Psi,\Psi)\}$ die-off, and have no pole, as $z \to \infty$.

(b) Cuts with $\sigma \in \{(\Phi,\Psi),(\Psi,\Phi)\}$ have a pole at $z \to \infty$ ($\mathcal{N} = 0, 1, 2$).

Figure 3.8: Illustration of two internal helicity configurations of the cut loop momenta.

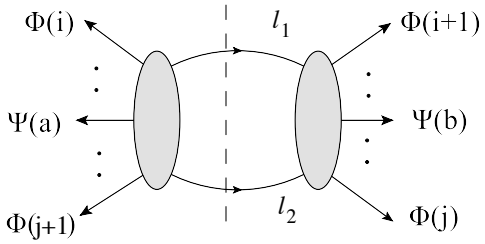

Figure 3.9: The two-particle cut that gives $\widehat{\mathcal{S}}^{(i,j)}_{\{a,b\},\mathcal{N}}$.

by:

$$\widehat{\mathcal{S}}^{(i,j)}_{\{a,b\},\mathcal{N}}\Big|_{\mathcal{O}(z^0)} = (\mathcal{N}-4)\mathcal{A}^{\text{tree}}_n \frac{\langle i,i+1\rangle\langle j,j+1\rangle}{\langle a,b\rangle^2} \frac{\langle a,\lambda\rangle^2\langle b,\lambda\rangle^2}{\langle j,\lambda\rangle\langle j+1,\lambda\rangle\langle i,\lambda\rangle\langle i+1,\lambda\rangle}, \quad (3.23)$$

where $\{a,b\}$ indicates the positions of the two sets of external negative-helicity states (within the Ψ multiplets). We have set $|l_2\rangle = |\lambda\rangle$. Since $\widehat{\mathcal{S}}^{(i,j)}_{\{a,b\},\mathcal{N}}$ is purely holomorphic in λ, we can straightforwardly rewrite the dLIPS integral (3.16) as a total derivative, and the bubble coefficient is given as:

$$\begin{aligned} C^{(i,j)}_{2\ \{a,b\}} &= \frac{-1}{2\pi i}\oint_{\tilde{\lambda}=\overline{\lambda}} P^2_{i+1,j}\frac{\langle\lambda,d\lambda\rangle[\tilde{\lambda},d\tilde{\lambda}]}{\langle\lambda|P_{i+1,j}|\tilde{\lambda}]^2}\ \widehat{\mathcal{S}}^{(i,j)}_{\{a,b\},\mathcal{N}}\Big|_{\mathcal{O}(z^0)} \\ &= \frac{1}{2\pi i}\oint_{\tilde{\lambda}=\overline{\lambda}} \langle\lambda,d\lambda\rangle d\tilde{\lambda}_{\dot{\alpha}}\frac{\partial}{\partial\tilde{\lambda}_{\dot{\alpha}}}\left[\frac{[\tilde{\lambda}|P_{i+1,j}|\alpha\rangle}{\langle\lambda|P_{i+1,j}|\tilde{\lambda}]\langle\lambda,\alpha\rangle}\ \widehat{\mathcal{S}}^{(i,j)}_{\{a,b\},\mathcal{N}}\Big|_{\mathcal{O}(z^0)}\right], \quad (3.24) \end{aligned}$$

where $|\alpha\rangle$ is a reference spinor. In this section, for convenience, we label the bubble coefficients $C_{2\,\{a,b\}}^{(i,j)}$ in the same way as the two-particle cut $\widehat{\mathcal{S}}_{\{a,b\},\mathcal{N}}^{(i,j)}$. There are two kinds of poles inside the total derivative, the four collinear poles of $\widehat{\mathcal{S}}_{\{a,b\},\mathcal{N}}^{(i,j)}$ in eq. (3.23) and the spurious pole $1/\langle\lambda,\alpha\rangle$. The spurious pole can be simply removed by the $\langle a,\lambda\rangle^2\langle b,\lambda\rangle^2$ factor in the numerator of eq. (3.23) if we choose the auxiliary spinor $|\alpha\rangle$ to be $|a\rangle$ or $|b\rangle$. Thus with this choice of reference spinor, the contributions to the bubble coefficient come solely from the collinear poles in $\widehat{\mathcal{S}}_{\{a,b\},\mathcal{N}}^{(i,j)}|_{\mathcal{O}(z^0)}$.

From eq. (3.23) we see that there are four collinear poles in $\widehat{\mathcal{S}}_{\{a,b\},\mathcal{N}}^{(i,j)}\big|_{\mathcal{O}(z^0)}$, each corresponding to λ becoming collinear with the adjacent external lines of the cut. Careful readers might find this puzzling, as the MHV tree amplitudes on both side of the cut only have collinear poles of the form $\langle l_1,i\rangle$, $\langle l_1,i+1\rangle$, $\langle l_2,j\rangle$ and $\langle l_2,j+1\rangle$. Recalling that here $|\lambda\rangle=|l_2\rangle$, one would instead expect collinear poles of the form, $[\lambda|P_{i+1,j}|i\rangle$, $[\lambda|P_{i+1,j}|i+1\rangle$, $\langle\lambda,j\rangle$ and $\langle\lambda,j+1\rangle$. The resolution is that eq. (3.23) is obtained by shifting $\langle l_1,i\rangle\to\langle l_1,i\rangle+z\langle l_2,i\rangle$ and expanding around $z\to\infty$, thus introducing the $\langle l_2,i\rangle$ poles:

$$\frac{1}{\langle l_1(z),i\rangle}\bigg|_{z\to\infty}=\frac{1}{z\langle l_2,i\rangle}+\mathcal{O}(\frac{1}{z^2}) \tag{3.25}$$

Since these poles originated from $\langle l_1(z),i\rangle$, we will abuse the terminology, as well as the figures, and still refer to them as collinear poles.[3]

To better track the contributions of the collinear poles, we rewrite the integrand as follows:

$$\begin{aligned}\widehat{\mathcal{S}}_{\{a,b\},\mathcal{N}}^{(i,j)}\bigg|_{\mathcal{O}(z^0)} &= (\mathcal{N}-4)\mathcal{A}_n^{\text{tree}}\frac{\langle a,\lambda\rangle\langle b,\lambda\rangle^2\langle i,i+1\rangle}{\langle a,b\rangle^2\langle i,\lambda\rangle\langle i+1,\lambda\rangle}\left(\frac{\langle a,j+1\rangle}{\langle j+1,\lambda\rangle}-\frac{\langle a,j\rangle}{\langle j,\lambda\rangle}\right)\\ &= (\mathcal{N}-4)\mathcal{A}_n^{\text{tree}}\frac{\langle a,\lambda\rangle\langle b,\lambda\rangle^2\langle j,j+1\rangle}{\langle a,b\rangle^2\langle j,\lambda\rangle\langle j+1,\lambda\rangle}\left(\frac{\langle a,i+1\rangle}{\langle i+1,\lambda\rangle}-\frac{\langle a,i\rangle}{\langle i,\lambda\rangle}\right)\end{aligned} \tag{3.26}$$

[3]In fact, this is not as much of an abuse as it may seem. Note that evaluating the pole at $z\to\infty$ is equivalent to evaluating the pole at the origin minus the poles at finite z. The former would be a true collinear pole, while the latter would be a collinear pole with shifted l_1.

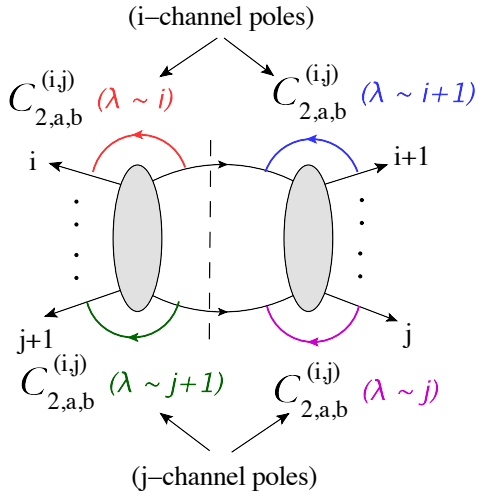

Figure 3.10: A graphical representation of eq. (3.28). The bubble coefficient of a given channel is separated into four terms, each having a different collinear pole as the origin of the holomorphic anomaly that gives a non-zero dLIPS integral. The 4-contributions can be grouped into two channels, the i- and the j-channel.

where the two equivalent representations focus on different adjacent collinear poles in the parentheses. The representation in eq. (3.26) allows us to compute the bubble coefficient in a manner that manifests the relation between collinear poles in adjacent channels. With auxiliary spinor $|\alpha\rangle$ in eq. (3.24) chosen to be $|a\rangle$, the bubble coefficient is

$$C^{(i,j)}_{2\,\{a,b\}} = C^{(i,j)}_{2\,\{a,b\}}(\lambda \sim j+1) \;+\; C^{(i,j)}_{2\,\{a,b\}}(\lambda \sim j) \;+\; C^{(i,j)}_{2\,\{a,b\}}(\lambda \sim i+1) \;+\; C^{(i,j)}_{2\,\{a,b\}}(\lambda \sim i)\,.$$

Here we have used $(\lambda \sim j)$ to indicate the contribution from the collinear pole $\langle \lambda, j\rangle$. For convenience, we will refer to $(\lambda \sim j)$ and $(\lambda \sim j+1)$ collinear poles as "j-channel poles", and $(\lambda \sim i)$ and $(\lambda \sim i+1)$ poles as "i-channel poles". A graphical illustration of eq. (3.28) is given in Fig. 3.10

Before proceeding, we point out a very important observation. Comparing the

first line of eq. (3.26) for $\widehat{\mathcal{S}}^{(i,j)}_{\{a,b\},\mathcal{N}}|_{\mathcal{O}(z^0)}$ with that for $\widehat{\mathcal{S}}^{(i,j-1)}_{\{a,b\},\mathcal{N}}|_{\mathcal{O}(z^0)}$,

$$\widehat{\mathcal{S}}^{(i,j-1)}_{a,b}\Big|_{\mathcal{O}(z^0)} = (\mathcal{N}-4)\mathcal{A}^{\text{tree}}_n \frac{\langle a,\lambda\rangle\langle b,\lambda\rangle^2\langle i,i+1\rangle}{\langle a,b\rangle^2\langle i,\lambda\rangle\langle i+1,\lambda\rangle}\left(\frac{\langle a,j\rangle}{\langle j,\lambda\rangle}-\frac{\langle a,j-1\rangle}{\langle j-1,\lambda\rangle}\right),$$

we immediately see that *terms containing the common collinear pole of the two adjacent cuts, i.e.* $1/\langle j,\lambda\rangle$*, are exactly the same but, crucially, have opposite signs.* This applies to all of the other terms in eq. (3.26), each having a counterpart in the adjacent channel, as illustrated in Fig. 3.1.

At this point, one is tempted to conclude that the contribution to the bubble coefficient from common collinear channels cancels. However there is one subtlety. In eq. (3.24), besides $\widehat{\mathcal{S}}^{(i,j)}_{\{a,b\},\mathcal{N}}|_{\mathcal{O}(z^0)}$, there is an extra factor in the total derivative that depends on the total momentum of the two-particle cut, $P_{i+1,j}$, which will be distinct for the adjacent cuts. Luckily these distinct factors become identical on the common collinear pole:

$$\frac{[\tilde{\lambda}|P_{i+1,j}|a\rangle}{\langle\lambda|P_{i+1,j}|\tilde{\lambda}]\langle\lambda,a\rangle}\Big|_{\langle\lambda,j\rangle=[\tilde{\lambda},j]=0} = \frac{[\tilde{\lambda}|P_{i+1,j-1}|a\rangle}{\langle\lambda|P_{i+1,j-1}|\tilde{\lambda}]\langle\lambda,a\rangle}\Big|_{\langle\lambda,j\rangle=[\tilde{\lambda},j]=0}, \tag{3.27}$$

where $|_{\langle\lambda,j\rangle=[\tilde{\lambda},j]=0}$ indicates that the loop momentum is evaluated in the limit where it is collinear with j.[4] Because the extra factors are identical on the common collinear pole (CCP), we now conclude that the contribution of the CCP to the bubble coefficient indeed cancels between adjacent channels. This can also be concretely checked against the result from the direct evaluation of the dLIPS integral:

$$\begin{aligned} C^{(i,j-1)}_{2\,\{a,b\}}(\lambda\sim j) &= -(\mathcal{N}-4)\mathcal{A}^{\text{tree}}_n \frac{\langle i,i+1\rangle}{\langle a,b\rangle^2}\frac{\langle a|P_{i+1,j-1}|j]}{\langle j+1|P_{i+1,j-1}|j]}\frac{\langle a,j\rangle\langle b,j\rangle^2}{\langle i,j\rangle\langle i+1,j\rangle}, \\ C^{(i,j)}_{2\,\{a,b\}}(\lambda\sim j) &= (\mathcal{N}-4)\mathcal{A}^{\text{tree}}_n \frac{\langle i,i+1\rangle}{\langle a,b\rangle^2}\frac{\langle a|P_{i+1,j}|j]}{\langle j|P_{i+1,j}|j]}\frac{\langle a,j\rangle\langle b,j\rangle^2}{\langle i,j\rangle\langle i+1,j\rangle}. \end{aligned}$$

[4]Since the contour of the dLIPS integral is taken to be real, $\tilde{\lambda}=\bar{\lambda}$, the collinear pole $1/\langle\lambda,j\rangle$ freezes the the loop momenta to satisfy $\langle\lambda,j\rangle=[\tilde{\lambda},j]=0$.

Adding these two equations, we find

$$\begin{aligned} & C^{(i,j)}_{2\,\{a,b\}}(\lambda \sim j) + C^{(i,j-1)}_{2\,\{a,b\}}(\lambda \sim j) \\ &= (4-\mathcal{N})\mathcal{A}_n^{\text{tree}} \frac{\langle i, i+1\rangle}{\langle a, b\rangle^2} \frac{\langle a, j\rangle\langle b, j\rangle^2}{\langle i, j\rangle\langle i+1, j\rangle} \left[-\frac{\langle a|P_{i+1,j}|j]}{\langle j|P_{i+1,j}|j]} + \frac{\langle a|P_{i+1,j-1}|j]}{\langle j|P_{i+1,j-1}|j]} \right] = 0, \end{aligned} \tag{3.28}$$

thus verifying our claim.

Since the four collinear poles for a generic two-particle cut are shared by four different adjacent channels as shown in Fig. 3.1, this immediately leads to the result that although the bubble coefficient for a generic two-particle cut is given by complicated rational functions *in summing over all two-particle cuts there is a pairwise cancellation of CCP, and thus a majority of bubble coefficient do not contribute to the final result.*

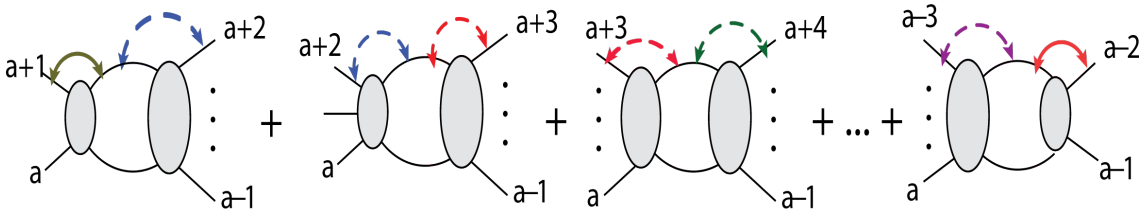

Figure 3.11: A schematic representation of the cancellation of CCP for adjacent MHV amplitude for SYM. Each colored arrow represents a collinear pole that contributed to the bubble coefficient. Pairs of dashed arrows in the same color cancel. Only those represented by the solid arrows one on the two ends remain; they are the only non-trivial contribution to the overall bubble coefficient.

The cancellation of CCP in adjacent channels leads to systematic cancellation in the sum of bubble coefficients, and the sum telescopes. However, there are "terminal cuts" which contain unique poles that are not canceled. Below, we demonstrate that these so-called "terminal poles" constitute the sole contribution to the overall bubble coefficient. First we focus on the simplest case, namely the two Ψ-lines a, b are adjacent. The general case is treated in section. 3.3.2.2.

3.3.2.1 Adjacent MHV amplitudes

We consider split-helicity MHV amplitudes where the Ψ lines a, b are adjacent, i.e. $b = a - 1$. The systematic cancellation is illustrated in Fig. 3.11, where the dashed lines indicate pairs of CCP that cancel in the sum. Note that there are no contributions from the collinear poles where the loop leg is collinear with the Ψ-lines, a and $a - 1$. This is because the residues of such poles are zero, as can be seen in eq. (3.26) and explicitly checked in eq. (3.28). One immediately sees that the summation is reduced to the two terminal poles. These are identified as poles in two-particle cuts with a 4-point tree amplitude on one side (and an n-point tree on the other), where the two loop momenta become collinear with the two external legs of the 4-point tree amplitude. A straightforward evaluation of the contribution of these two terminal poles yields the result for the sum of all bubble coefficients:

$$\begin{aligned} \mathcal{C}_{2\,\{a,a-1\}} &= C^{(a-3,a-1)}_{2\,\{a,a-1\}}(\lambda \sim a-2) + C^{(a+1,a-1)}_{2\,\{a,a-1\}}(\lambda \sim a+1) \\ &= -(\mathcal{N}-4)\mathcal{A}^{\text{tree}}_n + 0 = -\beta_0 \mathcal{A}^{\text{tree}}_n \,. \end{aligned} \tag{3.29}$$

with $\beta_0 = (\mathcal{N} - 4)$. Note that $C^{(a+1,a-1)}_{2\,\{a,a-1\}}(\lambda \sim a + 1) = 0$ is a result of our choice of reference spinor $|\alpha\rangle = |a\rangle$ in deriving eq. (3.28). Were we to make the other choice, $|\alpha\rangle = |b\rangle = |a - 1\rangle$, we would instead have $C^{(a-3,a-1)}_{2\,\{a,a-1\}}(\lambda \sim a - 2) = 0$ and $C^{(a+1,a-1)}_{2\,\{a,a-1\}}(\lambda \sim a + 1) = -\beta_0 \mathcal{A}^{\text{tree}}_n$.

For example take the six-point MHV amplitude with legs 1 and 6 to be negative helicity lines. The sum of bubble coefficient is given as

$$\begin{aligned} \mathcal{C}_{2\,\{1,6\}} &= C^{(2,6)}_{2\,\{1,6\}}(\lambda \sim 2) + C^{(2,6)}_{2\,\{1,6\}}(\lambda \sim 3) + C^{(3,6)}_{2\,\{1,6\}}(\lambda \sim 3) + C^{(3,6)}_{2\,\{1,6\}}(\lambda \sim 4) \\ &\quad + C^{(4,6)}_{2\,\{1,6\}}(\lambda \sim 4) + C^{(4,6)}_{2\,\{1,6\}}(\lambda \sim 5) \\ &= C^{(2,6)}_{2\,\{1,6\}}(\lambda \sim 2) + C^{(4,6)}_{2\,\{1,6\}}(\lambda \sim 5) = -\beta_0 \mathcal{A}^{\text{tree}}_n \,. \end{aligned} \tag{3.30}$$

We see that there are two pairs of common collinear poles, $\lambda \sim 3$ and $\lambda \sim 4$. The pairs cancel each other in the sum and one arrives at the two terminal pole which evaluates to the desired result. The cancellation is illustrated in Fig. 3.12.

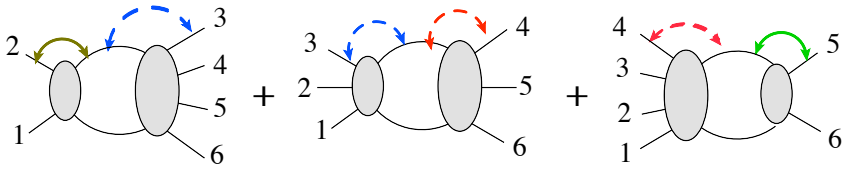

Figure 3.12: A schematic representation of the cancellation of CCP for adjacent six-point MHV amplitude. The dashed lines are common collinear poles which cancel pairwise.

Thus we have demonstrated that one of the terminal poles vanishes and *the sum of bubble coefficients for adjacent MHV amplitude, with arbitrary n, is given by a single terminal pole!*

3.3.2.2 Non-adjacent MHV amplitudes

The above case with the two Ψ-lines a, b being adjacent is simple because the j-channel poles (see below (3.26)) were absent. For MHV amplitudes with a, b being non-adjacent, the j-channel poles are now non-zero, and all the four collinear poles contribute in eq. (3.28). The sum of bubble coefficients can be conveniently separated into a summation of the i-channel poles, and a summation of the j-channel poles. Cancellation of CCP in both channels again reduces the summation to the terminal poles. For simplicity, we set $a = 1$ and $1 < b$. We denote the terminal cut in the summation of i-channel poles by i_t, j, and similarly for the terminal cut of the j-channel poles by i, j_t. The contribution of these uncancelled poles are identified as:

- i-channel:

$$C_{2\ \{1,b\}}^{(i_t,j)}(\lambda \sim i_t) \qquad \begin{array}{ll} \text{for } \ j = n, & i_t = 2 \\ \text{for } \ b \leq j < n, & i_t = 1 \end{array} ,$$

$$C^{(i_t,j)}_{2\ \{1,b\}}(\lambda\sim i_t+1) \qquad \begin{array}{ll} \text{for } \ j=b, & i_t=b-2 \\ \text{for } \ b<j\leq n, & i_t=b-1 \end{array} \ ,$$

- j-channel:

$$C^{(i,j_t)}_{2\ \{1,b\}}(\lambda\sim j_t) \qquad \begin{array}{ll} \text{for } \ i=b-1, & j_t=b+1 \\ \text{for } \ 1\leq i<b-1, & j_t=b \end{array} \ ,$$

$$C^{(i,j_t)}_{2\ \{1,b\}}(\lambda\sim j_t+1) \qquad \begin{array}{ll} \text{for } \ i=1, & i_t=n-1 \\ \text{for } \ 1<i\leq n-1, & j_t=n \end{array} \ .$$

In identifying the terminal poles, one has to take into account that, when summing over the i-channel poles, the value of j affects the possible values that i can take (and vice versa for the summation of j-channel poles). As discussed in section 3.3.2.1, the collinear poles where the loop momenta becomes collinear with a Ψ-line have vanishing residues. In the present context, this refers to $(\lambda\sim 1)$ and $(\lambda\sim b)$. Thus there are only four contributing terms in the sum of bubble coefficients

$$\mathcal{C}_{2\,\{1,b\}}=C^{(2,n)}_{2\ \{1,b\}}(\lambda\sim 2)+C^{(b-2,b)}_{2\ \{1,b\}}(\lambda\sim b-1)+C^{(b-1,b+1)}_{2\ \{1,b\}}(\lambda\sim b+1)+C^{(1,n-1)}_{2\ \{1,b\}}(\lambda\sim n)\,. \tag{3.31}$$

Extracting the corresponding expressions from eq. (3.28), one finds that the first and last terms vanish. This is again due to the choice of reference spinor $|\alpha\rangle=|a\rangle$. [5] Thus the only contributions to the sum of bubble coefficients come from $C^{(b-1,b+1)}_{2\ \{1,b\}}(\lambda\sim b+1)$

[5] If we were to use the other choice, $|\alpha\rangle=|b\rangle$, we would arrive at the result that the second and third terms of eq. (3.31) vanish. This apparent dependence of a particular double-cut on the reference spinor is illusory: with care, one can cancel the full $|\alpha\rangle$-dependence from each individual bubble coefficient. However, this cancellation comes at the expense of the manifest $a\leftrightarrow b$ symmetry present in the uncanceled form. This asymmetry causes one term to seemingly vanish while the other gives the full bubble-coefficient.

and $C^{(b-2,b)}_{2\,\{1,b\}}(\lambda \sim b-1)$, which sum to

$$\begin{aligned}\mathcal{C}_{2\,\{1,b\}} &= C^{(b-1,b+1)}_{2\;\{1,b\}}(\lambda \sim b+1) + C^{(b-2,b)}_{2\;\{1,b\}}(\lambda \sim b-1) \\ &= (4-\mathcal{N})\mathcal{A}_n^{\text{tree}} \frac{\langle 1,b-1\rangle\langle b,b+1\rangle + \langle b-1,b\rangle\langle 1,b+1\rangle}{\langle b-1,b+1\rangle\langle 1,b\rangle} = -(\mathcal{N}-4)\mathcal{A}_n^{\text{tree}} \end{aligned} \tag{3.32}$$

This agrees with eq. (3.2) with $\beta_0 = (\mathcal{N}-4)$.

In conclusion, for both adjacent and non-adjacent MHV amplitudes in $\mathcal{N} = 1, 2$ super Yang-Mills theory, the cancellation of CCP in the sum of bubble coefficients implies that *for n-point (non-)adjacent MHV amplitudes, only (two) one term in the sum of bubble coefficients gives a non-trivial contribution* $\beta_0\mathcal{A}_n^{\text{tree}}$. Thus the on-shell formalism achieves eq. (3.2) in a systematic and simple way.

3.3.3 MHV bubble coefficients for pure Yang-Mills

The observed structure of cancellations for $\mathcal{N} = 1, 2$ super Yang-Mills theory is present in pure Yang-Mills as well. However, it is more envolved to derive this since the $\mathcal{O}(z^0)$ part of the BCFW-shifted two-particle cut contains higher order collinear poles. Nevertheless, adjacent channels again share these higher order CCP, and their contribution to the sum of bubble coefficient also cancels. The cancellation of CCP renders the summation down to the terminal poles which evaluate to $11/6A_n^{\text{tree}}$. We spare the reader from the detailed derivation of this, here we would like to give a brief discussion on the nature of the terminal poles in pure Yang-Mills theory.

As discussed above, the terminal cuts are those where there is a 4-point tree amplitude on one side of the two-particle cut. The un-cancelled terminal poles can be identified as the poles that arise when the loop momenta become collinear with the pair of external legs of this 4-point tree amplitude. For pure Yang-Mills, summing over the internal helicity configurations *before* taking the dz and dLIPS integrals obscures the nature of the cancellation.

Additional structure reveals itself if we *first* evaluate the contributions to the bubble-coefficient for a given set of internal states, aka gluon helicity configuration, and *then* sum over internal states/helicities. Specifically, these double-forward terminal poles are non-zero only when the internal helicities of the loop legs leaving the n-point tree on one side of the cut, match with the helicities of the pair of external lines in the 4-point tree on the other side of the cut (see Fig. 3.13). These "helicity preserving" double-poles (which will henceforth be called "double-forward poles") give the entire bubble coefficient.

Consider the internal helicity configuration (l_1^+, l_2^-) as shown in Figs. 3.8(b) and 3.13. There are two "helicity preserving" terminal-cuts: diagram (a) and (b) in Fig.3.13. Choosing the reference spinor $|\alpha\rangle = |a\rangle$, diagram (b) vanishes, and diagram (a) evaluates to $11/6 A_n^{\text{tree}}$. If one were to make the other choice for the reference spinor, $|\alpha\rangle = |b\rangle$, we would instead have diagram (a) in Fig 3.13 vanishing, and diagram (b) giving $11/6 A_n^{\text{tree}}$. In fact, the helicity preserving property of the contributing poles can also be seen for the $\mathcal{N} = 1, 2$ super Yang-Mills theory, where one simply substitute the $+$ and $-$ helicity in the previous discussions with Ψ and Φ lines. This fact was obscured previously as the different internal multiplet configurations were summed to obtain the simple form of the two-particle cut in eq. (3.23).

Thus we conclude that in the pure Yang-Mills theory *the sum of bubble coefficients is simply given by the contribution of terminal poles where the helicity configuration is preserved, and where the loop momenta become collinear with the pair of external legs within the 4-point amplitude.* For simplicity we will call these double-forward poles, due to the nature of the kinematics. Now we present a general argument for the cancellation of CCP.

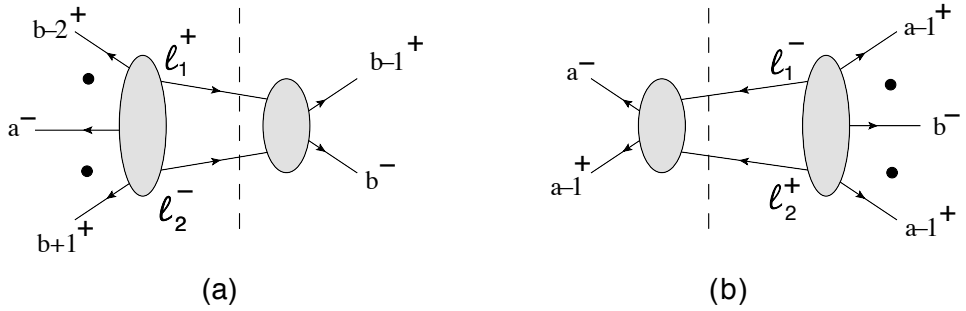

Figure 3.13: The two terminal cuts for a given helicity configuration for the loop legs. For the choice of reference spinor $|\alpha\rangle = |a\rangle$ only diagram (a) is non vanishing. If one instead choose $|\alpha\rangle = |b\rangle$, then it is diagram (b) that gives the non-trivial contribution.

3.4 Towards general cancellation of common collinear poles

In the above, we have shown that eq. (3.2) can be largely attributed to the fact that the bubble coefficient for a given cut, secretly shares the same terms with it's four adjacent cuts, leading to systematic cancellations between them. We have proven this for n-point MHV amplitudes in both $\mathcal{N} = 1, 2$ super Yang-Mills. One can also consider adjoint scalars and fermions minimally coupled to gluons. Since at one-loop, we can separate contributions from different spins inside the loop as

$$\begin{aligned} \text{fermions} \quad &\to \quad \big(\ \mathcal{N}=1 \text{ SYM}\ \big) \ - \ \big(\ \text{YM}\ \big) \\ \text{scalar} \quad &\to \quad \big(\ \mathcal{N}=2 \text{ SYM}\ \big) \ - \ \big(\ \mathcal{N}=1 \text{ SYM}\ \big) \ - \ \big(\ \text{fermions}\ \big)\,, \end{aligned} \tag{3.33}$$

proof of cancellation of CCP for each of the theories (for MHV scattering) on the RHS of eq. (3.33), implies that such cancellation occurs for each spin individually.

We would like to show this holds for N^{k}MHV amplitudes. Unfortunately, for N^{k}MHV amplitudes, multi-particle poles of the tree amplitude on both side of the cut contributes to the bubble coefficient, and the analysis becomes more complicated. However, we believe that the cancellation between CCP persists for arbitrary helicity

configuration. As an indication, we demonstrate that the residues of CCP for adjacent cut always have the same form and opposite signs, for any helicity configuration.

Collinear limits of tree level amplitudes in Yang-Mills theory, with $k_a = zk_P,\ k_b = (1-z)k_P$, factorize as

$$A_n^{\text{tree}}\left(...,a^{\lambda_a},b^{\lambda_b},...\right) \to \sum_{\lambda=\pm} \text{Split}_{-\lambda}^{\text{tree}}\left(z,a^{\lambda_a},b^{\lambda_b}\right) A_{n-1}^{\text{tree}}\left(...,P^{\lambda},...\right) \tag{3.34}$$

where the factor $\text{Split}_{-\lambda}^{\text{tree}}\left(z,a^{\lambda_a},b^{\lambda_b}\right)$ is the gluon splitting amplitude. Its form for various helicity configurations are given by [111, 113]:

$$\begin{aligned}
\text{Split}_{-}^{\text{tree}}\left(a^-,b^-\right) &= 0 \\
\text{Split}_{-}^{\text{tree}}\left(a^+,b^+\right) &= \frac{1}{\sqrt{z(1-z)}\langle ab\rangle} \\
\text{Split}_{+}^{\text{tree}}\left(a^+,b^-\right) &= \frac{(1-z)^2}{\sqrt{z(1-z)}\langle ab\rangle} \\
\text{Split}_{-}^{\text{tree}}\left(a^+,b^-\right) &= -\frac{z^2}{\sqrt{z(1-z)}[ab]}\,.
\end{aligned} \tag{3.35}$$

Without loss of generality, we focus on the common collinear pole, depicted in Fig. 3.5, in adjacent cuts $(1...i-1|i...n)$ and $(1...i|i+1...n)$. In other words, we study the collinear region with $l_1^{(i)} = \tau^{(i)}k_i$ and $l_1^{(i+1)} = \tau^{(i+1)}k_i$.[6] The two integrands become

$$\begin{aligned}
&\text{Cut}_{(1..i-1|i..n)}\big|_{\langle l_1 i\rangle} \\
&\quad = A_{i+1}\left(1,...,i-1,\tau^{(i)}i,l_2^{(i)}\right)\sum_{\lambda=\pm}\text{Split}_{-\lambda}^{\text{tree}}A_{n-i+2}\left(-l_2^{(i)},(1-\tau^{(i)})i,i+1,...,n\right)\ ,
\end{aligned} \tag{3.36}$$

[6] Strictly speaking, the condition $\langle l_1 i\rangle = 0$ only requires $\lambda_{l_1} \sim \lambda_i$. However since the dLIPS integration contour is along $\tilde{\lambda} = \overline{\lambda}$, the condition is equivalent to $l_1 \sim k_i$.

for cut $(1...i-1|i...n)$, and

$$\begin{aligned}&\mathrm{Cut}_{(1..i|i+1...n)}\big|_{\langle l_1 i\rangle} \qquad (3.37)\\ &= \sum_{\lambda=\pm} \mathrm{Split}^{\mathrm{tree}}_{-\lambda} A_{i+1}\left(1,...,(1+\tau^{(i+1)})i, l_2^{(i+1)}\right) A_{n-i+2}\left(-l_2^{(i+1)}, -\tau^{(i+1)}i, i+1,...,n\right)\ ,\end{aligned}$$

for cut $(1...i|i+1...n)$. The parameter $\tau^{(i)}$ can be fixed by the on-shell condition on $l_2^{(i)}$ since in the cut $(1...i-1|i...n)$, $l_2^{(i)} = P_{i-1} + \tau^{(i)} k_i$. Similar constraints from the cut $(1...i|i+1...n)$ fix $\tau^{(i+1)}$. This leads to

$$\begin{aligned}&\tau^{(i)} = \frac{P_{i-1}^2}{2k_i \cdot P_{i-1}} = \tau^{(i+1)} + 1\\ \rightarrow\ \ &l_2^{(i)} = P_{i-1} + \tau^{(i)} k_i = P_i + \tau^{(i+1)} k_i = l_2^{(i+1)}\,.\end{aligned}$$

Substituting these results back into eq. (3.36) and eq. (3.37), we see that the product of tree amplitudes are identical at their common collinear pole. Furthermore, identifying the kinematic variables in the splitting amplitudes for each cut as:

$$\begin{aligned}&(1...i-1|i...n): \qquad k_a = k_i,\ k_b = -\tau^{(i)} k_i,\ z = \frac{1}{1-\tau^{(i)}}\\ &(1...i|i+1...n): \qquad k'_a = k_i,\ k'_b = \tau^{(i+1)} k_i,\ z' = \frac{1}{1+\tau^{(i+1)}} = \frac{1}{\tau^{(i)}}\end{aligned}$$

we see that the splitting amplitudes for the two cuts are identical with a relative minus sign.[7]

The above analysis confirms that eq. (3.36) and eq. (3.37) are indeed identical up to a minus sign. Thus the residue of the *entire two-particle cut* on the common collinear poles, are identical and with opposite sign. This, however, does not directly lead to a proof of cancellation of CCP for bubble coefficients. This is because to extract the bubble coefficient, the two-particle cut must be translated into a total derivative, in order for one to use holomorphic anomaly generated by the collinear

[7]For consistency, we take the positive branch of the square root.

poles to isolate the dLIPS integral. It is not guaranteed that after translating the two cuts into a total derivative form, the residues on the CCP are still equal and opposite.

3.5 Conclusion and future directions

In this chapter, we study the proportionality between the sum of bubble coefficients and the tree amplitude, which is required for renormalizability. For theories where Feynman diagram analysis is tractable, such as scalar theory and pure scalar amplitudes of Yukawa theory, we find that the bubble coefficient only receives contributions from a small class of one-loop diagrams. The contribution of each diagram is proportional to a tree-diagram, and hence summing over all one-loop diagrams that give non-trivial contributions, is equivalent to summing over all tree-diagrams. This trivially leads to the proportionality condition. For some amplitudes of the Yukawa theory, the large-z behavior of the two-particle cut becomes intractable via Feynman diagrams, and we instead use helicity amplitudes. By requiring the sum to be proportional to tree amplitude, we find the known renormalization conditions derived from power counting analysis.

For (super)Yang-Mills theory, we show that the bubble coefficient for each cut can be organized in terms of their origin as collinear poles, which are responsible for the nontrivial contribution to the dLIPS integration. This representation manifests the cancellation of the residues of common collinear poles (CCP), which telescopes the sum of bubble coefficient down to terminal cuts. These terminal cuts correspond to cuts where there is a 4-point tree amplitude on one side of the cut. Further cancellation occurs for these terminal terms: for a given helicity configuration of the loop legs, there is a unique terminal term that contribute to the sum of bubble coefficients. *This term arises from the double-forward pole of the four-point tree amplitude in a terminal cut, helicities of the two external legs in the 4-point tree amplitude, match those of the loop legs.* Thus the proportionality constant is determined by only two

terms, one for each choice of states running in the loop, for arbitrary n-point MHV amplitude, and gives $11/6 + 11/6 = 11/3$ times A_n^{tree} for pure Yang-Mills theory, and $(\mathcal{N} - 4)$ times $\mathcal{A}_n^{\text{tree}}$ for $\mathcal{N} = 1, 2$ super Yang-Mills theory.

For more generic external helicity configurations, it will be interesting to see how the contributions from the multi-particle poles cancel with each other. As an indication for the existence of such cancellation, we explicitly prove that the forward pole contributions to the bubble coefficient in the Yang-Mills theory in the terminal cuts, with a given helicity configuration of the internal lines, indeed give 11/6 times the tree amplitude for split helicity n-point N^{k}MHV amplitudes. This implies heavy cancellations among contributions to the bubble coefficient from all other channels.

An even more interesting example would be gravity. It is well known that gravity is one-loop finite [114]. The bubble coefficient is non-vanishing for generic two-particle cut and hence massive cancellation must occur. The lack of color ordering for gravity amplitudes indicate the pole structure that gives rise to the non-trivial contributions for the dLIPS integral is more complicated than Yang-Mills, and presumably new cancellation mechanism would be required even for MHV amplitudes.

CHAPTER IV

Symmetries of Holographic Super-Minimal Models

4.1 Introduction

The AdS_3/CFT_2 correspondence is an attractive testing-ground for gauge/gravity dualities. On the gravity side, three-dimensional gravity possesses significantly fewer degrees of freedom than higher-dimensional analogues due to the fact that tensor fields with spin greater than one do not have any bulk degrees of freedom, but their dynamics are localized at the boundary. This fact even allows an exact computation of the partition function of the theory for the pure gravity case [115]. Therefore, gravity on AdS_3 spacetime is much simpler than its higher-dimensional counterparts. On the field theory side, the Virasoro algebra of the two-dimensional CFT imposes an infinite number of constraints on the dynamics, and this drastically facilitates the analysis of the theory.

Among various versions of the AdS_3/CFT_2 duality, the recently proposed duality [57] between pure gravity coupled to massless higher-spin gauge fields with two massive scalars in an AdS_3 background and the large-N limit of 2d $\mathcal{W}_N$ minimal models is of great interest. The key ingredients in this conjecture are the higher-spin fields. It has been shown that in a d-dimensional background with constant negative curvature, an infinite tower of massless higher-spin fields can be introduced with consistent interactions [116, 117]. Since the proposed CFT dual to this higher-spin theory, the

W_n-minimal model, is in principle solvable at any value of the 't Hooft coupling, this duality is supposed to be easier to study than the previously conjectured duality between higher-spin gravity in AdS_4 and the 3d $O(N)$ vector model [31]. Therefore, it serves as a useful tool to understand the connection between the large-N limit of gauge theory and gravity beyond the pure gravity limit [57].

Several nontrivial checks have been done on the duality: including the matching of the symmetries [66, 67, 68, 118], the spectra [57], the partition functions [65] and the correlation functions [119, 120]. Further studies of spacetime geometry in higher-spin gravity can be found in [121, 77, 86, 76] and of the higher-spin AdS_3/CFT_2 correspondence in [122, 123, 124, 125].

In this chapter, we discuss the $\mathcal{N} = 2$ supersymmetric version of the duality [61], with a particular emphasis on the correspondence of the symmetries. In the supersymmetric case, it was proposed in [61] that $\mathcal{N} = 2$ higher-spin supergravity in AdS_3 based on the higher-spin algebra $shs[\lambda]$ [126, 127] is dual to the 't Hooft limit of the $\mathcal{N} = 2$ $\mathbb{C}P^n$ minimal model defined in [128] by the coset

$$\frac{\widehat{SU(n+1)}_k \times \widehat{SO(2n)}_1}{\widehat{SU(n)}_{k+1} \times \widehat{U(1)}_{n(n+1)(k+n+1)}} \,. \tag{4.1}$$

The 't Hooft limit is defined by[1]

$$n,\ k \to \infty, \quad \lambda = \frac{n}{2(n+k)} \ :\ \text{fixed} \,. \tag{4.2}$$

Although supersymmetry is not necessary to take full control of the theories on both sides, it is still very useful to consider the supersymmetric version of the duality. First, with supersymmetry, calculations are easier thanks to the presence of more symmetry constraints. Secondly, there are new objects we can study such as chiral

[1]We follow the convention of [126, 127] for $shs[\lambda]$. Their λ is different from λ in [61] by a factor of two, and that is why there is two in the denominator of the following equation.

rings and spectral flow, which provide a larger stage to study the duality. Finally, the higher-spin theory is expected to be related to string theory in the small string tension limit [66]. So, to make a connection to superstring theory, it is very natural to consider the supersymmetrized version of the duality.

The chapter is organized as follows. In section 2, we review the Chern-Simons formulation of $\mathcal{N} = 2$ higher-spin supergravity based on the higher-spin algebra $shs[\lambda]$ [126, 127]. In section 3, we discuss the asymptotic symmetry of the higher-spin supergravity theory and obtain the non-linear super-$W_\infty[\lambda]$ algebra.[2] In section 4, we introduce the chiral superalgebra, denoted by $\mathcal{SW}_n$, of the dual $\mathbb{C}\mathrm{P}^n$ minimal model and provide two non-trivial checks on the correspondence of the symmetries. Finally, we conclude with a discussion in section 5.

4.2 Higher-spin supergravity as a Chern-Simons Theory

In [129, 130], it was shown that classical three-dimensional Einstein gravity in an AdS_3 background can be reformulated as an $SL(2,\mathbb{R})_L \times SL(2,\mathbb{R})_R$ Chern-Simons theory. Define the $SL(2,\mathbb{R})_L \times SL(2,\mathbb{R})_R$ connections

$$A = (\omega^a + \frac{1}{\ell} e^a) J^a \,, \qquad \tilde{A} = (\omega^a - \frac{1}{\ell} e^a) \tilde{J}^a \,, \qquad a = 1, 2, 3 \,, \tag{4.3}$$

where ℓ is the radius of AdS_3, J^a are generators of $SL(2,\mathbb{R})_L$, and $\tilde{J}^a$ are generators of $SL(2,\mathbb{R})_R$. The Einstein-Hilbert action can then be written as

$$I_{EH} = I_{CS}(A) - I_{CS}(\tilde{A}) \,, \qquad I_{CS}(A) = \frac{k_{CS}}{4\pi} \int_{\mathcal{M}} \mathrm{Tr}(A \wedge dA + \frac{2}{3} A \wedge A \wedge A) \,, \tag{4.4}$$

[2] This non-linear super-$W_\infty[\lambda]$ algebra should be distinguished from the linear super-W_∞ algebra obtained in [126, 127]. In the rest of the chapter, the super-$W_\infty[\lambda]$ algebra means the non-linear version unless otherwise mentioned.

where the Chern-Simons level k_{CS} is related to the Newton's constant in AdS_3 spacetime as

$$k_{CS} = \frac{\ell}{4G_3}\,, \tag{4.5}$$

and the trace Tr is taken over gauge indices throughout the chapter. One can show that e^a and ω^a behave in the same way as the vielbein and spin connection, respectively, in Einstein gravity on-shell [130]. This formulation is extended to particular types of higher-spin theories with and without supersymmetry in [131]. In this section, we discuss how to extend this Chern-Simons formulation to $\mathcal{N}=2$ higher-spin supergravity based on $shs[\lambda]$.

4.2.1 Supersymmetric higher-spin algebra $shs[\lambda]$

The $\mathcal{N}=2$ higher-spin supergravity theory is formulated as a Chern-Simons theory based on the super higher-spin algebra $shs[\lambda]$. We start with a briefly review of this algebra.

$shs[\lambda]$ is a one-parameter family of Lie superalgebras [126, 127]. It admits $\mathcal{N}=2$ supersymmetry and consists of two sets of bosonic generators $L_m^{(s)\pm}$ as well as two sets of fermionic generators $G_r^{(s)\pm}$. s is an integer and satisfies $s\geq 2$ for $L_m^{(s)+}$ and $G_r^{(s)\pm}$, and $s\geq 1$ for $L_m^{(s)-}$. m takes values in the integers satisfying $|m|<s$ and r is a half-integer satisfying $|r|<s-1$. Here, we only make two points:[127]

- The $shs[\lambda]$ algebra contains an $Osp(1,2)$ algebra generated by $L_m^{(2)+}$ and $G_r^{(2)+}$ as a subalgebra. $(L_m^{(s)+}, G_r^{(s)+})$ and $(L_m^{(s)-}, G_r^{(s+1)-})$ form $\mathcal{N}=1$ supermultiplets of the $Osp(1,2)$ subalgebra with $SL(2)$ spins $(s, s-1/2)$ and $(s, s+1/2)$, respectively. The $Osp(1,2)$ generators $L_m^{(2)+}$ and $G_r^{(2)+}$, together with $L_m^{(1)-}$ and $G_r^{(2)-}$ generate an $Osp(2,2)$ subalgebra, where $L_0^{(1)-}$ corresponds to the R-charge of the superalgebra.

- The $shs[\lambda]$ algebra can be truncated at a special value of λ. For $\lambda=1/4$, the

+ sector (of generators with a "+" index) and − sector decouple, and the + sector reduces to the $\mathcal{N}=1$ superalgebra, which was used to construct $\mathcal{N}=1$ higher-spin supergravity in [132, 131].

In the following, we relabel the generators in + sector and − sector as

$$L_m^{(s)} = L_m^{(s)+}, \qquad L_m^{(s+1/2)} = L_m^{(s)-}, \qquad G_r^{(s)} = G_r^{(s)+}, \qquad G_r^{(s+1/2)} = G_r^{(s+1)-} \tag{4.6}$$

for notational simplicity.

The $\mathcal{N}=2$ higher-spin supergravity theory is formulated as a Chern-Simons theory based on the gauge group $shs[\lambda]_L \times shs[\lambda]_R$.[3] The $shs[\lambda]_L \times shs[\lambda]_R$ super-connections are given by

$$\Gamma = \sum_{s,m} A_m^{(s)} L_m^{(s)} + \sum_{s,r} \psi_r^{(s)} G_r^{(s)} \,, \qquad \tilde{\Gamma} = \sum_{s,m} \tilde{A}_m^{(s)} \tilde{L}_m^{(s)} + \sum_{s,r} \tilde{\psi}_r^{(s)} \tilde{G}_r^{(s)} \,, \tag{4.7}$$

where A and $\tilde{A}$ are expressed using (particular linear combinations of higher-spin analogues of) vielbeins and spin connections as

$$A_m^{(s)} = \omega_m^{(s)} + \frac{1}{\ell} e_m^{(s)} \,, \qquad \tilde{A}^{(s)} = \omega_m^{(s)} - \frac{1}{\ell} e_m^{(s)} \,, \tag{4.8}$$

where ℓ is the AdS radius and the action is obtained as a difference of two Chern-Simons actions

$$I_{SHS} = I_{CS}(\Gamma) - I_{CS}(\tilde{\Gamma}) \,. \tag{4.9}$$

With the help of the equations of motion, $e^{(2)}$ and $\omega^{(2)}$ are identified with the vielbein and spin connection and $\psi^{(2)}$, $\tilde{\psi}^{(2)}$ are identified as two sets of gravitinos.

[3] There can be several ways to embed the gravity sector into the higher-spin algebra. We take $L_m^{(2)}$, $L_m^{(3/2)}$, $G_r^{(2)}$ and $G_r^{(3/2)}$ as the generators associated with the $\mathcal{N}=2$ supergravity.

4.2.2 Boundary conditions, constraints and gauge fixing

Now that the action is obtained, we discuss how one defines a consistent theory based on this action. First of all, in order for the variational principle to be well-defined, the variation of the action should not depend on the variation of the field at the boundary. The variation of the action is

$$\delta I_{CS} = -\frac{k_{CS}}{4\pi}\int_{\partial\mathcal{M}} \mathrm{Tr}(\Gamma_+\delta\Gamma_- - \Gamma_-\delta\Gamma_+) - \frac{k_{CS}}{4\pi}\int_{\mathcal{M}} (\text{e.o.m.}) \ , \tag{4.10}$$

where we use coordinates (t, ρ, θ) to parameterize the spacetime manifold $\mathcal{M}$, and define $x^{\pm} = t/\ell \pm \theta$. One can set the boundary contribution to zero by fixing Γ_- on the boundary:

$$\Gamma_-\big|_{\partial\mathcal{M}} = 0 \ . \tag{4.11}$$

We call this "minimal" boundary condition to distinguish it from the boundary condition we impose in the next section from which we obtain the asymptotic algebra super-$W_\infty[\lambda]$.

We also need to fix the gauge degrees of freedom. We choose the gauge fixing conditions, following [67], as

$$\Gamma_\rho = b^{-1}(\rho)\partial_\rho b(\rho) \ , \tag{4.12}$$

where $b(\rho)$ is an arbitrary, but fixed, function of the radial coordinate ρ and takes values in the group $shs[\lambda]$. In the later sections, we take $b(\rho)$ to be

$$b(\rho) = e^{\rho L_0^{(2)}} \tag{4.13}$$

for $shs[\lambda]$ Chern-Simons theory, but the discussions in this section are independent of the choice of $b(\rho)$. In the action, there is no time derivative of A_t, implying that

there is a constraint. The variation of the action with respect to A_t yields

$$\partial_\rho \Gamma_\theta + [\Gamma_\rho, \Gamma_\theta] = 0 \ . \tag{4.14}$$

This can be solved uniquely by

$$\Gamma_\theta = b^{-1}(\rho)\gamma(t,\theta)b(\rho) \ , \tag{4.15}$$

where $\gamma(t,\theta)$ is an arbitrary function of t and θ. Therefore, the degrees of freedom are reduced to $\gamma(t,\theta)$ by the gauge fixing and constraints.

4.2.3 Global symmetry

We are ready to discuss the global symmetry of the theory with our minimal boundary condition (4.11). The global symmetry is defined to be the residual symmetry after the gauge fixing that leaves the boundary condition (4.11) and the gauge fixing condition (4.12) invariant. The invariance of the gauge fixing condition (4.12), $\delta\Gamma_\rho = 0$, implies that the gauge transformation parameter Λ should satisfy

$$\partial_\rho \Lambda + [\Gamma_\rho, \Lambda] = 0 \ . \tag{4.16}$$

This can be solved uniquely by

$$\Lambda = b^{-1}(\rho)\lambda(t,\theta)b(\rho) \ . \tag{4.17}$$

Now, the invariance of the boundary condition (4.11) imposes a further constraint

$$\partial_- \Lambda\big|_{\partial\mathcal{M}} = 0 \ . \tag{4.18}$$

This implies that

$$\lambda(t,\theta) = \lambda(x^+) \ . \tag{4.19}$$

So, the time dependence of the transformations are fixed by the θ dependence. Thus the gauge degrees of freedom are completely fixed to $\lambda(x^+)$.

What we are interested in is to discuss the global algebra generated by these transformations. Note that the global charge of this algebra is given by [133, 134]

$$Q[\Lambda] = -\frac{k_{CS}}{2\pi}\int_{\partial\Sigma} d\theta \ \mathrm{Tr}(\Lambda\Gamma_\theta) \ , \tag{4.20}$$

where Σ is a constant time slice. From our boundary conditions and gauge fixing, we have (4.15) and (4.17), which lead to

$$Q[\Lambda] = -\frac{k_{CS}}{2\pi}\int_{\partial\Sigma} d\theta \ \mathrm{Tr}(\lambda(\theta)\gamma(\theta)) \ . \tag{4.21}$$

¿From this expression, given that the symmetry transformation parameters are $\lambda(\theta)$, the generators of the global symmetries are $\gamma(\theta)$ and their algebra is obtained by considering the symmetry transformations of $\gamma(\theta)$. Namely,

$$\delta\gamma(\theta) = \{Q,\gamma(\theta)\} = -\frac{k_{CS}}{2\pi}\int d\theta' \ \lambda(\theta')\{\gamma(\theta'),\gamma(\theta)\} \ , \tag{4.22}$$

where $\{\cdot,\cdot\}$ is the Poisson bracket. $\delta\gamma(\theta)$ on the left hand side can be derived from the original gauge transformation of Γ_θ. To see this, note that the gauge transformation of Γ_θ is given by

$$\begin{aligned} \delta\Gamma_\theta &= \partial_\theta\Lambda - [\Gamma_\theta,\Lambda] \\ &= b^{-1}(\rho)(\partial_\theta\lambda(\theta) - [\gamma(\theta),\lambda(\theta)])b(\rho) \ . \end{aligned} \tag{4.23}$$

Then, by comparing this with $\delta\Gamma_\theta = b^{-1}\delta\gamma(\theta)b$, one obtaines

$$\delta\gamma(\theta) = \partial_\theta\lambda(\theta) - [\gamma(\theta), \lambda(\theta)] \ . \tag{4.24}$$

If one expands $\gamma(\theta)$ in terms of the generators of the gauge group T^a as $\gamma(\theta) = \sum \gamma^a(\theta)T^a$, then the transformations (4.24) can be reproduced by the following Poisson bracket:

$$\{\gamma^a(\theta), \gamma^b(\theta')\} = \frac{2\pi}{k_{CS}}\left[K^{ab}\delta'(\theta-\theta') - f^{ab}{}_c\gamma^c(\theta)\delta(\theta-\theta')\right] \ , \tag{4.25}$$

where K^{ab} is the inverse of the Killing form K_{ab} and $f^{ab}{}_c$ are the structure constants of the gauge group. One can expand $\gamma^a(\theta)$ in modes as

$$\gamma^a(\theta) = \frac{1}{k_{CS}}\sum_{n=-\infty}^{\infty}\gamma^a_m e^{-im\theta} \ . \tag{4.26}$$

Then, we get the affine Kac-Moody algebra associated with the gauge group:

$$\{\gamma^a_m, \gamma^b_n\} = imk_{CS}K^{ab}\delta_{m+n,0} - f^{ab}{}_c\gamma^c_{m+n} \ . \tag{4.27}$$

Note that this result is true for general gauge group. As a summary of this section, we reviewed how higher spin supergravity is realized as a Chern-Simons theory and the global symmetry of the theory with the minimal boundary condition (4.11). In the next section, we impose a more restrictive boundary condition and see the super-$W_\infty[\lambda]$ is realized as the asymptotic symmetry.

4.3 Super-$W_\infty[\lambda]$ algebra as the asymptotic symmetry

The goal of this section is to obtain the non-linear super-$W_\infty[\lambda]$ as the asymptotic symmetry by imposing additional boundary conditions. Super-$W_\infty[\lambda]$ is a higher-spin

extension of the $\mathcal{N}=2$ super-Virasoro algebra. The boundary condition to obtain the super-Virasoro algebra from the affine Kac-Moody algebra is known in the literature [135, 136], and we use the same boundary condition and extend their analysis to higher spin cases.

4.3.1 Boundary condition for super-$W_\infty[\lambda]$ algebra

In order to obtain the super-$W_\infty[\lambda]$ symmetry, we, impose a boundary condition:[4]

$$(\Gamma - \Gamma_{AdS_3})\big|_{\partial\mathcal{M}} = \mathcal{O}(1) \ , \tag{4.28}$$

in addition to the minimal boundary condition (4.11), where Γ_{AdS} is the gauge field configuration corresponding to the global AdS geometry and is given explicitly by

$$\Gamma_{AdS_3} = \left[e^{\rho}L_1^{(2)} + \frac{1}{4}e^{-\rho}L_{-1}^{(2)}\right] d\theta + b(\rho)^{-1}\partial_\rho b(\rho) d\rho + \Gamma_t dt \ . \tag{4.29}$$

where $b(\rho)$ is the same as that in (4.13). The boundary condition (4.28) imposes constraints on $\gamma(\theta)$. To see that, we expand $\gamma(\theta)$ in terms of the $shs[\lambda]$ generators as

$$\gamma(\theta) = \sum_{s,m} a_m^{(s)}(\theta) L_m^{(s)} + \sum_{s,r} \psi_r^{(s)}(\theta) G_r^{(s)} \ . \tag{4.30}$$

This, together with (4.12) and (4.15), fixes the super-connection as:

$$\Gamma = b^{-1}(\rho)\left(a_m^{(s)}L_m^{(s)} + \psi_r^{(s)}G_r^{(s)}\right) b(\rho) d\theta + b^{-1}(\rho)\partial_\rho b(\rho) d\rho + \Gamma_t dt \ , \tag{4.31}$$

where the repeated indices are summed over. Here, the Γ_t is equal to Γ_θ at the boundary due to the boundary condition (4.11), though in the bulk, there is no restriction on it. This time component, however, is expected not to affect the global

[4]This boundary condition (4.28) has been extensively studied in three-dimensional gravity and its supersymmetric extensions [137, 138, 139, 135, 136].

symmetry of the theory because the charge integral (4.21) is taken on a constant time slice, and the dependence on the time component of the gauge field disappear. Therefore, we will not discuss Γ_t in the rest of the chapter.

The $shs[\lambda]$ commutation relations read

$$[L_0^{(2)}, L_m^{(s)}] = -mL_m^{(s)}, \qquad [L_0^{(2)}, G_r^{(s)}] = -rG_r^{(s)} \ . \tag{4.32}$$

which reflect the fact that the commutator of any generator with $L_0^{(2)}$ just gives the conformal weight of the generator. Together with the Baker-Campbell-Hausdorff formula and (4.13), (4.31) can be rewritten as

$$\Gamma = \left(e^{m\rho} a_m^{(s)} L_m^{(s)} + e^{\rho r} \psi_r^{(s)} G_r^{(s)}\right) d\theta + b^{-1}(\rho)\partial_\rho b(\rho) d\rho + \Gamma_t dt \ . \tag{4.33}$$

The boundary condition (4.28) implies that, at the boundary $\rho \to \infty$, the difference between (4.33) and (4.29) is order one. This imposes the following constraints:

$$a_1^{(2)} = 1 \ , \tag{4.34}$$

$$a_m^{(s)} = 0 \qquad (s \geq 3,\ m > 0) \ , \qquad \psi_r^{(s)} = 0 \quad (i > 0) \ . \tag{4.35}$$

The constraints (4.35) are first class because the Poisson bracket, given in (4.25), between any pair of them closes into a linear combination of (4.35).[5] Therefore, each of these first class constraints generates a gauge symmetry. These $(\lfloor s \rfloor - 1) + (\lfloor s \rfloor - 1)$ gauge symmetries are fixed by the following $(\lfloor s \rfloor - 1) + (\lfloor s \rfloor - 1)$ gauge fixing conditions

$$a_m^{(s)} = 0 \quad (-\lfloor s \rfloor + 1 < m \leq 0), \qquad \psi_r^{(s)} = 0 \quad (\lfloor -s \rfloor + 3/2 < m < 0) \ , \tag{4.36}$$

where $\lfloor \cdot \rfloor$ is the "floor" function. These conditions are second class because generally

[5]Note that a Poisson bracket between positive frequency modes close into a linear combination of positive frequency modes.

commutators $[a_m^{(s)}, a_{-m+1}^{(s)}]$ and $\{\psi_r^{(s)}, \psi_{-r+1}^{(s)}\}$ close into certain linear combinations of constraints plus $a_1^{(2)}$, which is non-vanishing under the constraints. Therefore, the only unconstrained fields are

$$a_{1-\lfloor s\rfloor}^{(s)} \equiv \frac{2\pi}{k_{CS} N_s^B} a_s \ , \qquad\qquad \psi_{3/2+\lfloor -s\rfloor}^{(s)} \equiv \frac{2\pi}{k_{CS} N_s^F} \psi_s \ . \tag{4.37}$$

where the normalization functions are defined by $N_s^B = \mathrm{Tr}(L_{-\lfloor s\rfloor+1}^{(s)} L_{\lfloor s\rfloor-1}^{(s)})$ and $N_s^F = \mathrm{Tr}(G_{\lceil s\rceil-3/2}^{(s)} G_{\lfloor -s\rfloor+3/2}^{(s)})$ with $\lceil\cdot\rceil$ being the "ceiling" function.

The $\gamma(\theta)$ in (4.30) is thus constrained by (4.35), (4.36) to be

$$\gamma(\theta) = L_1 + \frac{2\pi}{k_{CS}} \sum_{s\geq 3/2, s\in\frac{1}{2}\mathbb{Z}} \left(\frac{1}{N_s^B} a_s(\theta) L_{-\lfloor s\rfloor+1}^{(s)} + \frac{1}{N_s^F} \psi_s(\theta) G_{\lfloor -s\rfloor+3/2}^{(s)} \right) \ . \tag{4.38}$$

This is the most general form of the super-connection that is compatible with the boundary condition (4.28). In the next subsection, we will derive the symmetry algebra that leaves the form of the super-connection (4.38) invariant.

4.3.2 Super-$W_\infty[\lambda]$ symmetries

We are now ready to discuss the asymptotic symmetry under the boundary condition (4.28). For convenience, we expand the gauge transformation parameter Λ, and the gauge variations of fields $a(\theta)$ and $\psi(\theta)$ in terms of the generators of $shs[\lambda]$ as

$$\Lambda = \sum_{s\geq 3/2, s\in\frac{1}{2}\mathbb{Z}} \left(\sum_{m\in\mathbb{Z}} \xi_m^{(s)} L_m^{(s)} + \sum_{r\in\mathbb{Z}+1/2} \epsilon_r^{(s)} G_r^{(s)} \right) \ , \tag{4.39}$$

$$\delta a = \sum_s \sum_m c_{s,m}^B L_m^{(s)} \ , \qquad \delta\psi = \sum_s \sum_r c_{s,r}^F G_r^{(s)} \ , \tag{4.40}$$

where we omit the argument θ. Then, under the gauge transformation (4.24), $c^B_{s,m}$ and $c^F_{s,r}$ are found to be

$$\begin{aligned} c^B_{s,m} &= \partial_+\xi^{(s)}_m + (-m+\lfloor s\rfloor)\xi^{(s)}_{m-1} \\ &\quad +\sum_t \Bigg[\sum_u a^{(t)}_{-\lfloor t\rfloor+1}\ \xi^{(s+u-t)}_{m+\lfloor t\rfloor-1}\ g^{t,s+u-t}_u\big(-\lfloor t\rfloor+1, m+\lfloor t\rfloor-1;\lambda\big) \\ &\quad -\sum_v \psi^{(t)}_{\lfloor -t\rfloor+3/2}\ \epsilon^{(s+v-t)}_{m+\lfloor -t\rfloor-3/2}\ \tilde{g}^{t,s+v-t}_v\big(\lfloor -t\rfloor+3/2, m+\lfloor -t\rfloor-3/2;\lambda\big)\Bigg] \qquad (4.41) \\ c^F_{s,r} &= \partial_+\epsilon^{(s)}_r + (-r+\lfloor s+1/2\rfloor-1/2) \\ &\quad +\sum_t \Bigg[\sum_v a^{(t)}_{-\lfloor t\rfloor+1}\ \xi^{(s+v-t)}_{r+\lfloor t\rfloor-1}\ h^{t,s+v-t}_v\big(-\lfloor t\rfloor+1, r+\lfloor t\rfloor-1;\lambda\big) \\ &\quad -\sum_u \psi^{(t)}_{\lfloor -t\rfloor+3/2}\ \epsilon^{(s+u-t)}_{r+\lfloor -t\rfloor-3/2}\ \tilde{h}^{t,s+u-t}_u\big(\lfloor -t\rfloor+3/2, r+\lfloor -t\rfloor-3/2;\lambda\big)\Bigg] \qquad (4.42) \end{aligned}$$

where g^{st}_u, $\tilde{g}^{st}_u$, h^{st}_u and $\tilde{h}^{st}_u$ are the structure constants of $shs[\lambda]$. The ranges of summations in (4.41) are

$$\max(1+|m+\lceil t\rceil-1|, 1+\lfloor s\rfloor-\lfloor t\rfloor) \le \lfloor s+u-t\rfloor \qquad \text{and} \qquad 1\le u\le 2s-\frac{1}{2} \tag{4.43a}$$

$$\max(\frac{3}{2}+\big|m+\lfloor t\rfloor-\frac{3}{2}\big|, 2+\lceil s\rceil-\lfloor t\rfloor) \le \lceil s+v-t\rceil \qquad \text{and} \qquad 1\le v\le 2s-\frac{1}{2} \tag{4.43b}$$

The ranges of summations in (4.42) are

$$\max(\frac{3}{2}+\big|m+\lfloor t\rfloor-1\big|, 1+\lceil s\rceil-\lfloor t\rfloor) \le \lceil s+v-t\rceil \qquad \text{and} \qquad 1\le v\le 2s-\frac{1}{2} \tag{4.44a}$$

$$\max(1+|m+\lceil t\rceil-1|, 1+\lceil s\rceil-\lceil t\rceil) \le \lfloor s+u-t\rfloor \qquad \text{and} \qquad 1\le u\le 2s-\frac{1}{2} \tag{4.44b}$$

The global symmetry consists of the transformations which preserve the structure (4.38). In terms of $c^B_{s,m}$ and $c^F_{s,r}$, preserving (4.38) implies:

$$c^B_{s,m} = 0 \quad \text{for } m \neq -\lfloor s \rfloor + 1 \quad \text{and} \quad c^F_{s,r} = 0 \quad \text{for } r \neq \lfloor -s \rfloor + 3/2 \; . \tag{4.45}$$

One can solve these conditions. As a result, we find that the only independent transformation parameters are

$$\eta_s \equiv \xi^{(s)}_{\lfloor s \rfloor - 1} \qquad \text{and} \qquad \epsilon_s \equiv \epsilon^{(s)}_{\lceil s \rceil - 3/2} \tag{4.46}$$

and all other parameters can be expressed in terms of these independent parameters.

Once all the transformation parameters $\xi^{(s)}_m$, $\epsilon^{(s)}_r$ are solved in terms of η_s and ϵ_s, one can compute the variation of a's and ψ's (4.40). These variations can be written as:

$$\begin{aligned} \delta^B_s a_t &= \frac{k_{CS}}{2\pi} N^B_t c^B_{t,1-\lfloor t \rfloor}(\eta_s) \; , \qquad \delta^F_s a_t = \frac{k_{CS}}{2\pi} N^B_t c^B_{t,1-\lfloor t \rfloor}(\epsilon_s) \; , \\ \delta^B_s \psi_t &= \frac{k_{CS}}{2\pi} N^F_t c^F_{t,\lfloor -t \rfloor + 3/2}(\eta_s) \; , \quad \delta^F_s \psi_t = \frac{k_{CS}}{2\pi} N^F_t c^F_{t,\lfloor -t \rfloor + 3/2}(\epsilon_s) \; . \end{aligned} \tag{4.47}$$

where $\delta^{B(F)}_s$ represents a variation corresponding to the bosonic (fermionic) generator with spin s. The argument (η_s) means that we turn on η_s and set ϵ_s to zero, and similar for (ϵ_s).

Calculating the global symmetry algebra amounts to solve (4.45) and express all $\xi^{(s)}_m$ and $\epsilon^{(s)}_r$ in (4.47) in terms of η_s and ϵ_s. While solving (4.45) in full generality is a difficult task, we focus on the variations including the lower spin generators. First

of all, we find that the variations including $s = 3/2$ and $s = 2$ are given by

$$\delta_2^B a_2 = 2a_2\eta' + a_2'\eta - \frac{k_{CS}}{4\pi}\eta''' \,, \tag{4.48a}$$

$$\delta_2^B a_{3/2} = 0 \,, \tag{4.48b}$$

$$\delta_{3/2}^B a_{3/2} = -\frac{k_{CS}}{\pi}\eta' \,, \tag{4.48c}$$

$$\delta_2^B \psi_2 = \frac{3}{2}\psi_2\eta' + \psi_2'\eta + \frac{\pi}{k_{CS}}a_{3/2}\psi_{3/2}\eta \,, \tag{4.48d}$$

$$\delta_2^B \psi_{3/2} = \frac{3}{2}\psi_{3/2}\eta' + \psi_{3/2}'\eta + \frac{\pi}{k_{CS}}a_{3/2}\psi_2\eta \,, \tag{4.48e}$$

$$\delta_{3/2}^B \psi_2 = \psi_{3/2}\eta \,, \tag{4.48f}$$

$$\delta_{3/2}^B \psi_{3/2} = \psi_2\eta \,, \tag{4.48g}$$

$$\delta_2^F \psi_2 = -2a_2\epsilon + \frac{\pi}{k_{CS}}a_{3/2}^2\epsilon + \frac{k_{CS}}{\pi}\epsilon'' \,, \tag{4.48h}$$

$$\delta_2^F \psi_{3/2} = 2a_{3/2}\epsilon' + a_{3/2}'\epsilon \,, \tag{4.48i}$$

$$\delta_{3/2}^F \psi_{3/2} = 2a_2\epsilon - \frac{\pi}{k_{CS}}a_{3/2}^2\epsilon - \frac{k_{CS}}{\pi}\epsilon'' \,, \tag{4.48j}$$

where η' represents $\frac{\partial\eta(\theta)}{\partial\theta}$ and the subscripts s of η_s, which are the same s as in the $\delta_s^{B(F)}$, are omitted.

To reproduce the standard form of the $\mathcal{N} = 2$ super-Virasoro algebra, one first needs to, as in [136], redefine the a_2 as

$$a_2^{\mathrm{SVA}} = a_2 + \frac{\pi}{2k_{CS}}a_{3/2}a_{3/2} \tag{4.49}$$

and the fermionic generators as $\psi_+^{\mathrm{SVA}} = \frac{1}{2}(\psi_2 + \psi_{3/2})$ and $\psi_-^{\mathrm{SVA}} = \frac{1}{2}(\psi_2 - \psi_{3/2})$, where $\psi_\pm^{\mathrm{SVA}}$ has $U(1)_R$ charge ± 1. Then, one can convert the variation into Poisson bracket using (4.22) and expand the fields into modes using

$$\mathcal{O}(\theta) = \frac{1}{2\pi}\sum_{p\in\mathbb{Z}}\mathcal{O}_p e^{ip\theta} \,. \tag{4.50}$$

Plugging this into the Poisson bracket gives the commutators between the modes. Finally, one needs to modify the zero mode of $a_2^{\rm SVA}$ as

$$a_{2,p}^{\rm SVA} \to a_{2,p}^{\rm SVA} - \frac{k_{CS}}{4}\delta_{p,0}\,. \tag{4.51}$$

For example, the commutator between two a_2^{SVA}'s reproduces the Virasoro algebra:

$$[(a_2)_m,\ (a_2)_n] = (m-n)(a_2)_{m+n} + \frac{c_{\rm AdS}}{12}(m^3-m)\delta_{m+n,0}, \qquad \text{where } c_{\rm AdS} = 6k_{CS}\,. \tag{4.52}$$

This is how we obtain the standard form of the $\mathcal{N}=2$ super-Virasoro algebra.

We have also shown that the variations of a_s and ψ_s with $s = 3/2, 2$ with respect to generators with the spin greater than two satisfy

$$\delta_n^B a_2 = \lfloor n \rfloor a_n \eta' + (\lfloor n \rfloor - 1) a_n' \eta - \frac{k_{CS}}{4\pi}\eta'''\delta_{n,2}\,, \tag{4.53a}$$

$$\delta_n^F a_2 = (\lfloor -n \rfloor + 1/2)\psi_n \epsilon' + (\lfloor -n \rfloor + 3/2)\psi_n' \epsilon + FB_{n,2}\,, \tag{4.53b}$$

$$\delta_n^B a_{3/2} = 0\,, \qquad \delta_{n-1/2}^B a_{3/2} = 0\,, \tag{4.53c}$$

$$\delta_{n-1/2}^F a_{3/2} = -\psi_n \epsilon\,, \tag{4.53d}$$

$$\delta_n^F a_{3/2} = -\psi_{n-1/2}\epsilon\,, \tag{4.53e}$$

$$\delta_n^B \psi_2 = (n-1/2)\psi_n \eta' + (n-1)\psi_n' \eta + BF_{n,2}\,, \tag{4.53f}$$

$$\delta_{n-1/2}^B \psi_2 = \psi_{n-1/2}\eta\,, \tag{4.53g}$$

$$\delta_n^F \psi_2 = -2a_n \epsilon + FF_{n,2}\,, \tag{4.53h}$$

$$\delta_{n-1/2}^F \psi_2 = (2-2n)a_{n-1/2}\epsilon' + (3-2n)a_{n-1/2}'\epsilon\,, \tag{4.53i}$$

$$\delta_n^B \psi_{3/2} = (n-1/2)\psi_{n-1/2}\eta' + (n-1)\psi_{n-1}'\eta + BF_{n,3/2}\,, \tag{4.53j}$$

$$\delta_{n-1/2}^B \psi_{3/2} = \psi_n \eta\,, \tag{4.53k}$$

$$\delta_n^F \psi_{3/2} = (2n-2)a_{n-1/2}\epsilon' + (2n-3)a_{n-1/2}'\epsilon\,, \tag{4.53l}$$

$$\delta_{n-1/2}^F \psi_{3/2} = 2a_n \epsilon + FF_{n-1/2,3/2}\,, \tag{4.53m}$$

where $n \in \mathbb{Z}$ and $BF_{i,j}, FB_{i,j}$ and $FF_{i,j}$ represent the non-linear terms. The results (4.53a) and (4.53b) correspond to the conditions that a's and ψ's are primary fields at least at linear order.

Finally, we present the variations including $s = 5/2$ and $s = 3$[6]. The bosonic variations of a's are

$$\delta^B_{5/2} a_{5/2} = \frac{1-4\lambda}{3}\left[2a_{5/2}\eta' + a'_{5/2}\eta\right] - N^B_{5/2}\left[2a_2\eta' + a'_2\eta\right] + \frac{k_{CS}N^B_{5/2}}{4\pi}\eta''' \,, \tag{4.54}$$

$$\delta^B_{5/2} a_3 = 3a_{7/2}\eta' + a'_{7/2}\eta + \frac{1-4\lambda}{15}\left[3a_3\eta' + a'_3\eta\right] + BB_{5/2,3} \,, \tag{4.55}$$

$$\begin{aligned}\delta^B_3 a_3 = {} & 4a_4\eta' + 2a'_4\eta - \frac{N^B_3}{12}\left[2a'''_2\eta + 9a''_2 + 15a'_2\eta'' + 10a_2\eta'''\right] \\ & + \frac{1-4\lambda}{60}\left[2a'''_{5/2}\eta + 9a''_{5/2} + 15a'_{5/2}\eta'' + 10a_{5/2}\eta'''\right] + \frac{k_{CS}N^B_3}{48}\eta'''' + BB_{3,3} \,,\end{aligned} \tag{4.56}$$

where $BB_{i,j}$ are the non-linear terms. The bosonic variations of ψ's are

$$\delta^B_{5/2}\psi_{5/2} = \psi_4\eta + \frac{1-4\lambda}{15}\left[5\psi_{5/2}\eta' + 2\psi'_{5/2}\eta\right] - \frac{N^B_3}{12}\left[6\psi_2\eta'' + 4\psi'_2\eta' + \psi''_2\eta\right] + BF_{5/2,5/2} \,, \tag{4.57}$$

$$\delta^B_{5/2}\psi_3 = \eta\psi_{7/2} + \frac{1-4\lambda}{15}\left[2\eta\psi'_3 + 5\eta'\psi_3\right] - \frac{N^F_3}{12}\left[\eta\psi''_{3/2} + 4\eta'\psi'_{3/2} + 6\eta''\psi_{3/2}\right] + BF_{5/2,3} \,, \tag{4.58}$$

$$\begin{aligned}\delta^B_3\psi_3 = {} & \frac{7}{2}\eta'\psi_4 + 2\eta\psi'_4 - \frac{1-4\lambda}{30}\left[2\eta\psi''_{5/2} + 6\eta'\psi'_{5/2} + 5\eta''\psi_{5/2}\right] \\ & - \frac{N^F_3}{24}\left[4\eta\psi'''_2 + 15\eta'\psi''_2 + 20\eta''\psi'_2 + 10\eta'''\psi_2\right] + BF_{3,3} \,.\end{aligned} \tag{4.59}$$

[6]The computations of the variations including $s = 5/2$ and $s = 3$ were done using computer.

The fermionic variations of ψ's are

$$\begin{aligned}
\delta^F_{5/2}\psi_{5/2} &= 2a_4\epsilon + \frac{1-4\lambda}{15}\left[3a''_{5/2}\epsilon + 10a'_{5/2}\epsilon' + 10a_{5/2}\epsilon''\right] \\
&\quad -\frac{N^B_3}{6}\left[3a''_2\epsilon + 10a'_2\epsilon' + 10a_2\epsilon''\right] + \frac{k_{CS}N^B_3}{12\pi}\epsilon'''' + FF_{5/2,5/2}\,, \quad (4.60)\\
\delta^F_{5/2}\psi_3 &= -3a'_{7/2}\epsilon - 6a_{7/2}\epsilon' + \frac{2(1-4\lambda)}{15}\left[a'_3\epsilon + 2a_3\epsilon'\right] \\
&\quad +\frac{N^B_3}{12}\left[a'''_{3/2}\epsilon + 4a''_{3/2}\epsilon' + 6a'_{3/2}\epsilon'' + 4a_{3/2}\epsilon'''\right] + FF_{5/2,3}\,, \quad (4.61)\\
\delta^F_3\psi_3 &= -2a_4\epsilon - \frac{1-4\lambda}{15}\left[3a''_{5/2}\epsilon + 10a'_{5/2}\epsilon' + 10a_{5/2}\epsilon''\right] \\
&\quad +\frac{N^B_3}{6}\left[3a''_2\epsilon + 10a'_2\epsilon' + 10a_2\epsilon''\right] - \frac{k_{CS}N^B_3\epsilon''''}{12\pi} + FF_{3,3}\,. \quad (4.62)
\end{aligned}$$

Note that the variation (4.54) does not have any non-linear terms, it can be converted into a commutator of the algebra after the shift (4.51)

$$[(a_{\frac{5}{2}})_m,\,(a_{\frac{5}{2}})_n] = \frac{1-4\lambda}{3}(m-n)(a_{\frac{5}{2}})_{m+n} - N^B_{5/2}(m-n)(a_2)_{m+n} - \frac{k_{CS}N^B_{5/2}}{2}(m^3-m)\delta_{m+n,0} \quad (4.63)$$

This plays an important role in section 4.4, where we compare it with the commutator in the dual CFT.

The super-$W_\infty[\lambda]$ we have just obtained is non-linear due to the non-vanishing curvature of AdS_3. As in the bosonic case [140, 68], these non-linear terms drop once the curvature is taken to zero, and the super-$W_\infty[\lambda]$ algebra further reduces to the $shs[\lambda]$ algebra if one takes its wedge subalgebra. To see this, one first converts the shift in mode (4.51) back to a shift in the energy-momentum tensor according to (4.50):

$$a_2 \to a_2 - \frac{k_{CS}}{8\pi}\,. \quad (4.64)$$

Applying this to the variations of the super-$W_\infty[\lambda]$ algebra will generate some linear terms from the nonlinear terms. The remaining nonlinear terms are negligible in the vanishing curvature limit. The mode expansion according to (4.50) then takes us

back to the $shs[\lambda]$ algebra.

[7]

4.4 Identification with the $\mathbb{C}\mathrm{P}^n$ chiral algebras

In this section, we examine the duality between $\mathcal{N}=2$ higher-spin supergravity and $\mathcal{N}=2$ $\mathbb{C}\mathrm{P}^n$ model at large n [61] from the perspective of the symmetry. The authors of [61] proposed in their work that $\mathcal{N}=2$ higher-spin supergravity based on $shs[\lambda]\times shs[\lambda]$ algebra is equivalent to the large-n limit of the $\mathcal{N}=2$ Kazama-Suzuki type coset model (4.1) (known as $\mathbb{C}\mathrm{P}^n$ model [128]) with

$$n,k\to\infty\ ,\qquad \lim_{n,k\to\infty}\frac{n}{2(n+k)}=\lambda\ ,\qquad c_{\mathrm{AdS}}=c_{\mathrm{CFT}}\ . \tag{4.65}$$

One can check that the relation between the central charge and the Chern-Simons level is consistent with the asymptotic super-Virasoro algebra (See (4.48a), for example.). The central charge of the coset model c_{CFT} is known to be $3nk/(n+k+1)$, so after taking the 't Hooft limit, one obtains the identification

$$k_{CS}=\frac{n(1-2\lambda)}{2}\ . \tag{4.66}$$

The goal of this section is to check this duality by understanding the underlying symmetries. The global symmetry of the higher-spin supergravity forms the super-$W_\infty[\lambda]$ algebra we obtained in the previous section, and the procedure we followed to get the super-$W_\infty[\lambda]$ algebra coincides with the classical Drinfeld-Sokolov (CDS) reduction of the $shs[\lambda]$ algebra. On the other side of the duality, we consider the large-n limit of the chiral algebra $\mathcal{SW}_n$ of the $\mathcal{N}=2$ $\mathbb{C}\mathrm{P}^n$ model which comes from the quantum Drinfeld-Sokolov (QDS) reduction of the Lie superalgebra $A(n,n-1)$

[7] Here we do not consider the central terms in the super-W_∞ algebra.

[141, 142, 143]. We propose that the $\mathcal{SW}_n$ algebra in the large n limit coincides with the super-$W_\infty[\lambda]$ with the parameter identifications (4.65). In the following two subsections, we carry out two non-trivial checks to support the above proposal. We first check the matching of the two algebras and then the matching of the representations of the two algebras.

4.4.1 Large n limits of the $\mathbb{C}\mathrm{P}^n$ chiral algebra

In this section, we match the two algebras by explicitly showing that the variation of the higher-spin fields $a_{\frac{5}{2}}$ under the asymptotic symmetry transformation agrees with the OPE of the corresponding operators in the 't Hooft limit of the $\mathbb{C}\mathrm{P}^n$ model. This non-trivial check partially supports the claim that the two algebras are identical.

Before the actual check, we briefly review the chiral algebra structure of the $\mathbb{C}\mathrm{P}^n$ minimal model. The chiral algebra $\mathcal{SW}_n$ can be derived from $A(n, n-1)$ by the QDS reduction [143]. Concretely, the higher-spin currents can be obained from the super-Lax operator

$$L(Z) \equiv : (aD - \Theta_{2n+1}(Z))(aD - \Theta_{2n}(Z)) \cdots (aD - \Theta_1(Z)) : , \tag{4.67}$$

where $Z = (z, \theta)$ is the $\mathcal{N} = 1$ superspace coordinate with z being bosonic and θ being fermionic, $D = \frac{\partial}{\partial\theta} + \theta\frac{\partial}{\partial z}$ is the super-covariant derivative, : : denotes the normal ordering, a is a bosonic parameter from the QDS reduction and $\Theta_i(Z) = (-1)^{i-1}(\Lambda_i - \Lambda_{i-1},\ D\Phi(Z))$. Here, Λ_i is a fundamental weight of $A(n, n-1)$ with $\Lambda_0 = 0 = \Lambda_{2n+1}$, Φ is a free chiral superfield, taking values in the root space of $A(n, n-1)$ and $(\cdot, \cdot)$ represents the inner product on the root space. One can expand $L(Z)$ in terms of aD by moving aD to the very right of the expression, then the coefficients of different powers of aD are the generators of the super-W_n algebra

[144]:

$$L(Z) = (aD)^{2n+1} + \sum_{i=2}^{2n+1} W_{\frac{i}{2}}(Z)(aD)^{2n+1-i} \ . \tag{4.68}$$

The superfields W_k decompose into components fields. We present here how the first few W_k's are decomposed:

$$\begin{aligned}
W_1(Z) &= W_1^-(z) + i\theta[G_2^+(z) + G_2^-(z)] \ , \\
W_{\frac{3}{2}}(Z) &= a[iG_2^-(z) + \theta W_2^+(z)] \ , \\
W_2(Z) &= W_2^-(z) + i\theta[G_3^+(z) + G_3^-(z)] \ , \\
W_{\frac{5}{2}}(Z) &= a[iG_3^-(z) + \theta W_3^+(z)] \ ,
\end{aligned}$$

where $W_i^\pm$ are bosonic generators with conformal weight i and $G_i^\pm$ are fermionic generators with conformal weight $i - \frac{1}{2}$. We identify W_1^- and W_2^+ with the familiar $U(1)$ charge and the energy momentum tensor J and T respectively. In addition to the matching of the central charge, we can match the higher spin fields on the both side of the duality now. The dictionary between the higher-spin fields in the asymptotic algebra and the primaries in the $\mathbb{C}\mathrm{P}^n$ model is:

$$a_s \leftrightarrow W_s^+ \ , \quad a_{t+1/2} \leftrightarrow W_t^- \ , \quad \psi_s \leftrightarrow G_s^+ \ , \quad \psi_{t+1/2} \leftrightarrow G_{t+1}^-$$

$$s, t \in \mathbb{Z}, \quad s \geq 2 \ , \quad t \geq 1 \ . \tag{4.69}$$

where the spin of the fields in the AdS side is matched with the conformal weight of the operators in the CFT side.

The OPEs between these operators can be computed from the free field realization of $\mathcal{SW}_n$ algebra [144, 145], where the results are explicitly known for $n = 3$. Computing the OPEs in the 't Hooft limit requires the knowledge of the OPEs at general n, which is complicated in general. Our strategy is to compute the OPEs

at several small n first and then extrapolate to results at general n. However, this extrapolation is possible in principle but difficult in practice, because there are non-linear terms in the OPE between higher spin operators. These non-linear terms make the extrapolation to general n difficult. Nevertheless, in the supersymmetric setting, there are examples such as the $W_2^- W_2^-$ OPE that is linear. This makes the general n extrapolation straightforward. For this reason, we restrict our attention to the $W_2^- W_2^-$ OPE.

Since our goal is to compare the algebra in the AdS side and that in the CFT side, we need to redefine the operators in the CFT side in such a way that the higher spin operators in the CFT are in the same bases as the ones in the AdS side. Up to the W_2^- operator, this can be done as follows:

1. Compute the relevant OPEs for $n = 2, 3, 4, 5$ and extrapolating the results to the general n expressions.

2. Redefine the super-Virasoro operators, T and $G^{\pm}$ to $\widetilde{T}$ and $\widetilde{G}^{\pm}$ so that the OPEs between the redefined operators match the variations on the AdS side (4.48).

3. Redefine the W_2^- operator so that its OPEs with the operators J and the $\widetilde{T}$ match with the corresponding variation on the AdS side (4.53c) and (4.53a).

The redefinitions are explicitly given by

$$T \to \widetilde{T} = T - \frac{1}{2}\partial J - \frac{:JJ:}{2n\left(1+a^2+na^2\right)} \tag{4.70a}$$

$$W_2^- \to \widetilde{W}_2^- = W_2^- + \frac{1}{2}\left(a^2 - na^2\right)\partial J + \frac{(1-n):JJ:}{2n} - \frac{\left(1+a^2+n^3a^4-n\left(1+a^2+a^4\right)\right)\tilde{T}}{-1+3n^2a^2+3n\left(1+a^2\right)} \tag{4.70b}$$

Now we carry out the OPE between the modified operators $\widetilde{W}_2^-$ on the CFT side

$$\begin{aligned}\widetilde{W}_2^-(z)\widetilde{W}_2^-(w) &= -\frac{(-1+n)n\left(-1+a^2n\right)\left(1+a^2+a^2n\right)\left(2+a^2+a^2n\right)\left(1+2a^2+a^2n\right)}{2\left(-1+3n+3a^2n+3a^2n^2\right)(z-w)^4} \\ &- \frac{2(1+n)\left(1+a^2n\right)\left(1+a^2+2a^2n\right)\ \widetilde{W}_2^-}{\left(-1+3\left(1+a^2\right)n+3a^2n^2\right)(z-w)^2} \\ &- \frac{2(-1+n)n\left(-1+a^2n\right)\left(1+a^2+a^2n\right)\left(2+a^2+a^2n\right)\left(1+2a^2+a^2n\right)\widetilde{T}}{\left(-1+3\left(1+a^2\right)n+3a^2n^2\right)^2(z-w)^2} \\ &- \frac{(1+n)\left(1+a^2n\right)\left(1+a^2+2a^2n\right)\partial\widetilde{W}_2^-}{\left(-1+3\left(1+a^2\right)n+3a^2n^2\right)(z-w)} \\ &- \frac{n(-1+n)\left(-1+a^2n\right)\left(1+a^2+a^2n\right)\left(2+a^2+a^2n\right)\left(1+2a^2+a^2n\right)\partial\widetilde{T}}{\left(-1+3\left(1+a^2\right)n+3a^2n^2\right)^2(z-w)} .\end{aligned} \tag{4.71}$$

According to the duality proposed in [61], we take the 't Hooft limit (4.65):

$$n,k\to\infty\ , \qquad \lim_{n,k\to\infty} na^2 = -\lim_{n,k\to\infty}\frac{n}{n+k+1} = -2\lambda\ . \tag{4.72}$$

then the above OPE can be rewritten as

$$\begin{aligned}\widetilde{W}_2^-(z)\widetilde{W}_2^-(w)\Big|_{\text{'t Hooft limit}} &= -\frac{(2\lambda+1)(2\lambda-1)(1-\lambda)n}{3(z-w)^4} \\ &-\frac{2(3(1-4\lambda)\widetilde{W}_2^- + 2(2\lambda+1)(\lambda-1)\widetilde{T})}{9(z-w)^2} \\ &-\frac{3(1-4\lambda)\partial\widetilde{W}_2^- + 2(2\lambda+1)(\lambda-1)\partial\widetilde{T}}{9(z-w)} ,\end{aligned} \tag{4.73}$$

where we keep only the leading term at large n.

The OPEs in the CFT are functions of complex variables z and w, while the variations of higher-spin fields under the asymptotic symmetry are functions of variable θ, so we cannot compare them directly. Therefore, we first convert the results on the both sides to commutators between modes. The converting in the AdS side is given in (4.50) and the discussion there. The mode expansion on the CFT side is defined

by:

$$\widetilde{W} = \sum_{n\in\mathbb{Z}} \widetilde{W}_n z^{-n-h_{\widetilde{W}}} \tag{4.74}$$

where $h_{\widetilde{W}}$ is the conformal weight of $\widetilde{W}$. Plugging this into the OPE (4.73) and redefining $\widetilde{W}_2^- \to -\widetilde{W}_2^-$ yield

$$\begin{aligned}[\widetilde{W}^-_{2,m},\ \widetilde{W}^-_{2,n}] \ &= \ \frac{(1+2\lambda)(1-2\lambda)(1-\lambda)n}{18}(m^3-m)\delta_{m+n,0} \\ &\quad + \frac{2(1+2\lambda)(1-\lambda)}{9}(m-n)\widetilde{T}_{m+n} + \frac{(1-4\lambda)}{3}(m-n)\widetilde{W}^-_{2,m+n}\end{aligned} \tag{4.75}$$

From the dictionary (4.69), we expect that this commutation relation should match with the $[(a_{\frac{5}{2}})_m,\ (a_{\frac{5}{2}})_n]$ commutator (4.63) in the asymptotic symmetry algebra. Using the relation between the central charge and the Chern-Simons level (4.66) and $N_B^{5/2} = (2/9)(-1+\lambda)(1+2\lambda)$, one sees that this commutator exactly agrees with the one in the CFT side (4.75), including the numerical coefficients!

This computation is possible only in the supersymmetric case, since in the bosonic case, the OPE between any pair of higher-spin generators contains non-linear terms and the large-n extrapolation is difficult as discussed above. However, in the supersymmetric case, there exists an OPE (4.73) that is linear and the extrapolation is straightforward to carry out. Note that the generator $\widetilde{W}_2^-$ is introduced by the $\mathcal{N}=2$ supersymmetry so the possibility of this check is available to us only by introducing supersymmetry.

4.4.2 Degenerate representations

In this section, we compare the degenerate representations, whose Verma modules are truncated by null vectors, on both AdS and CFT sides. We show that any degenerate representation of the $\mathbb{C}\mathrm{P}^n$ model in the 't Hooft limit can be a degenerate representation of the asymptotic symmetry algebra of the higher-spin supergravity theory and vice versa.

Finding the degenerate representations on the CFT side is straightforward. The chiral algebra of the $\mathcal{N}=2$ $\mathbb{C}\mathrm{P}^n$ minimal model is shown to be the $\mathcal{SW}_n$ algebra that can be derived from the Lie superalgebra $A(n,n-1)$ by the QDS reduction [144]. We can find the degenerate representations by explicitly constructing the null vectors in the modules and the resulting expressions for the degenerate representations are known (see e.g. [146, 144] and reference therein). We then take the 't Hooft limit by simply applying the limit (4.65) to the representations.

The degenerate representations of the asymptotic algebra are not explicitly known in the literature. We thus take a step back and find them indirectly. First, note that the way we get the asymptotic super-$W_\infty[\lambda]$ algebra on the AdS side is the same as the classical Drinfeld-Sokolov reduction of $shs[\lambda]$. Secondly, we utilize the fact that $shs[\lambda]$ is realized by analytically continuing $A(n,n-1)$ to $n=-2\lambda$ [147, 65]. Thirdly, we know that the Quantum Drinfeld-Sokolov reduction of $A(n,n-1)$ gives $\mathcal{SW}_n$ algebra and we know how to find its degenerate representations. Finally, one can take the classical limit that reduces the Quantum Drinfeld-Sokolov reduction to the Classical Drinfeld-Sokolov reduction. This limit corresponds to taking the level of QDS reduction, k_{DS}, to infinity[8]. Thus, we can start with any degenerate representation of the algebra $\mathcal{SW}_n$ and apply the combination of these operation: $n=-2\lambda, k_{DS}\to\infty$, then the resulting representation is a degenerate representation of the super-$W_\infty[\lambda]$ algebra.

With this reasoning in mind, we can compare the degenerate representations on both sides by starting with any degenerate representation of $\mathcal{SW}_n$, taking the two limits, (i) Super-higher-spin limit: $n=-2\lambda, k_{DS}\to\infty$ and (ii) the 't Hooft limit: $n,k\to\infty$, $\lim_{n\to\infty}\frac{n}{n+k+1}=2\lambda$. Then we compare the spectra of conformal weights and the $U(1)$ charges of the two resulting representations. The relation is clear in the

[8]In the duality, the central charges on both sides are identified. Since the central charge diverges in the 't Hooft limit in the CFT side, this implies that the central charge of the AdS side should also diverges. This is equivalent to taking $k_{DS}\to\infty$, according to (4.79) and $n=-2\lambda$, $\alpha_-^2=k_{DS}+1$.

following diagram:

$$\begin{array}{ccc} A(n,n-1) & \xrightarrow{n\to -2\lambda} & shs[\lambda] \\ \downarrow \text{QDS} & & \downarrow \text{CDS} \\ \mathcal{SW}_n & \xrightarrow[\substack{n\to -2\lambda \\ k_{DS}\to\infty}]{\text{classical limit}} & \text{super-}W_\infty[\lambda] \end{array} \qquad \begin{array}{ccc} & \text{AdS}_3/\text{CFT}_2 \text{ Proposal} & \\ \mathcal{SW}_n & \xrightarrow[?]{\text{'t Hooft limit}} & \text{super-}W_\infty[\lambda] \end{array}$$

Let us now move on to computing the degenerate representations. We start from any degenerate representation of $\mathcal{SW}_n$. In the bosonic sector, the highest weight state of the module is characterized by a weight of the form:

$$\Lambda = \alpha_+ \Lambda_+ + \alpha_- \Lambda_- \ , \tag{4.76}$$

where $\alpha_- = -\sqrt{k_{DS}+1}$ and $\alpha_-\alpha_+ = -1$. Λ_+ and Λ_- are linear combinations of fundamental weights with non-negative integer coefficients. For a given Λ, the conformal dimension is represented as [143, 146]

$$h(\Lambda) = \frac{1}{2}(\Lambda, \Lambda + 2\alpha_-\rho) \ , \tag{4.77}$$

where ρ is the dual Weyl vector. The $U(1)_R$ charge is given by

$$Q(\Lambda) = -\alpha_-(\Lambda, \nu) \ , \tag{4.78}$$

where ν is the generator of the center of the $A(n, n-1)$ algebra.

We first consider the spectrum in the CFT side. To find out the relation between k_{DS} and the level in the coset model k, we match the central charge of $\mathcal{SW}_n$ from the

QDS reduction with that of the $\mathbb{C}\mathrm{P}^n$ coset model [143, 144, 146]. It yields

$$\begin{aligned} c_{mm} &= \frac{3nk}{n+k+1} \\ c_{DS} &= 3n(1-(n+1)\alpha_-^2) \qquad (4.79) \\ c_{mm} = c_{DS} \Rightarrow k_{DS}+1 &= \frac{1}{n+k+1}\,, \qquad (4.80) \end{aligned}$$

where the subscript mm stands for the minimal model. Therefore, $k_{DS}+1 \to 0$ ($\alpha_- \to 0^-$ and $\alpha_+ \to \infty$) in the 't Hooft limit. What we are interested in is to extract representations with finite conformal dimensions in the 't Hooft limit. The finiteness of the conformal dimensions yields strong constraints on the allowed value of weight Λ. Plugging the Λ given in (4.76) into (4.77), we have the following expression for the conformal weight of a general degenerate representation:[9]

$$h_{mm}(\Lambda) = \frac{n+k+1}{2}(\Lambda_+,\Lambda_+) - (\Lambda_-,\Lambda_+) + \frac{(\Lambda_-,\Lambda_-)}{2(n+k+1)} - (\Lambda_+,\rho) + \frac{(\Lambda_-,\rho)}{n+k+1}\,. \qquad (4.81)$$

To further evaluate the inner products between weights, we decompose the weight Λ_+ and Λ_- of the Lie superalgebra $sl(n+1|n)$ into sums of weights $\Lambda_\pm^{(1)}, \Lambda_\pm^{(2)}, Q_\pm$ of the bosonic subalgebra $sl(n+1)\oplus sl(n)\oplus u(1)$ of the $sl(n+1|n)$. This decomposition has already been considered in [143]. It reads

$$\Lambda_\pm = \Lambda_\pm^{(1)} + \Lambda_\pm^{(2)} + Q_\pm \nu/(n+1)\,, \qquad (4.82)$$

where we have factored out the explicit n dependence in the $U(1)$ part, according to the analysis in [143] so that $Q_\pm \sim \mathcal{O}(1)$. We can further choose sets of orthogonal bases e_i, d_i of the $sl(n+1)$ and $sl(n)$ on which the $\Lambda_\pm^{(1)}$ and $\Lambda_\pm^{(2)}$ can be expanded. The bases satisfy

$$e_i \cdot e_j = \delta_{ij}\,, \qquad d_i \cdot d_j = -\delta_{ij}\,, \qquad (4.83)$$

[9] We replace the α_+^2's in various places by $k_{DS}+1$ to simplify the expressions.

where the negative signatures of the inner products between d_i bases are required due to the negative signature of the $sl(n)$ part of the $sl(n+1|n)$. An advantage to adopt this decomposition is that we can directly use the results in the bosonic computation in [65]. Thus, as in [65], we consider the following formal expansion of the weights:

$$\Lambda_+^{(1)} = \sum_{i=1}^{n+1} l_i\, e_i\,, \qquad l_i = r_i^{(1+)} - \frac{B^{(1+)}}{n+1}\,, \quad B^{(1+)} = \sum r_i^{(1+)}\,, \tag{4.84}$$

$$\Lambda_+^{(2)} = \sum_{i=1}^{n} k_i\, d_i\,, \qquad k_i = r_i^{(2+)} - \frac{B^{(2+)}}{n}\,, \quad B^{(2+)} = \sum r_i^{(2+)}\,, \tag{4.85}$$

$$\Lambda_-^{(1)} = \sum_{i=1}^{n+1} p_i\, e_i\,, \qquad p_i = r_i^{(1-)} - \frac{B^{(1-)}}{n+1}\,, \quad B^{(1-)} = \sum r_i^{(1-)}\,, \tag{4.86}$$

$$\Lambda_-^{(2)} = \sum_{i=1}^{n} q_i\, d_i\,, \qquad q_i = r_i^{(2-)} - \frac{B^{(2-)}}{n}\,, \quad B^{(2-)} = \sum r_i^{(2-)}\,, \tag{4.87}$$

where r_i^x is the number of boxes in the i^{th} row of the Young tableau corresponding to the weight x, and B^x represent the total number of boxes in the Young tableau. With these notations, we can compute the conformal weights in the two limits and express the results in terms of the Young tableau associated to each of the bosonic weights.

Requiring the representations to have finite conformal weights in the 't Hooft limit yields the following conditions:

$$B^{(2+)} = B^{(1+)}, \qquad \sum (r_i^{(2+)})^2 = \sum (r_i^{(1+)})^2 \qquad Q_+ = 0\,. \tag{4.88}$$

The conformal weight is thus[10]

$$h_{mm}(\Lambda) = 2\lambda(B^{(1-)} - B^{(2-)}) + \sum_{i=1}^{n} r_i^{(1+)}(i - r_i^{(1-)}) + \sum_{i=1}^{n-1} r_i^{(2+)}(r_i^{(2-)} - i) - B^{(1+)}\,. \tag{4.89}$$

[10]The λ-dependent part can be shown to be non-negative. From the decomposition (4.82) (see

One can also compute the $U(1)$ charge (4.78) under the requirement (4.88). It reads

$$q_{mm}(\Lambda) = 2\lambda\, Q_- \,. \tag{4.90}$$

The fermionic sector represents the affine Lie algebra $SO(2n)$ at level one. The degenerate representation is characterized by a weight $\tilde{\Lambda}$ and the contributions to the conformal weight and the $U(1)_R$ charge are $\frac{1}{2}\tilde{\Lambda}^2$ and $\sum_i \tilde{\Lambda}_i$, respectively [128]. Therefore, the conformal weight of a degenerate representation ends up with

$$h_{mm}(\Lambda) = 2\lambda(B^{(1-)} - B^{(2-)}) + \sum_{i=1}^{n} r_i^{(1+)}(i - r_i^{(1-)}) + \sum_{i=1}^{n-1} r_i^{(2+)}(r_i^{(2-)} - i) - B^{(1+)} + \frac{1}{2}\tilde{\Lambda}^2 \,, \tag{4.91}$$

and the $U(1)_R$ charge with

$$q_{mm}(\Lambda, \tilde{\Lambda}) = 2\lambda Q_- + \sum_i \tilde{\Lambda}_i \,. \tag{4.92}$$

Then, we compute the conformal weights and $U(1)_R$ charges of degenerate representations of the symmetry algebra in the AdS side. We take the limits $n \to -2\lambda$ and $k_{DS} \to \infty$, where the general expression for the conformal weight reads

$$h_{HS}(\Lambda) = \frac{(\Lambda_+, \Lambda_+)}{2(k_{DS}+1)} - (\Lambda_-, \Lambda_+) + \frac{(k_{DS}+1)}{2}(\Lambda_-, \Lambda_-) - (\Lambda_+, \rho) + (k_{DS}+1)(\Lambda_-, \rho) \,. \tag{4.93}$$

In this limit, one needs to set $\Lambda_- = 0$ to get representations with finite conformal

also [144]) and (4.84)-(4.87) (see also [65]), one can show that

$$\begin{aligned} B^{(1-)} &= \sum_{s=1}^{N} s(m_{2s-1} + m_{2s}) = \sum_{s=1}^{N} s\, m_{2s} + \sum_{s'=0}^{N-1} (s'+1)\, m_{2s'+1} \\ B^{(2-)} &= \sum_{s=1}^{N-1} s(m_{2s} + m_{2s+1}) = \sum_{s=1}^{N-1} s\, m_{2s} + \sum_{s=1}^{N-1} s\, m_{2s+1} \\ \Rightarrow \quad & B^{(1-)} - B^{(2-)} = N m_{2N} + \sum_{s=1}^{N} m_{2s-1} \geq 0 \,, \end{aligned}$$

where the m_i is a non-negative Dynkin coefficient of the weight Λ of the original $sl(n+1|n)$ algebra.

weights. The conformal weight can be evaluated as

$$h_{HS}(\Lambda,\tilde{\Lambda}) \;=\; 2\lambda(B^{(1+)}-B^{(2+)})+\sum_{i=1}^{n} ir_i^{(1+)}-\sum_{i=1}^{n-1} ir_i^{(2+)}-B^{(1+)}+\frac{1}{2}\tilde{\Lambda}^2 \quad (4.94)$$

The $U(1)_R$ charge is evaluated as

$$q_{HS}(\Lambda,\tilde{\Lambda}) \;=\; 2\lambda Q_+ +\sum_i \tilde{\Lambda}_i \ . \quad (4.95)$$

Note that in these expressions, the symbols $B, r, \tilde{\Lambda}$ are different from those in the other limit.

Now, we can compare the two limits. We see that the spectra of $U(1)$ charges match in a simple way. The spectra of λ-dependent part of the conformal dimensions also match straightforwardly. But the matching of the λ-independent part in the conformal dimensions is not obvious since they have different expressions. We thus leave a more careful check of the matching of the λ-independent part in future work and we conclude here that any degenerate representation of the CFT in the 't Hooft limit *can* be a representation of the bulk higher-spin theory and vise versa.

The agreement of the spectrum of degenerate representations indicates that the representation in the 't Hooft limit of the $\mathbb{C}\mathrm{P}^n$ model can be a representation of the asymptotic $\mathcal{SW}_\infty$ algebra on the AdS side and vice versa. This provides another piece of evidence for the validity of the duality.

4.5 Conclusion

In this chapter, we have analyzed the asymptotic symmetry of the supergravity theory supersymmetrically coupled to an infinite tower of higher-spin fields. The matching of this asymptotic symmetry algebra with the chiral algebra of the $\mathbb{C}\mathrm{P}^n$ CFT model in the 't Hooft limit provides another non-trivial check of the recently proposed

supersymmetric duality [61]. We have also shown that the degenerate representations on gravity sides can be mapped to the degenerate representations of the $\mathbb{C}\mathrm{P}^n$ model and vice versa.

For future directions, it would be interesting to extend the matching of the symmetry algebras to higher order. Due to the technical difficulties, we found it hard to obtain the commutators for higher-spin generators in the coset CFT for general n. It is, however, possible in principle, and should provide firmer evidence for the duality. Another direction is to compute the partition function and correlation functions on both sides and see the agreement so as to provide other strong evidence for the duality. The one-loop partition function was discussed in the recent paper [148].

CHAPTER V

Dualities from higher-spin supergravity

5.1 Introduction

The AdS/CFT duality with higher-spin fields on both sides has drawn a lot of attention in recent years.

As mentioned in Chapter I, in this chapter we extend the analysis of [86] to the supersymmetric setting. We consider the 3d spin-3 supergravity that can be described as a Chern-Simons theory with $sl(3|2)$ gauge fields.[1] The supergravity sector is represented by an $osp(1|2)$ subalgebra. It turns out that there are three different ways to embed an $osp(1|2)$ into the defining $sl(3|2)$. The vacuum solutions corresponding to these 3 embeddings are labeled as $\text{AdS}^{(1)}$, $\text{AdS}^{(2)}$ and $\text{AdS}^{(\text{p})}$.[2] We analyze the vacuum structure of each embedding and explicitly construct a holographic RG flow from $\text{AdS}^{(1)}$ to $\text{AdS}^{(\text{p})}$ and from $\text{AdS}^{(2)}$ to $\text{AdS}^{(\text{p})}$, respectively. In this sense, we identify $\text{AdS}^{(\text{p})}$ as an IR theory and the $\text{AdS}^{(1)}$, $\text{AdS}^{(2)}$ as two different UV theories. Thus a duality is found between the two UV theories in the sense that the two theories, each with a chemical potential turned on, flow to the same IR theory. Moreover, this structure is very similar to the known structure of the Hamiltonian reduction of

[1] In this theses, we adopt the convention that names with capital letters, such as $SL(3)$, represent Lie (super)groups and names with lower case letters, such as $sl(3)$, represent the corresponding Lie (super)algebra.

[2] In this chapter, we will abuse the notation $\text{AdS}^{(\cdot)}$ for both the higher-spin theory with a certain $osp(1|2)$ embedding and its AdS vacuum solution.

the 2d Wess-Zumino-Witten (WZW) model with $sl(3|2)$-valued currents. It has been shown by Ahn, Ivanov and Sorin [149] that three different reductions of the $sl(3|2)$ WZW model exist, each containing the usual Virasoro algebra as a subalgebra of its chiral algebra. They have also shown that one of the three reductions can be obtained from the other two by secondary Hamiltonian reductions. We find an exact match between the chiral symmetries of these three resulting theories and the asymptotic symmetries of the three different embeddings. This gives a hint of a duality between the 3d higher-spin supergravity and some extended version of the Hamiltonian reduced 2d WZW models, as argued in [150, 151] for the bosonic case. In addition, our analysis suggests a physical interpretation of the Hamiltonian reduction procedures as RG flows.

5.2 3d higher-spin gravity, its AdS vacua and the RG flow

In this section, we review the known results about the higher-spin gravity in 3-dimensional AdS spacetime. We then briefly summarize the result in [86], namely the two distinct AdS vacua that correspond to the two different $sl(2,\mathbb{R})$ embeddings into $sl(3,\mathbb{R})$ and the RG flow between them.

We first review the result in [86]. In the Chern-Simons language, the gauge connections that correspond to the AdS vacuum read:

$$\Gamma_{\text{AdS}} = e^{\rho} L_1 dx^+ + L_0 d\rho\,, \qquad \tilde{\Gamma}_{\text{AdS}} = -e^{\rho} L_{-1} dx^- - L_0 d\rho\,, \tag{5.1}$$

where $L_{0,\pm1}$ are the $sl(2,\mathbb{R})$ generators and we omit the superscript (2) in $L_i^{(2)}$. Then we can compute the metric of the corresponding geometric

$$ds^2 = d\rho^2 - e^{2\rho} dx^+ dx^-\,, \tag{5.2}$$

which represents an AdS_3 spacetime.

This simple computation tells us that the properties, most importantly the trace structure, of the $sl(2,\mathbb{R})$ generators $L_{0,\pm1}$ determines the metric of the geometry. Since it is known that there can be different ways to embed an $sl(2,\mathbb{R})$ algebra to a higher rank Lie algebra, it is natural to ask what happens to the geometry if we consider different $sl(2,\mathbb{R})$ embeddings.

For the special case $sl(3,\mathbb{R})$, there are two different $sl(2,\mathbb{R})$ embeddings: a principal embedding and a non-principal which is usually called the "diagonal" embedding. The work [86] showed that the gauge connections (5.1) corresponding to the principal embedding give an AdS_3 vacuum with unit radius, which we denote as $AdS^{(p)}$ with p standing for "principal". The gauge connections corresponding to the diagonal embedding were shown to describe an AdS_3 vacuum with radius 1/2. We denote it as $AdS^{(d)}$ where d stands for "diagonal".

We can further consider perturbation solutions around any AdS_3 vacuum that goes back to the vacuum solution asymptotically. For instance, we can consider the perturbed asymptotic $AdS^{(p)}$ solution

$$\Gamma = \left(e^{\rho}L_1 - \frac{2\pi}{k_{CS}}e^{-\rho}\mathcal{L}(x^+)L_{-1} - \frac{\pi}{2k_{CS}}e^{-2\rho}\mathcal{W}(x^+)W_{-2}\right)dx^+ + L_0 d\rho\,, \tag{5.3}$$

where $\mathcal{L}(x^+), \mathcal{W}(x^+)$ are asymptotic fields. Due to the topological nature of the Chern-Simons action, much of the information about this perturbation is encoded in the asymptotic symmetry which is the gauge symmetry that preserves the form of (5.3). Following the procedure shown in [67, 68], the asymptotic symmetry of the principal embedding $AdS^{(p)}$ can be shown to be the W_3 algebra, which contains a spin-2 generator and a spin-3 generator. The authors of [86] showed that the asymptotic symmetry of the $AdS^{(d)}$ vacuum is the $W_3^{(2)}$ algebra, which contains a spin-2 generator, 2 spin-3/2 generators and one spin-1 generator.

Another interesting result in [86] is the RG flow from $\mathrm{AdS}^{(\mathrm{d})}$ to $\mathrm{AdS}^{(\mathrm{p})}$. This flow was explicitly constructed as an interpolation solution between the two vacua

$$\Gamma = \lambda\, e^{\rho} L_1 dx^+ + e^{2\rho} \hat{L}_1 dx^- + L_0 d\rho\,, \tag{5.4}$$

where L_1 ($\hat{L}_1$) are the spin-2 generators of the principal (diagonal) embedding. A similar expression exists for the $\tilde{\Gamma}$ connection. This solution approaches to the $\mathrm{AdS}^{(\mathrm{d})}$ in the $\rho \to \infty$ limit, while it approaches to the $\mathrm{AdS}^{(\mathrm{p})}$ in the $\rho \to -\infty$ limit. In this sense, we get an RG flow from the $\mathrm{AdS}^{(\mathrm{d})}$ vacuum in the UV to the $\mathrm{AdS}^{(\mathrm{p})}$ vacuum in the IR.

The authors of [86] also found the relations between UV fields and IR fields. This is done by adding both the UV and IR perturbations

$$\begin{aligned} \delta\Gamma \;=\; & \left(\mathcal{L}_{IR} e^{-\rho} L_{-1} + \mathcal{W}_{IR} e^{-2\rho} W_{-2}\right) dx^+ && (5.5)\\ & + \left(J_{UV} W_0 + G^{(1)}_{UV} e^{-\rho} L_{-1} + G^{(2)}_{UV} e^{-\rho} W_{-1} + T_{UV} e^{-2\rho} W_{-2}\right) dx^- && (5.6) \end{aligned}$$

to the gauge connection of the interpolation solution (5.4). Then solving the linearized equation of motion leads to the relations between UV fields $\mathcal{O}_{UV}$ and IR fields $\mathcal{O}_{IR}$.

5.3 Higher-spin supergravity with different $osp(1|2)$ embeddings

In this section, we review the Chern-Simons formalism for higher-spin supergravity. We will use this formalism to study the spin-3 supergravity which can be expressed in terms of the Chern-Simons theory based on the Lie superalgebra $sl(3|2)$. To prepare for later sections, we discuss the different $osp(1|2)$ embeddings of the $sl(3|2)$ algebra, which is the supersymmetric version of the $sl(2,\mathbb{R})$ embedding of the $sl(3,\mathbb{R})$ algebra.

5.3.1 Higher-spin supergravity as a Chern-Simons theory

Higher spin supergravity can be written as a Chern-Simons theory based on some superalgebra $\mathcal{G}$. We consider the $\mathcal{N}=2$ higher-spin supergravity, where the relevant gauge superalgebra is $\mathcal{G}=sl(n|n-1)$ [61, 70]. For this choice the higher-spin gauge theory contains $\mathcal{N}=2$ supermultiplets with spin ranging from 2 to n. The action reads

$$I_{HS}=I_{CS}(\Gamma,k_{CS})-I_{CS}(\tilde{\Gamma},k_{CS})\ ,\qquad I_{CS}(\Gamma,k_{CS})=\frac{k_{CS}}{4\pi}\int\limits_{\mathcal{M}}\mathrm{STr}(\Gamma\wedge d\Gamma+\frac{2}{3}\Gamma\wedge\Gamma\wedge\Gamma)\ , \tag{5.7}$$

where Γ is the gauge super-connection that evaluates in $\mathcal{G}$. The connections can be expanded in terms of the bosonic and fermionic generators of $\mathcal{G}$

$$\Gamma=\sum_{s,m}A_m^{(s)}L_m^{(s)}+\sum_{s,r}\psi_r^{(s)}G_r^{(s)}\ ,\qquad \tilde{\Gamma}=\sum_{s,m}\tilde{A}_m^{(s)}\tilde{L}_m^{(s)}+\sum_{s,r}\tilde{\psi}_r^{(s)}\tilde{G}_r^{(s)}\ , \tag{5.8}$$

where $L_m^{(s)}$ ($\tilde{L}_m^{(s)}$) are bosonic generators, $G_m^{(s)}$ ($\tilde{G}_m^{(s)}$) are fermionic generators, $A_m^{(s)}$ ($\tilde{A}_m^{(s)}$) are the bosonic fields and $\psi_m^{(s)}$ ($\tilde{\psi}_m^{(s)}$) are fermionic fields.

We realize the superalgebra $\mathcal{G}=sl(n|n-1)$ as supermatrices following the convention [152] where $\mathcal{G}$ is spanned by matrices of the form

$$M=\begin{pmatrix} E & B \\ C & D \end{pmatrix}\ , \tag{5.9}$$

in which E and D are $n\times n$ and $(n-1)\times(n-1)$ matrices that generate the $gl(n)$ and $gl(n-1)$ algebra respectively, B and C are $n\times(n-1)$ and $(n-1)\times n$ matrices respectively. The "STr" in (5.7) stands for the super-trace and is defined as

$$\mathrm{STr}(M)=\mathrm{Tr}(E)-\mathrm{Tr}(D)\,. \tag{5.10}$$

Every element $g \in sl(n|n-1)$ satisfies $\mathrm{STr}(g) = 0$. Note that in this chapter we follow the normalization of super-trace in [152], which is different from that in [70].

To minimize the confusion caused by different notations, we will use the representation of the $sl(3|2)$ algebra in the Racah basis following [147]. In [147], the bosonic generators of $sl(n|n-1)$ are

$$T^s_m\,, \quad 0 \le s \le n-1,\ -s \le m \le s,\ \text{and}\ U^t_u\,, \quad 0 \le t \le n-2,\ -t \le u \le t\,, \tag{5.11}$$

and the fermionic generators are

$$Q^r_p\,, \quad 1/2 \le r \le n-3/2,\ -p \le r \le p,\ \text{and}\ \bar{Q}^{\bar{r}}_q\,, \quad 1/2 \le \bar{r} \le n-3/2,\ -q \le \bar{r} \le q\,. \tag{5.12}$$

Each of these generators is associated with a $(2n-1)\times(2n-1)$ matrix, see [147] for the concrete matrix realization of all the generators.

Coming back to (5.7), the relation between k_{CS} and the parameter ℓ is

$$k_{CS} = \frac{\ell}{4G_3}\frac{1}{(-\mathrm{STr}(L_0^{(2)})^2)}\,. \tag{5.13}$$

where $L^{(2)}_{0,\pm1}$ are the bosonic generators of an $osp(1|2)$ subalgebra of $\mathcal{G}$. The metric can be computed from the connection

$$g_{\mu\nu} = \frac{\ell^2}{4\,\mathrm{Tr}L_0^2}\mathrm{STr}((\tilde{\Gamma}_\mu - \Gamma_\mu)(\tilde{\Gamma}_\nu - \Gamma_\nu))\,. \tag{5.14}$$

5.3.2 Normalization

In this chapter, we will consider different $osp(1|2)$ subalgebras of $sl(n|n-1)$. Therefore, the $\mathrm{STr}(L_0^{(2)})^2)$ can be different for different embeddings. To compare results from different embeddings, we need a proper normalization. To simplify our notation, we will omit the (2) in $L_0^{(2)}$ throughout this chapter.

In the current supersymmetric case key identity relating the frame-like language and the Chern-Simons language is

$$(\mathrm{STr}L_0^2)\, k_{CS} = \frac{\ell}{4G_3}\,, \tag{5.15}$$

where on the right hand side of the equation, the parameter ℓ is related to the cosmological constant and G_3 is the 3-dimensional gravity constant. On the left hand side of the equation, k_{CS} is the Chern-Simons level and the $\mathrm{STr}L_0^2$ is related to the different embeddings. This equation is valid for all different embeddings. Since the factor $\mathrm{STr}L_0^2$ changes among different embeddings, the k_{CS} and ℓ cannot be fixed at the same time. We fix the value of k_{CS} among different embeddings, since the higher spin action (5.7) is unchanged when we identify different generators to span the $osp(1|2)$ subalgebra[3].

Then suppose we identify some different $L'_{0,\pm1}$ as the bosonic generators of the $osp(1|2)$. We have the identification:

$$k_{CS} = \frac{\ell'}{4G_3}\frac{1}{(\mathrm{STr}(L'_0)^2)}\,. \tag{5.16}$$

Since k_{CS} is fixed in the two identifications, we develop a relation between ℓ and ℓ':

$$\ell/(\mathrm{STr}(L_0)^2) = \ell'/(\mathrm{STr}(L'_0)^2) \Rightarrow \Lambda(\mathrm{STr}(L_0)^2)^2 = \Lambda'(\mathrm{STr}(L'_0)^2)^2\,. \tag{5.17}$$

Thus we see different identifications of the $osp(1|2)$ subalgebra, which in general have different values of $\mathrm{STr}(L_0)^2$, correspond to spacetimes with different cosmological constants.

[3]We thank Thomas Hartman for clarifying this point to us.

5.3.3 $osp(1|2)$ embeddings of $sl(3|2)$

In this subsection, we construct the three different $osp(1|2)$ embeddings into the Lie superalgebra $sl(3|2)$. The results in this section are useful for later discussions.

In [153], the authors discussed the $osp(1|2)$ embeddings of the $sl(n+1|n)$ superalgebra in general. For our case $sl(3|2)$, we will see that there are three different embeddings. Here we want to derive the explicit form of the decomposition of the adjoint representations of $sl(3|2)$ for each of the embeddings. In other words, we want to find the explicit grouping of the generators of the $sl(3|2)$ algebra into the representations of the $osp(1|2)$ subalgebra. This is a supersymmetric generalization of the bosonic $sl(2,\mathbb{R})$ embedding considered in [153, 86]. It is shown in [153] that any $osp(1|2)$ embedding in a basic Lie superalgebra $\mathcal{G}$ can be considered as the superprincipal $osp(1|2)$ embedding of a regular subsuperalgebra $\mathcal{K}$ of $\mathcal{G}$. Further notice that not all the basic Lie superalgebras admit an $osp(1|2)$ superprincipal embedding. The basic Lie superalgebras admitting a superprincipal $osp(1|2)$ are the following [152]:

$$sl(n\pm1|n),\ osp(2n\pm1|2n),\ osp(2n|2n),\ osp(2n+2|2n),\ D(2,1;\alpha)\ \text{ with } \alpha\neq 0,-1,\infty$$

where $D(2,1;\alpha)$ is a one-parameter family of exceptional Lie superalgebras with rank 3 and dimension 17. For the algebra $\mathcal{G}=sl(3|2)$, there are three different regular subsuperalgebras $\mathcal{K}=sl(3|2)$, $sl(2|1)$, $sl(1|2)$, so there are three different $osp(1|2)$ embeddings into $sl(3|2)$. We study each of the three embeddings in the following 3 subsections.

5.3.3.1 The principal embedding: $\mathcal{K} = sl(3|2)$

This is the principal embedding. Following the notation in [153], the decomposition of the adjoint representation of $sl(3|2)$, which is the algebra itself, reads

$$\frac{\mathbf{Ad}[sl(3|2)]}{sl(3|2)} = \mathcal{R}_2 \oplus \mathcal{R}_{3/2} \oplus \mathcal{R}_1 \oplus \mathcal{R}_{1/2}\,. \tag{5.18}$$

where $\mathcal{R}_j$ is an irreducible representation of $osp(1|2)$ algebra with spin j. Notice that $\mathcal{R}_j$ can be decomposed as $\mathcal{R}_j = \mathcal{D}_j \oplus \mathcal{D}_{j-1/2}$ with $\mathcal{D}_j$ being the spin-j representation of $sl(2)$. From this, we see that the bosonic sector of $sl(3|2)$,

$$sl(3|2)\big|_B = sl(3) \oplus sl(2) \oplus u(1)\,. \tag{5.19}$$

decomposes as

$$\mathbf{Ad}[sl(3|2)]\big|_B = \mathcal{D}_2 \oplus \mathcal{D}_1 \oplus \mathcal{D}'_1 \oplus \mathcal{D}_0\,. \tag{5.20}$$

Notice that $\mathcal{D}_2, \mathcal{D}_1, \mathcal{D}_0$ comes from the $sl(3)$ subalgebra, while the $\mathcal{D}'_1$ comes from the $sl(2)$ subalgebra.[4] These correspond to a spin-2 representation,[5] two spin-1 representations and a spin-0 (singlet) representation, which agrees with [70].

The fermionic sector contains

$$\mathbf{Ad}[sl(3|2)]\big|_F = 2\mathcal{D}_{3/2} \oplus 2\mathcal{D}_{1/2}\,. \tag{5.21}$$

We see there are 2 spin-3/2 representations and 2 spin-1/2 representations, which again agrees with the result in [70]. As a simple consistency check, we count the number of bosonic and fermionic states. From (5.20), there are $5+3+3+1=12$ bosonic states. From (5.21), there are $2\times 4 + 2\times 2 = 12$ fermionic states, which is the same as the number of bosonic states. This agrees with the well known property

[4] In this section, we use "$'$" to indicate any representation coming from the $sl(2)$ part in (5.19).
[5] In this section, "spin" refers to the $sl(2)$ spin, the spacetime spin is the $sl(2)$ spin plus one.

of the $sl(n|n-1)$ supealgebra.

5.3.3.2 Non-principal embedding I : $\mathcal{K} = sl(2|1)$

In this section, we consider the $osp(1|2)$ superprincipal embedding of $\mathcal{K} = sl(2|1)$ in $\mathcal{G} = sl(3|2)$

$$\frac{\mathbf{Ad}[sl(3|2)]}{sl(2|1)} = \mathcal{R}_1 \oplus 3\mathcal{R}_{1/2} \oplus 2\tilde{\mathcal{R}}_{1/2} \oplus 2\mathcal{R}_0 \oplus 2\tilde{\mathcal{R}}_0 \,, \tag{5.22}$$

where $\tilde{\mathcal{R}}_j = \tilde{\mathcal{D}}_j \oplus \tilde{\mathcal{D}}_{j-1/2}$ represents a spin-j representation of $osp(1|2)$ but with "wrong" statistics, in the sense that $\tilde{\mathcal{D}}_i$ is spanned by fermionic (bosonic) generators if i is an integer (half integer). In addition, $\tilde{\mathcal{R}}_0 = \tilde{\mathcal{D}}_0$, $\mathcal{R}_0 = \mathcal{D}_0$. We see that there is only one $sl(2)$ subalgebra in the decomposition (5.22): the $\mathcal{D}_1$ in $\mathcal{R}_1$. The decomposition of the bosonic subalgebra (5.19) under this $osp(1|2)$ embedding reads

$$\mathbf{Ad}[sl(3|2)]\big|_B = \mathcal{D}_1 \oplus 2\tilde{\mathcal{D}}_{1/2} \oplus 2\mathcal{D}_0 \oplus 3\mathcal{D}'_0 \,. \tag{5.23}$$

Thus we see that the $sl(3)$ subalgebra in the decomposition (5.19) gives the unique $sl(2)$ subalgebra, 2 (bosonic) spin-1/2 representations of the $sl(2)$ and 2 singlets. The $sl(2)$ part in (5.19) decomposes into 3 singlets.

The decomposition of the fermionic part under this $osp(1|2)$ embedding reads

$$\mathbf{Ad}[sl(3|2)]\big|_F = 4\mathcal{D}_{1/2} \oplus 4\tilde{\mathcal{D}}_0 \,. \tag{5.24}$$

We see the fermionic part breaks into 4 spin-1/2 representations and 4 singlets of $sl(2)$. We can do a similar state counting here. From (5.23), there are $3+2\times 2+5\times 1 = 12$ bosonic states. From (5.24), there are $4\times 2 + 4\times 1 = 12$ fermionic states, which is the same as the number of bosonic states.

5.3.3.3 Non-principal embedding II : $\mathcal{K} = sl(1|2)$

In this section, we consider the case of $\mathcal{K} = sl(1|2)$. This embedding reads

$$\frac{\mathbf{Ad}[sl(3|2)]}{sl(1|2)} = \mathcal{R}'_1 \oplus 5\mathcal{R}_{1/2} \oplus 4\mathcal{R}_0 \,. \tag{5.25}$$

We can again decompose the bosonic subalgebra into spin-s representations $\mathcal{D}_s$ of $sl(2,\mathbb{R})$

$$\mathbf{Ad}[sl(3|2)]\big|_B = \mathcal{D}'_1 \oplus 9\mathcal{D}_0 \,. \tag{5.26}$$

Thus we learn that under this embedding, the bosonic subalgebra $sl(2)$ gives the only spin-1 representation, corresponding to the gravitational sector, and the $sl(3)$ subalgebra decomposes to 9 singlets.

The decomposition of the fermionic part in this $osp(1|2)$ embedding reads

$$\mathbf{Ad}[sl(3|2)]\big|_F = 6\mathcal{D}_{1/2} \,. \tag{5.27}$$

This means that there are 6 spin-1/2 representations. From (5.26), there are $3+9\times1 = 12$ bosonic states. From (5.27), there are $6 \times 2 = 12$ fermionic states, which agrees with the number of bosonic states.

5.4 The asymptotic symmetry

Following the procedure in [67, 68] for the bosonic case and [70] in the supersymmetric case, we can derive the asymptotic symmetries corresponding to the 3 different embeddings that we presented in section 5.3.3.1, 5.3.3.2, and 5.3.3.3.

5.4.1 The asymptotic symmetry of the principal embedding

We want to find the asymptotic symmetry algebra corresponding to the principal embedding. This can be done by a truncation of the result in [70]. The important

lessons from that computation are (i) the asymptotic symmetry corresponding to the principal embedding being the super-$\mathcal{W}_3$ algebra [145] and (ii) the value of the central charge being $c = 18k_{CS}$.

In the next two sections, we proceed to compute the asymptotic symmetry algebra following the exact procedure of [68, 70].

5.4.2 The asymptotic symmetry of the non-principal embedding I

Motivated by (5.22), we realize the non-principal embedding in section 5.3.3.2 by giving explicit expressions for the generators of the different $osp(1|2)$ representations in (5.22). We spare the reader for the concrete matrix realizations. Symbolically, the $\{\hat{L}_{-1}, \hat{L}_0, \hat{L}_1\}$ generate the $sl(2)$ subalgebra. The $\{\hat{M}_{-1/2}, \hat{M}_{1/2}\}$ and $\{\hat{N}_{-1/2}, \hat{N}_{1/2}\}$ form 2 bosonic spin-1/2 representations of the $sl(2)$ and the $\hat{J}_i$, $i = 1, ..., 5$ are the 5 $sl(2)$ singlets.

Now we can perform the standard procedure to get the asymptotic symmetry algebra. We expand the gauge connections in terms of the above generators

$$\begin{aligned}
\Gamma &= \Gamma_+ dx^+ + \Gamma_- dx^- + \Gamma_\rho d\rho, \\
\Gamma_+ &= e^{-\rho \hat{L}_0}\, \gamma\, e^{\rho \hat{L}_0}, \qquad \Gamma_\rho = e^{-\rho \hat{L}_0}\, \partial_\rho e^{\rho \hat{L}_0}, \qquad \Gamma_- = 0\,, \\
\gamma &= \hat{L}_1 + \frac{2\pi}{k_{CS}} \mathcal{L} \hat{L}_{-1} + \frac{2\pi}{k_{CS}} (\mathcal{M} \hat{M}_{-1/2} + \mathcal{N} \hat{N}_{-1/2} + \sum_{i=1}^{5} \mathcal{J}_i \hat{J}_i) \\
&\quad + \frac{2\pi}{k_{CS}} (\sum_{i=-1,-2,1,2} \mathcal{G}_i \hat{G}^i_{-1/2} + \sum_{i=1}^{4} \mathcal{X}_i \hat{X}_i)\,,
\end{aligned} \tag{5.28}$$

where all the fields, denoted by calligraphic letters, only depend on x^+. Following the procedure in [70], we find the asymptotic symmetry algebra corresponding to the

non-principal embedding (5.22). With the following mode expansions

$$\mathcal{L}(\phi) = \frac{1}{2\pi}\sum_n L_n e^{in\phi}\,, \qquad \mathcal{J}_a(\phi) = \frac{1}{2\pi}\sum_n J^a_n e^{in\phi}\,, \qquad \mathcal{X}_a(\phi) = \frac{1}{2\pi}\sum_n X^a_n e^{in\phi}\,,$$
$$\mathcal{G}_j(\phi) = \frac{1}{2\pi}\sum_n G^j_n e^{in\phi}\,, \qquad \bar{\mathcal{G}}_j(\phi) = \frac{1}{2\pi}\sum_n \bar{G}^j_n e^{in\phi}\,,$$
$$\mathcal{M}_j(\phi) = \frac{1}{2\pi}\sum_n M^j_n e^{in\phi}\,, \qquad \mathcal{N}_j(\phi) = \frac{1}{2\pi}\sum_n N^j_n e^{in\phi}\,.$$

We compute the commutation relations that agrees with the non-linear $u(2|1)$-extended superconformal algebra discovered in [154]. To match our result with the expressions in [154], we employ the following dictionary

$$\mathcal{J}_1 \to \Sigma^{11}, \qquad \mathcal{J}_2 \to \Sigma^{12}, \qquad \mathcal{J}_3 \to \Sigma^{21}, \qquad \mathcal{J}_4 \to \Sigma^{22},$$
$$\mathcal{J}_5 \to \Sigma^{33}, \qquad \mathcal{X}_1 \to \Sigma^{13}, \qquad \mathcal{X}_2 \to \Sigma^{31}, \qquad \mathcal{X}_3 \to \Sigma^{23}, \qquad \mathcal{X}_4 \to \Sigma^{32}\,,$$
$$\mathcal{G}_i \to G^i, \quad i = 1, 2\,, \qquad \mathcal{G}_i \to \bar{G}^{-i}, \quad i = -1, -2\,, \quad \mathcal{N} \to G^3\,, \quad \mathcal{M} \to \bar{G}^3, \tag{5.29}$$

at the following value of the parameters in [154]

$$\kappa = k_{CS}\,, \qquad \kappa' = k_{CS}\,, \qquad \epsilon = 0\,, \qquad \phi = -2\,, \qquad \phi' = -1\,, \qquad a = -2k_{CS}\,.$$

As stated in [154], the resulting algebra is a nonlinear superconformal algebra (SCA) with $u(2|1)$-supersymmetry. We call this algebra $u(2|1)$-SCA. The spin-1 currents $\mathcal{J}_{1\ldots5}$, $\mathcal{X}_{i=1,4}$ fall into the adjoint representation of the Lie superalgebra $u(2|1)$. The multiplet $(\mathcal{G}_1, \mathcal{G}_2, \mathcal{N})$ and $(\mathcal{G}_{-1}, \mathcal{G}_{-2}, \mathcal{M})$ are the fundamental and anti-fundamental representations of the $u(2|1)$ respectively. The spin-2 field $\mathcal{L}$ is a singlet of $u(2|1)$. The central charge of this algebra is $c = 12\,\mathrm{STr}(\hat{L}_0^2)\,(k_{CS}) = 6\,k_{CS}$.

• **The quantum algebra.** Note that what we have derived here is the classical version of the $\mathcal{N} = 2$ super-conformal algebra with quadratic non-linearity [154]. To get the full quantum algebra, we require all the commutators to satisfy the Jacobi

identities. We can start with our classical result, set all coefficients of the non-linear commutators as well as the central charge as independent parameters. Requiring this ansatz to satisfy the Jacobi identities yields the full quantum algebra. The result turns out to be the same as those presented in [154], which is not surprising since our classical solution coincides with the ansatz in [154]. The key result for us is the new quantum corrected central charge

$$c = 6k_{CS} + 3\,. \tag{5.30}$$

For the full algebra that satisfying the Jacobi identities, we refer the reader to [154].

5.4.3 The asymptotic symmetry of the non-principal embedding II

The non-principal embedding (5.25) similar to the last section. One difference of this embedding is that the super-trace $\mathrm{STr}L_0^2 < 0$. Then from the relation (5.15), keeping k_{CS} unchanged means ℓ changes sign. But this is fine: ℓ itself is not so important since it is related to the cosmological constant by $\Lambda = -\frac{2}{\ell^2}$, so it is $|\ell|$ that represents the AdS radius.

A more convenient way to understand this extra minus sign goes like this. After we get the embedding (5.25), we turn off all other fields and leave only the gravitational sector. The resulting action of the higher-spin theory[6]

$$I_{HS}^{(2)} = I_{CS}^{(2)}(\Gamma, k_{CS}) - I_{CS}^{(2)}(\tilde{\Gamma}, k_{CS})\,, \tag{5.31}$$

is the same as the Einstein-Hilbert action (4.9). However, as discussed above, $\ell < 0$ for this non-principal embedding. This means the relation between the gauge fields

[6]The superscript "(2)" represents the fact that only the spacetime spin-2 sector is left after the truncation.

and the vielbeins are

$$\Gamma^{(2)} = \omega^{(2)} - \frac{1}{|\ell|} e^{(2)} \,, \qquad \tilde{\Gamma}^{(2)} = \omega^{(2)} + \frac{1}{|\ell|} e^{(2)} \,. \tag{5.32}$$

This looks a little unfamiliar comparing with the more conventional (4.8) where $\ell > 0$ by default and is interpreted as the AdS radius. Then it is natural to consider the following rewriting of the action (5.31)

$$I^{(2)}_{HS} = I^{(2)}_{CS}(\Gamma', -k_{CS}) - I^{(2)}_{CS}(\tilde{\Gamma}', -k_{CS}) \,, \tag{5.33}$$

where $\Gamma' = \tilde{\Gamma}$ and $\tilde{\Gamma}' = \Gamma$. This is identical to the original formula (5.31) and we simply switch the role of the Γ and $\tilde{\Gamma}$. The benefit of this rewriting is that the relations between the new gauge connection $\Gamma'^{(2)}$ ($\tilde{\Gamma}'^{(2)}$) and the vielbein/spin-connection take the conventional form as (4.8)

$$\Gamma'^{(2)} = \omega^{(2)} + \frac{1}{|\ell|} e^{(2)} \,, \qquad \tilde{\Gamma}'^{(2)} = \omega^{(2)} - \frac{1}{|\ell|} e^{(2)} \,. \tag{5.34}$$

After this redefinition, nothing is special for this embedding except for the minus sign in front of the k_{CS} in (5.33). This minus sign is crucial to get the correct expression for the central charge in the later computation.

This rewriting (5.33) should be carried over to the full higher-spin gauge connections for consistency and we will use the relabeled gauge connections Γ' and $\tilde{\Gamma}'$ to do all the following computations. But to simpify the notation, we drop the "$'$" everywhere. Then the computation can be carried out in exactly the same was as in the previous two subsections with only one important thing to keep in mind: the Chern-Simons level used in this computation becomes $-k_{CS}$. Now we carry out the explicit computation. The super-connection takes the general form as in (5.28) after

imposing the asymptotic AdS boundary condition gauge fixing

$$\begin{aligned}
\Gamma &= \Gamma_+ dx^+ + \Gamma_- dx^- + \Gamma_\rho d\rho, \\
\Gamma_+ &= e^{-\rho \hat{L}_0}\, \gamma\, e^{\rho \hat{L}_0}, \qquad \Gamma_\rho = e^{-\rho \hat{L}_0}\, \partial_\rho e^{\rho \hat{L}_0}, \qquad \Gamma_- = 0\,, \\
\gamma &= \hat{L}_{-1} + \frac{2\pi}{-k_{CS}} \left(\mathcal{L} \hat{L}_1 + \sum_{i=1}^{9} \mathcal{J}_i\, \hat{J}_i + \sum_{i=-1,-2,-3,1,2,3} \mathcal{G}_i\, \hat{G}^i_{1/2} \right).
\end{aligned}$$

After field redefinitions

$$\mathcal{G}_i \to \bar{\mathcal{S}}_i\,, \quad i = 1..3\,, \qquad \mathcal{G}_i \to \mathcal{S}_{-i}, \quad i = -1..-3\,, \tag{5.35}$$

and a mode expansion

$$\begin{aligned}
\mathcal{L}(\phi) &= \frac{1}{2\pi} \sum_n L_n e^{in\phi}\,, \qquad \mathcal{J}_a(\phi) = \frac{1}{2\pi} \sum_n J^a_n e^{in\phi}\,, \\
\mathcal{S}_j(\phi) &= \frac{1}{2\pi} \sum_j S^j_n e^{in\phi}\,. \qquad \bar{\mathcal{S}}_j(\phi) = \frac{1}{2\pi} \sum_j \bar{S}^j_n e^{in\phi}\,,
\end{aligned}$$

we get the asymptotic algebra following the procedure used in the previous section, and we find the central charge to be related to k_{CS} by $c = 12\,\mathrm{STr}(\hat{\hat{L}}_0^2)\,(-k_{CS}) = 6\,k_{CS}$.

Remarkably, this algebra is precisely the 2-dimensional nonlinear superconformal algebra with $u(3)$-supersymmetry [155, 156]. We call this algebra $u(3)$-SCA. To compare with the results in [156], we can use the following dictionary

$$A^a \to \lambda^a\,, \quad \mathcal{J}_a \to W_a\,, \quad \mathcal{S}_i \to G_i\,, \quad \bar{\mathcal{S}}_i \to \bar{G}_i$$

and the value of the parameter

$$B = 2\,, \qquad 2k_{CS} = S = S_0\,.$$

The spin-1 currents form the adjoint representation of the $u(3)$ symmetry algebra,

and $\mathcal{S}_i$ and $\bar{\mathcal{S}}_i$ are the fundamental and anti-fundamental representations of the $u(3)$ algebra respectively. Once again, the spin-2 field $\mathcal{L}$ is a singlet of $u(3)$.

• **The quantum algebra.** As in the previous case, the above algebra we derived is a classical version of the algebra in [157, 155, 156]. We follow the same procedure to solve the Jacobi identities and since our classical solution once again coincides with the ansatz in [155, 156], the quantum algebra agrees with the result in [155, 156]. The key result for us is the new quantum corrected central charge

$$c = \frac{6k_{CS}^2 + 13k_{CS} + 2}{k_{CS} + 2}\,. \tag{5.36}$$

For the full algebra that satisfying the Jacobi identities, we refer the reader to [155, 156].

Summary: In this section, we have computed the asymptotic symmetries corresponding to the different $osp(1|2)$ embeddings. The results of this section can be summarized in the following table

embedding	asymptotic symmetry	central charge	known results
principal embedding (5.18)	super-$\mathcal{W}_3$	$c = 18k_{CS}$	[158, 159, 145, 160]
non-principal embedding (5.22)	$u(2\|1)$-SCA	$c = 6k_{CS}$	[154]
non-principal embedding (5.25)	$u(3)$-SCA	$c = 6k_{CS}$	[157, 155, 156]

Table 5.1: This table lists the asymptotic symmetries (column 2) corresponding to the different $osp(1|2)$ embeddings (column 1). The central charges of each of the asymptotic symmetries are given in the third column.

Further notice that the two different non-principal embeddings really give two different theories. This is because

1. The spectra of the asymptotic states are different. In the non-principal embedding (5.22), which is denoted as $\text{AdS}^{(1)}$, there are states with "wrong" statistics: the bosonic fields $\mathcal{M}$, $\mathcal{N}$ with spin $s = 1/2$ and the fermionic fields $\mathcal{X}_i$, $i = 1, ..., 4$ with spin $s = 0$. However, all fields in the non-principal embedding (5.25) have "correct" statistics.

2. When we were deriving the asymptotic symmetry, which describes the global symmetry of the asymptotic AdS_3 spacetime, we imposed different boundary conditions for the different embeddings. This is reflected in the different forms of the asymptotic AdS_3 connections (5.28) and (5.35) since their forms are determined by the boundary condition.

3. The asymptotic symmetries of the three different embeddings are different. This gives a hint that the dual CFTs should also be different.

5.5 Geometry corresponding to the different embeddings

In the previous sections, we have studied different $osp(1|2)$ embeddings of the $sl(3|2)$ higher-spin supergravity. Physically, this means identifying different states in the higher-spin theory as the gravity sector. In other words, we have identified different fields with vielbeins and spin connections in different embeddings. Thus if we consistently turn off all fields other than the gravity sector, each embedding admits a vacuum solution of the higher-spin theory. This means the $sl(3|2)$ higher-spin supergravity possesses three vacua configurations.[7] Each vacuum solution is obtained by solving the vacuum Einstein equation, which is the flatness condition in the Chern-Simons language

$$d\Gamma + \Gamma \wedge \Gamma = 0\,, \qquad d\tilde{\Gamma} + \tilde{\Gamma} \wedge \tilde{\Gamma} = 0\,, \tag{5.37}$$

[7] We will shortly show that the three vacua are different.

where the gauge connection Γ, $\tilde{\Gamma}$ contains only the gravity sector with all other fields turned off. The AdS vacuum sulotion reads

$$\Gamma_{\rm AdS} = e^{\rho} L_1 dx^+ + L_0 d\rho\,, \qquad \tilde{\Gamma}_{\rm AdS} = -e^{\rho} L_{-1} dx^- - L_0 d\rho \tag{5.38}$$

where $L_{0,\pm 1}$ are the gravitational $sl(2,\mathbb{R})$ generators for each $osp(1|2)$ embedding.

In this section, we will discuss the properties of the AdS vacua and the relations among them.

5.5.1 AdS vacua corresponding to different embeddings

For the three different embeddings, the metrics of the AdS vacuum of the three corresponding embeddings all take the standard form:

$$ds^2 = \ell_i^2 (d\rho^2 - e^{2\rho} dx_+ dx_-)\,, \qquad i = p, 1, 2\,. \tag{5.39}$$

They represent AdS_3 vacua with AdS radius ℓ_{AdS} being $|\ell_p|$, $|\ell_1|$, $|\ell_2|$ respectively.

As discussed earlier in section 5.3.2, we fix the k_{CS} in different embeddings, which leads to different AdS radii for different embeddings. In our specific case, we have

$$4\, G_3\, k_{CS} = \frac{\ell_p}{\mathrm{STr}(L_0^2)} = \frac{\ell_1}{\mathrm{STr}(\hat{L}_0^2)} = \frac{\ell_2}{\mathrm{STr}(\hat{\hat{L}}_0^2)}\,. \tag{5.40}$$

Following the definition (5.10), the super-traces can be computed as

$$\mathrm{STr}(L_0^2) = \frac{3}{2}\,, \qquad \mathrm{STr}(\hat{L}_0^2) = \frac{1}{2}\,, \qquad \mathrm{STr}(\hat{\hat{L}}_0^2) = -\frac{1}{2}\,. \tag{5.41}$$

Then the AdS radii corresponding to the two non-principal embeddings are 1/3 of the AdS radius of the principal embedding.

5.5.2 RG flows between different AdS vacua

In this subsection, we will show that the theories derived from different embeddings are related by RG flows. We will identify the two non-principal embeddings as two UV theories and the principal embedding as an IR theory. We will construct interpolation solutions from each UV vacuum to the IR vacuum. Then we verify our proposal by showing that the solution flow to the UV vacuum at $\rho \to \infty$ and to the IR vacuum at $\rho \to -\infty$, which is similar to the construction in [86].

Before doing that, we want to address the motivation of the RG flow. We understand the holographic RG flow in the following sense

1. From what we will show next, we can explicitly construct solutions of the Chern-Simons equation of motion (5.37) that interpolate between different AdS vacua. This is the conventional treatment of the holographic RG flow.

2. As mentioned at the end of the previous section, different embeddings give different theories. So the interpolation solutions are not trivial field relabeling since they connect distinct theories.

3. From the dual CFT point of view, we will find operators triggering the RG flows by analyzing the asymptotics of the interpolation solutions.

To simplify our notation, we call the vacuum corresponding to the principal embedding $\text{AdS}^{(\text{p})}$, the vacuum corresponding to the embedding (5.22) $\text{AdS}^{(1)}$ and the vacuum corresponding to the embedding (5.25) $\text{AdS}^{(2)}$.

5.5.2.1 RG flow from UV vacuum $\text{AdS}^{(1)}$ to the IR vacuum $\text{AdS}^{(\text{p})}$

To find the relation between different AdS vacua, we construct solutions of the equation of motion (5.37) interpolating between them. Unlike the bosonic case, the $sl(2)$ generators $L_0,\ \hat{L}_0,\ \hat{\hat{L}}_0$ of different embeddings are not proportional to each other, so the simple solution in [86] does not hold in the current supersymmetric case.

As a result, we consider the solution

$$\Gamma = \mu\bigg((\frac{16}{9}e^{e^\rho/2+\rho} - \frac{4}{9}e^\rho)L_1 - \frac{4}{3}(e^{e^\rho/2+\rho} - e^\rho)K_1\bigg)dx^+ + e^{e^\rho+2\rho}\hat{L}_1 dx^- + (L_0 + e^\rho\hat{L}_0)d\rho \quad (5.42)$$
$$\tilde{\Gamma} = -\mu\bigg((\frac{16}{9}e^{e^\rho/2+\rho} - \frac{4}{9}e^\rho)L_{-1} - \frac{4}{3}(e^{e^\rho/2+\rho} - e^\rho)K_{-1}\bigg)dx^- - e^{e^\rho+2\rho}\hat{L}_{-1}dx^+ - (L_0 + e^\rho\hat{L}_0)d\rho\,.$$

Note that the μ is an arbitrary constant parameter. In the $\rho \to \infty$ limit, we have $e^\rho \gg \rho$, $e^{e^\rho} \gg e^{e^\rho/2}$, so the dominant terms in the above solution are

$$\begin{aligned} \Gamma &= e^{e^\rho}\hat{L}_1 dx^- + e^\rho\hat{L}_0 d\rho\,, \\ \tilde{\Gamma} &= -e^{e^\rho}\hat{L}_{-1}dx^+ - e^\rho\hat{L}_0 d\rho\,. \end{aligned} \quad (5.43)$$

We can define $\tilde{\rho} = e^\rho$, then the above result reads

$$\begin{aligned} \Gamma &= e^{\tilde{\rho}}\hat{L}_1 dx^- + \hat{L}_0 d\tilde{\rho}\,, \\ \tilde{\Gamma} &= -e^{\tilde{\rho}}\hat{L}_{-1}dx^+ - \hat{L}_0 d\tilde{\rho}\,, \end{aligned} \quad (5.44)$$

which is the standard AdS vacuum (5.38) after switching x^+ with x^-. This means the interpolation solution (5.42) approaches to the $\mathrm{AdS}^{(1)}$ vacuum in the UV.

In the $\rho \to -\infty$ limit, we have $e^\rho \to 0$, $e^\rho \gg e^{2\rho}$, so the solution (5.42) reads

$$\begin{aligned} \Gamma &= \frac{4}{3}\,\mu\, e^\rho L_1 dx^+ + L_0 d\rho\,, \\ \tilde{\Gamma} &= -\frac{4}{3}\mu\, e^\rho L_{-1}dx^- - L_0 d\rho\,. \end{aligned} \quad (5.45)$$

Then a shift $\rho \to \tilde{\rho} = \rho + \ln\frac{4\mu}{3}$ will take it to the standard form (5.38). This means the interpolation solution (5.42) approaches the $\mathrm{AdS}^{(\mathrm{p})}$ vacuum in the IR.

Further, notice that the interpolation only flows in one direction: we cannot find a solution that approaches the $\mathrm{AdS}^{(\mathrm{p})}$ at large ρ and approaches to $\mathrm{AdS}^{(1)}$ vacuum

at small ρ.[8]

5.5.2.2 RG flow from UV vacuum AdS$^{(2)}$ to the IR vacuum AdS$^{(p)}$

For this case, we consider the solution[9]

$$\begin{aligned}\Gamma &= \Big(\frac{1}{3}(4e^{\mu\rho}-e^{e^\rho+\mu\rho})L_1-(e^{\mu\rho}-e^{e^\rho+\mu\rho})K_1\Big)dx^+ + (\mu L_0+e^\rho\hat{\hat{L}}_0)d\rho\,,\\ \tilde{\Gamma} &= -\Big(\frac{1}{3}(4e^{\mu\rho}-e^{e^\rho+\mu\rho})L_{-1}-(e^{\mu\rho}-e^{e^\rho+\mu\rho})K_{-1}\Big)dx^- - (\mu L_0+e^\rho\hat{\hat{L}}_0)d\rho\,,\end{aligned} \tag{5.46}$$

In the limit $\rho\to\infty$, the above solution approaches to

$$\begin{aligned}\Gamma &= \Big(-\frac{1}{3}e^{e^\rho}L_1+e^{e^\rho}K_1\Big)dx^+ + e^\rho\hat{\hat{L}}_0 d\rho\,,\\ \tilde{\Gamma} &= \Big(\frac{1}{3}e^{e^\rho}L_{-1}-e^{e^\rho}K_{-1}\Big)dx^- - e^\rho\hat{\hat{L}}_0 d\rho\,,\end{aligned} \tag{5.47}$$

Notice that since $\hat{\hat{L}}_{\pm1}=K_{\pm1}-\frac{1}{3}L_{\pm1}$, we can rewrite the above result as

$$\begin{aligned}\Gamma &= e^{e^\rho}\hat{\hat{L}}_1 dx^+ + e^\rho\hat{\hat{L}}_0 d\rho\,,\\ \tilde{\Gamma} &= -e^{e^\rho}\hat{\hat{L}}_{-1}dx^- - e^\rho\hat{\hat{L}}_0 d\rho\,,\end{aligned} \tag{5.48}$$

which gives the standard form (5.38) after the redefinition $\tilde{\rho}=e^\rho$.

In the limit $\rho\to-\infty$, the solution (5.46) approaches to

$$\begin{aligned}\Gamma &= e^{\mu\rho}L_1 dx^+ + \mu\, L_0 d\rho\,,\\ \tilde{\Gamma} &= -e^{\mu\,\rho}L_{-1}dx^- - \mu\, L_0 d\rho\,.\end{aligned} \tag{5.49}$$

[8]For example, if we naively change e^ρ to $e^{-\rho}$ in the $d\rho$ term of (5.42), then the solution does not flow to the desired AdS vacuum solution at least in one of the two limits.

[9]We do not find interpolation solutions with UV and IR generators in different components, namely with both dx^+ and dx^- non-vanishing as (5.42).

Then a rescaling $\rho \to \tilde{\rho} = \mu\rho$ gives the standard gauge connection for the AdS vacuum

$$\begin{aligned} \Gamma &= e^{\tilde{\rho}} L_1 dx^+ + L_0 d\tilde{\rho} \\ \tilde{\Gamma} &= -e^{\tilde{\rho}} L_{-1} dx^- - L_0 d\tilde{\rho} \,. \end{aligned} \tag{5.50}$$

As shown in the previous subsection, a key point for us to understand this solution as an RG flow is that it is a one-direction flow: we do not find a solution which approaches the $\mathrm{AdS}^{(\mathrm{p})}$ vacuum in the $\rho \to \infty$ limit and approaches the $\mathrm{AdS}^{(2)}$ vacuum in the $\rho \to -\infty$ limit.

5.5.2.3 Interpolations between the two UV vacua $\mathbf{AdS}^{(1)}$ and $\mathbf{AdS}^{(2)}$

We can also find interpolation solutions between $\mathrm{AdS}^{(1)}$ and $\mathrm{AdS}^{(2)}$. But they should not be understood as RG flows: there are solutions interpolating in both the two directions. Consider the following interpolation solution

$$\begin{aligned} \Gamma &= e^{a(\rho)} \hat{L}_1 dx^+ + e^{b(\rho)} \hat{\hat{L}}_1 dx^- + \big(a'(\rho)\hat{L}_0 + b'(\rho)\hat{\hat{L}}_0\big) d\rho \,, \\ \tilde{\Gamma} &= -e^{a(\rho)} \hat{L}_{-1} dx^+ - e^{b(\rho)} \hat{\hat{L}}_{-1} dx^- - \big(a'(\rho)\hat{L}_0 + b'(\rho)\hat{\hat{L}}_0\big) d\rho \,, \end{aligned} \tag{5.51}$$

where $a(\rho)$ and $b(\rho)$ are arbitrary functions of ρ.

• Interpolating from $\mathrm{AdS}^{(1)}$ to $\mathrm{AdS}^{(2)}$ as ρ decreases.

Now consider $a(\rho) = e^{\rho}$ and $b(\rho) = e^{-\rho}$, then at $\rho \to \infty$, $a(\rho) \gg b(\rho)$, $e^{a(\rho)} \gg e^{b(\rho)}$ and the solution (5.51) approaches $\mathrm{AdS}^{(1)}$ after a field redefinition $\rho \to \tilde{\rho} = e^{\rho}$

$$\begin{aligned} \Gamma &= e^{\tilde{\rho}} \hat{L}_1 dx^+ + \hat{L}_0 d\tilde{\rho} \,, \\ \tilde{\Gamma} &= -e^{\tilde{\rho}} \hat{L}_{-1} dx^+ - \hat{L}_0 d\tilde{\rho} \,. \end{aligned} \tag{5.52}$$

In the $\rho \to -\infty$ limit, $a(\rho) \ll b(\rho)$, $e^{a(\rho)} \ll e^{b(\rho)}$ and the solution (5.51) approaches

$\mathrm{AdS}^{(2)}$ after a field redefinition $\rho \to \tilde{\rho}' = e^{-\rho}$

$$\begin{aligned} \Gamma &= e^{\tilde{\rho}'} \hat{L}_1 dx^+ + \hat{L}_0 d\tilde{\rho}' \,, \\ \tilde{\Gamma} &= -e^{\tilde{\rho}'} \hat{L}_{-1} dx^+ - \hat{L}_0 d\tilde{\rho}' \,. \end{aligned} \tag{5.53}$$

• Interpolating from $\mathrm{AdS}^{(2)}$ to $\mathrm{AdS}^{(1)}$ as ρ decreases.

Now consider $a(\rho) = e^{-\rho}$ and $b(\rho) = e^{\rho}$, then at $\rho \to \infty$, $a(\rho) \ll b(\rho)$, $e^{a(\rho)} \ll e^{b(\rho)}$ and the solution (5.51) approaches $\mathrm{AdS}^{(2)}$ after a field redefinition $\rho \to \tilde{\rho} = e^{\rho}$

$$\begin{aligned} \Gamma &= e^{\tilde{\rho}} \hat{L}_1 dx^+ + \hat{L}_0 d\tilde{\rho} \,, \\ \tilde{\Gamma} &= -e^{\tilde{\rho}} \hat{L}_{-1} dx^+ - \hat{L}_0 d\tilde{\rho} \,. \end{aligned} \tag{5.54}$$

In the limit $\rho \to -\infty$, $a(\rho) \gg b(\rho)$, $e^{a(\rho)} \gg e^{b(\rho)}$ and the solution (5.51) approaches $\mathrm{AdS}^{(1)}$ after a field redefinition $\rho \to \tilde{\rho}' = e^{-\rho}$

$$\begin{aligned} \Gamma &= e^{\tilde{\rho}'} \hat{L}_1 dx^+ + \hat{L}_0 d\tilde{\rho}' \,, \\ \tilde{\Gamma} &= -e^{\tilde{\rho}'} \hat{L}_{-1} dx^+ - \hat{L}_0 d\tilde{\rho}' \,. \end{aligned} \tag{5.55}$$

The origin of the existence of interpolations in both the two directions is the following commutators

$$[\hat{L}_0, \hat{\hat{L}}_{\pm 1}] = 0 \,, \qquad [\hat{\hat{L}}_0, \hat{L}_{\pm 1}] = 0 \,. \tag{5.56}$$

This means the $sl(2,\mathbb{R})$ generators of these two embeddings decouple and the solution (5.51) is really a "direct sum" of two mutually commuting solutions

$$\Gamma = \Gamma^{(1)} + \Gamma^{(2)} \,, \qquad \tilde{\Gamma} = \tilde{\Gamma}^{(1)} + \tilde{\Gamma}^{(2)} \,, \tag{5.57}$$

where

$$\Gamma^{(1)} = e^{a(\rho)}\hat{L}_1 dx^+ + a'(\rho)\hat{L}_0 d\rho\,, \quad \Gamma^{(2)} = e^{b(\rho)}\hat{\bar{L}}_1 dx^- + b'(\rho)\hat{\bar{L}}_0 d\rho\,,$$
$$\tilde{\Gamma}^{(1)} = -(e^{a(\rho)}\hat{L}_{-1} dx^+ + a'(\rho)\hat{L}_0 d\rho)\,, \quad \tilde{\Gamma}^{(2)} = -(e^{b(\rho)}\hat{\bar{L}}_{-1} dx^- + b'(\rho)\hat{\bar{L}}_0 d\rho)\,.$$

In this language, the commutators (5.56) translate to

$$\Gamma^{(1)} \wedge \Gamma^{(2)} = 0\,, \tag{5.58}$$

which allows $\Gamma^{(1)}$, $\Gamma^{(2)}$ and Γ to be flat connections simultaneously. This gives another piece of evidence showing that the two non-principal embeddings give two different theories at UV.[10] We are free to tune $a(\rho)$ and $b(\rho)$ independently, and as shown above, we can interpolate between the two AdS vacua in both directions with special choices of $a(\rho)$ and $b(\rho)$.

Actually, we can further rewrite (5.57) in the following way

$$\Gamma^{(1)} = e^{a(\rho)}\hat{L}_1 dx^+ + \hat{L}_0 d\,a(\rho)\,, \quad \Gamma^{(2)} = e^{b(\rho)}\hat{\bar{L}}_1 dx^- + \hat{\bar{L}}_0 d\,b(\rho)\,, \tag{5.59}$$
$$\tilde{\Gamma}^{(1)} = -(e^{a(\rho)}\hat{L}_{-1} dx^+ + \hat{L}_0 d\,a(\rho))\,, \quad \tilde{\Gamma}^{(2)} = -(e^{b(\rho)}\hat{\bar{L}}_{-1} dx^- + \hat{\bar{L}}_0 d\,b(\rho))\,. \tag{5.60}$$

Hence we see that $(A^{(1)}, \bar{A}^{(1)})$ describes an AdS_3 vacuum with radial coordinate $\tilde{\rho} = a(\rho)$, and $(A^{(2)}, \bar{A}^{(2)})$ describes an AdS_3 vacuum with radial coordinate $\tilde{\rho} = b(\rho)$. Therefore the solution (5.51) is a trivial combination of two independent solutions and do not behave as a standard RG flow.

Alternatively, the existence of interpolations in both the two directions might be understood as an RG cycle. As we will show in section 5.5.6, the UV theories in our discussion are non-unitary so the c-theorem, which requires unitarity of the CFT,

[10] This is because the two UV theories being the same means $\Gamma^{(1)} \sim \Gamma^{(2)}$ up to relabeling, then the flat condition (or equation of motion) should read $d\Gamma^{(1)} + \Gamma^{(1)} \wedge \Gamma^{(2)} = 0$ with an extra $d\Gamma^{(1)}$ term.

does not forbid the existence of such an RG cycle.[11] Note that our observation in this section does not behave in the same way as the limit cycles in 4D [161, 162]: our interpolation is constructed from two RG flows, each ending at a CFT. In addition, we have to turn on chemical potentials to trigger each of the constituent RG flows. Therefore, the conclusion in [163] (as well as in the updated version of [162]) that the limit cycles are equivalent to conformal fixed points does not apply to our observation.

Summary: From the explicit computations we have done in this section, we show that the two non-principal embeddings give two UV theories that flow to the IR theory corresponding to the principal embedding. Thus we find a duality between the two UV theories in the sense that they flow to the same IR theory provided that some chemical potentials or operator perturbations are turned on.

5.5.3 Comparison with the bosonic spin-3 gravity

In this subsection, we want to investigate the relation between our results and the results in [86]. It is well understood that the principal embedding in our discussion is the $\mathcal{N} = 2$ supersymmetric extension of the principal embedding into the $sl(3)$ algebra. We claim that our non-principal embedding I, namely the $\text{AdS}^{(1)}$, in section 5.3.3.2 is a direct supersymmetrization of the diagonal embedding in [86]. The evidence is as follows

1. From the embedding itself, we can truncate our non-principal embedding I in 5.3.3.2 to the diagonal embedding of $sl(3)$ discused in [86]. We can truncate our result in two steps: first, turn off all the fermionic part of the $sl(3|2)$ superalgebra, which means we neglect (5.24); second, truncate out the $sl(2) \oplus u(1)$ part of the bosonic subalgebra (5.19), which means we drop the $3\mathcal{D}'_0 \oplus \mathcal{D}_0$ representations of the decomposition (5.23). Then the resulting decomposition of the $sl(3)$ algebra from the truncation of (5.23) reads $sl(3) = \mathcal{D}_1 \oplus 2\tilde{\mathcal{D}}_{1/2} \oplus \mathcal{D}_0$.

[11] We thank Thomas Hartman for suggesting this interpretation to us.

This is precisely the decomposition obtained from the diagonal embedding of $sl(3)$ discussed in [86].

2. The RG flow solution (5.42) is similar to the RG solution in the bosonic case in the sense that the UV generators and the IR generators sit in opposite-chirality-components of the solution. In other words, the chemical potential term is separable from the AdS_3 vacuum solution in the UV.

While using a similar reasoning, we conclude that our non-principal embedding II, namely $AdS^{(2)}$, in section 5.3.3.3 is a new result due to the presence of supersymmetry and has no counterpart in the bosonic case. The argument goes as

1. If we consider a similar truncation of the non-principal embedding II (5.25), we reach the decomposition $sl(3) = 8\mathcal{D}_0$. This is not observed in the bosonic case since this embedding is trivial and no spin-1 representation of the $sl(2)$, who has spacetime spin-2, is present. The resulting theory will not contain the gravity sector and thus should not be considered in the discussion in [86].

2. The RG solution (5.46) looks very different from that in the bosonic case since there is only a dx^+ component and the perturbations are not manifestly separable as in the bosonic case.

Therefore, we conclude that the non-principal $osp(1|2)$ embedding of $sl(3|2)$ in section 5.3.3.2, i.e. $AdS^{(1)}$, is a simple supersymmetric extension of the diagonal $sl(2)$ embedding of $sl(3)$ in [86]. While the other non-principal $osp(1|2)$ embedding of $sl(3|2)$ in section 5.3.3.3, i.e. $AdS^{(2)}$, is brought to us purely by supersymmetry. As a result, the duality we have claimed at the end of the previous subsection is also a bonus relation of supersymmetry.

The origin of this duality is not clear at this moment, but it must have something to do with the structure of the Lie superalgebra $sl(n|n-1)$. The bosonic subalgebra

of $sl(n|n-1)$ lookes like $sl(n|n-1)\big|_B = sl(n) \oplus sl(n-1) \oplus u(1)$. And the two sides of the duality correspond to identifying the (bosonic) gravitational $sl(2)$ subalgebra from $sl(n)$ and $sl(n-1)$, respectively. This is at least true for the $n = 3$ case. We would like to study this structure in full detail in the future.

5.5.4 Operators generating the RG flows

The above interpolation solutions can be obtained by adding terms to the AdS vacua solutions at UV and solving the equation of motion. Those extra terms trigger the RG flows.

• **The operators triggering the RG flow from AdS$^{(1)}$ to AdS$^{(p)}$.**

From UV point of view, the RG flow is triggered by the μ term in (5.42). In the bases of the UV theory, the μ term reads $\mu(\frac{8\sqrt{2}}{3}e^{e^\rho/2+\rho}(\hat{M}_{1/2}+\hat{N}_{1/2}) - \frac{4}{3}e^\rho\, i\hat{J}_3)$, which is real and the "i" shows up because "$\hat{J}_3$" is defined to be imaginary. However, this is not the final result due to the explicit ρ dependence. The correct expression for the UV theory should be obtained by taking the $\rho \to \infty$ limit, where the leading terms are $\mu\, \frac{8\sqrt{2}}{3}e^{e^\rho/2}(\hat{M}_{1/2}+\hat{N}_{1/2})$, with spin-3/2 generators $\hat{M}_{1/2}+\hat{N}_{1/2}$. So the RG flow is triggered by adding this term to the AdS vacuum solution, which corresponds to adding "bosonic" spin-3/2 currents to the Lagrangian. This is very similar to the observation in the bosonic case [86].

But the situation is a little more involved in the current supersymmetric case. First of all, in the bosonic case [86] the $\hat{L}_0$ generator in the UV theory is proportional to the L_0 generator in the IR theory. So the interpolation solution (2.27) in [86] has a simple $d\rho$ term. But in the supersymmetric case, the $\hat{L}_0$ generator in the UV theory is not proportional to the L_0, therefore from the solution (5.42), we have to include L_0 in $d\rho$ terms, which corresponds to $\frac{1}{2}i(\hat{J}_1 - \hat{J}_4) + 2\hat{L}_0$ in the UV bases. Thus in order to construct the interpolation solution, we have to turn on some spin-1 fields corresponding to $\hat{J}_1 - \hat{J}_4$ as well. Secondly, in the μ dependent term, there is another

spin-1 field $\hat{J}_3$ turned on. Although it is suppressed in the UV limit $\rho \to \infty$, it is still required to solve the equation of motion.

In summary, in addition to the spin-3/2 fields, the spin-1 currents corresponding to $\hat{J}_1$, $\hat{J}_3$, $\hat{J}_4$ are also needed to solve the equation of motion.

• **The operators triggering the RG flow from AdS$^{(2)}$ to AdS$^{(p)}$.**

As discussed in section (5.5.2.2), there is no solution that separate the chemical potential, i.e. μ, term from the AdS vacuum term. So the fields triggering the flow do not stand separately as in the previous case. Inspired from the analysis of the previous RG flow, we can capture the triggering fields by investigating the sub-leading fields in the UV limit $\rho \to \infty$. From the form of the solution (5.46), we can see that in the $d\rho$ term we need to turn on field L_0, which reads $\hat{\hat{L}}_0 + \hat{\hat{J}}_3 + \sqrt{3}\hat{\hat{J}}_8$ in the second UV bases. Although it is suppressed at $\rho \to \infty$, this term will become more and more important as we flow to the IR theory and will be dominant there. Besides, in the UV limit $\rho \to \infty$ the dx^+ term also possesses a subleading term $\frac{4}{3}\, e^{\mu\rho} L_1 - e^{\mu\rho} K_1$, which reads $-2(\hat{\hat{J}}_1 - i\,\hat{\hat{J}}_2 - \hat{\hat{J}}_6 + i\,\hat{\hat{J}}_7)e^{\mu\rho}$ in the second UV bases. Again due to the explicit ρ dependence, this subleading term in the UV becomes more and more relevant when flowing to the IR theory.

In summary, to trigger the flow, we need to add subleading terms proportional to $\hat{\hat{J}}_3 + \sqrt{3}\hat{\hat{J}}_8$, $\hat{\hat{J}}_1 - i\,\hat{\hat{J}}_2 - \hat{\hat{J}}_6 + i\,\hat{\hat{J}}_7$ in the UV AdS vacuum. This corresponds to turning on some certain combinations of the spin-1 currents in the Lagrangian. From the UV point of view, the μ parameter sources the L_0 generator in the $d\rho$ term of the interpolation solution (5.46) as a chemical potential. However, it enters the dx^+ term of the solution in an unfamiliar exponential way. We hope to investigate the role of μ in detail in the future. Nevertheless, as we will see in the next section, the μ drops out when we try to relate fields in the UV theory AdS$^{(2)}$ and the fields in the IR theory AdS$^{(p)}$.

5.5.5 Relations between UV and IR operators

As discussed in the previous subsection, we can construct interpolation solutions between UV theories and the IR theory. In this subsection, we want to find what fields in the IR theory do UV fields flow to. In practice, we consider the perturbations around the interpolation solutions. By solving the linearized equation of motion,[12] we get the relations between UV and IR fields.

In the case we are considering, the L_0, $\hat{L}_0\,\hat{\hat{L}}_0$ generators in different embeddings are not proportional to each other. So the interpolation solutions have complicated $d\rho$ terms. A consequence of this complication is that the ρ dependence of various fields are not separable in general: we cannot factor out the ρ dependence for each field as in the bosonic case [86]. However, as we will see below, this non-trivial ρ dependence allows us to keep track of how do different fields mix along the flow, which is not observed in the bosonic case.

5.5.5.1 Relations between operators in $\mathrm{AdS}^{(1)}$ and $\mathrm{AdS}^{(\mathrm{p})}$

We start by perturbing the RG flow, i.e. the interpolation solution (5.42), by adding all possible fields in the highest weight gauge

$$\Gamma = \mu\bigg((\frac{16}{9}e^{e^\rho/2+\rho} - \frac{4}{9}e^\rho)L_1 - \frac{4}{3}(e^{e^\rho/2+\rho} - e^\rho)K_1\bigg)dx^+ + e^{e^\rho+2\rho}\hat{L}_1 dx^- \tag{5.61}$$

$$+(L_0 + e^\rho\hat{L}_0)d\rho + (\mathcal{L}'_{IR}L_{-1} + \mathcal{A}'_{IR}K_{-1} + \mathcal{W}'_{IR}W_{-2} + \mathcal{J}'_{IR}J)dx^+ \tag{5.62}$$

$$+(\mathcal{L}'_{UV}\hat{L}_{-1} + \mathcal{P}'_{UV}\hat{M}_{-1} + \mathcal{Q}'_{UV}\hat{N}_{-1} + \sum_{i=1}^{5}\mathcal{J}'_{UV}\hat{J}^i_{-1})dx^- \tag{5.63}$$

where all the fields $\mathcal{O}'_{IR}\,(\mathcal{O}'_{UV})$ depend on $(x^+,\, x^-,\, \rho)$. The $\tilde{\Gamma}$ connection is similar so we only focus on the Γ connection.

Solving the $dx^+d\rho$ and $dx^-d\rho$ components of the equation of motion respectively,

[12] The equation of motion of the perturbed RG flow from $\mathrm{AdS}^{(2)}$ to $\mathrm{AdS}^{(\mathrm{p})}$ is linear due to the simple form of (5.46), therefore linearization is not necessary.

we work out the explicit ρ dependence of various fields

$$\begin{aligned}\Gamma^{(1p)} =& \mu\bigg((\frac{16}{9}e^{e^\rho/2+\rho} - \frac{4}{9}e^\rho)L_1 - \frac{4}{3}(e^{e^\rho/2+\rho} - e^\rho)K_1 \bigg) dx^+ + e^{e^\rho+2\rho}\hat{L}_1 dx^- \\ &+ (L_0 + e^\rho \hat{L}_0)d\rho + \bigg(\mathcal{J}_{IR} J + \frac{1}{9}\big(4e^{-\frac{e^\rho}{2}-\rho}(\mathcal{A}_{IR} + 3\mathcal{L}_{IR}) - e^{-\rho}(4\mathcal{A}_{IR} + 3\mathcal{L}_{IR})\big) L_{-1} \\ &+ \frac{1}{3}\big(e^{-\rho}(4\mathcal{A}_{IR} + 3\mathcal{L}_{IR}) - 4e^{-\frac{e^\rho}{2}-\rho}(\mathcal{A}_{IR} + 3\mathcal{L}_{IR})\big) K_{-1} + \mathcal{W}_{IR} e^{-e^\rho-2\rho} W_{-2} \bigg) dx^+ \\ &+ \bigg(e^{-e^\rho-2\rho}\hat{\mathcal{L}}_{UV}\hat{L}_{-1} + e^{-\frac{e^\rho}{2}-\rho}\mathcal{M}_{UV}\hat{M}_{-1} + e^{-\frac{e^\rho}{2}-\rho}\mathcal{N}_{UV}\hat{N}_{-1} \\ &+ \sum_{i=1,4,5} \hat{\mathcal{J}}^i_{UV}\hat{J}^i_{-1} + e^{-\rho}\sum_{i=2,3}\hat{\mathcal{J}}^i_{UV}\hat{J}^i_{-1} \bigg) dx^- \,. \end{aligned} \tag{5.64}$$

Now all the fields $\mathcal{O}_{IR}\,(\mathcal{O}_{UV})$ depend on $(x^+,\, x^-)$ but not on ρ. Furthermore, in the UV limit $\rho \to \infty$, the dx^- term in (5.64) reduces to the bosonic part of the asymptotic $\mathrm{AdS}^{(1)}$ vacuum (5.28) up to normalization factor $\frac{2\pi}{k_{CS}}$. In the IR limit $\rho \to -\infty$, the dx^+ term in (5.64) reduces to the bosonic part of the asymptotic $\mathrm{AdS}^{(\mathrm{p})}$ vacuum up to normalization factor $\frac{2\pi}{k_{CS}}$.

Now consider the linearized dx^+dx^- component of the equation of motion, which gives the following relations between the IR operators and the UV operators

$$\hat{\mathcal{L}}_{UV} = -3\,\frac{\partial_+^2(\mathcal{A}_{IR} + 3\,\mathcal{L}_{IR})}{512\mu^3}\,, \tag{5.65a}$$

$$\mathcal{M}_{UV} = \sqrt{2}\,\frac{\partial_+(\mathcal{A}_{IR} + 3\,\mathcal{L}_{IR}) + 24\mu\,\mathcal{W}_{IR}}{64\mu^2}\,, \tag{5.65b}$$

$$\mathcal{N}_{UV} = \sqrt{2}\,\frac{\partial_+(\mathcal{A}_{IR} + 3\,\mathcal{L}_{IR}) - 24\mu\,\mathcal{W}_{IR}}{64\mu^2}\,, \tag{5.65c}$$

$$\hat{\mathcal{J}}^1_{UV} + \hat{\mathcal{J}}^4_{UV} + 3\,\hat{\mathcal{J}}^5_{UV} = \frac{-i}{\mu}(\mathcal{A}_{IR} + 3\,\mathcal{L}_{IR})\,, \tag{5.65d}$$

$$\partial_+(\hat{\mathcal{J}}^1_{UV} + \hat{\mathcal{J}}^4_{UV}) = 6i\,\partial_-\mathcal{J}_{IR}\,, \tag{5.65e}$$

$$\partial_+\hat{\mathcal{J}}^2_{UV} = i\,\big(\frac{3}{2\mu}e^{-e^\rho/2}\partial_+\mathcal{W}_{IR} + (1 - 4e^{-e^\rho/2})\partial_-\mathcal{L}_{IR} + \frac{4}{3}(1 - e^{-e^\rho/2})\partial_-\mathcal{A}_{IR}\big)\,, \tag{5.65f}$$

as well as the relations

$$\begin{aligned}
\partial_+\hat{\mathcal{L}}_{UV} &= \frac{2\sqrt{2}\mu}{3}\,\partial_-(\mathcal{M}_{UV}-\mathcal{N}_{UV})\,, && (5.66a)\\
\partial_+(\mathcal{M}_{UV}-\mathcal{N}_{UV}) &= \frac{2\sqrt{2}\mu}{3i}\,\partial_-(\hat{\mathcal{J}}^1_{UV}+\hat{\mathcal{J}}^4_{UV}+3\,\hat{\mathcal{J}}^5_{UV})\,, && (5.66b)\\
\partial_+\hat{\mathcal{J}}^3_{UV} &= \frac{4\mu}{3}(\hat{\mathcal{J}}^1_{UV}-\hat{\mathcal{J}}^4_{UV})\,, && (5.66c)\\
\partial_+(\hat{\mathcal{J}}^1_{UV}-\hat{\mathcal{J}}^4_{UV}) &= -\frac{8\mu}{3}\hat{\mathcal{J}}^2_{UV}\,. && (5.66d)
\end{aligned}$$

The various factors "i" in the above expressions are not essential, they come from our complexification of the generators, we can absorb all the "i" in the definition and the results will no longer involve any "i". In addition, we see a mixing between $\mathcal{A}_{IR}$ and $\mathcal{L}_{IR}$ in both (5.64) and (5.65). This is a result of the $\mathcal{N}=2$ supersymmetry that produces another set of spin-1 generators K_i besides the L_i. The fact that the commutation relations $[L_I,\cdot]$ and $[K_I,\cdot]$, where $\cdot$ stands for other generators in the algebra, are almost identical directly leads to the mixing observed above.

From (5.65d), we see that the IR field $\mathcal{L}_{IR}$ is locally related to spacetime spin-1 fields in the UV, which agrees with the observation in the bosonic case [86]. From (5.65b) and (5.65c), we see the IR spin-3 field is related to a certain combination of the spin-3/2 fields in the UV by $\mathcal{W}_{IR}=\frac{2\sqrt{2}\mu}{3}\,(\mathcal{M}_{UV}-\mathcal{N}_{UV})$, which is a reasonable extension of the observation in the bosonic case [86].

Equation (5.65) also tells us how do the dimensions of various UV operators change along the flow. The operators $\hat{\mathcal{L}}_{UV}$, $\mathcal{M}_{UV}$, $\mathcal{N}_{UV}$, $\mathcal{J}^i_{UV}$ have conformal dimension $4,3,3,2$ in the IR respectively. The conformal dimensions of these fields are all doubled, we do not know if this is accidental or not.

Equation (5.66) represents the chiral conservation of the UV currents $\mathcal{L}_{UV}$, $(\mathcal{M}_{UV}-\mathcal{N}_{UV})$, $\hat{\mathcal{J}}^3_{UV}$, $(\hat{\mathcal{J}}^1_{UV}-\hat{\mathcal{J}}^4_{UV})$. This is because μ is turned off when we perturb around the UV vacua (i.e. in the UV limit),[13] which makes the right hand side of equation

[13] We are allowed to do this because (5.66) are relations among UV fields, and they make sense if

(5.66) vanish identically. From the conservation laws, our choice of the generators does not seem to be a best one when studying the behaviors of different operators. A certain recombination, namely $\check{\mathcal{J}}_{UV} = \hat{\mathcal{J}}^1_{UV} - \hat{\mathcal{J}}^4_{UV}$, $\check{\mathcal{M}}_{UV} = (\mathcal{M}_{UV} - \mathcal{N}_{UV})$ might be more fundamental since their conservations are explicit in this analysis.

In addition to the agreement with the bosonic case, the unconventional ρ dependence is not observed in the bosonic case. This is because the relation $\hat{L}_0 = L_0/2$ there leads to very simple ρ dependences. Although our result seems a little complicated, it reveals the explicit ρ dependences of various fields and hence tells explicitly how fields evolve along the flow. A good example is (5.65f), where ρ is an explicit parameter characterizing the running of the UV (spacetime) spin-1 current $\hat{\mathcal{J}}^2_{UV}$. The relations between the UV and the IR operators shown in (5.65) as well as those in the bosonic case [86] can be regarded as expansions of the UV operators in the set of bases of the IR operators. The special feature of (5.65f) is that the expansion coefficients change along the flow, representing the renormalization of the current. Concretely, in the UV limit $\rho \to \infty$, we have

$$\partial_+ \hat{\mathcal{J}}^2_{UV} = i\,\partial_-(\mathcal{L}_{IR} + \frac{4}{3}\mathcal{A}_{IR})\,. \tag{5.67}$$

But this is not really the relation between UV operator $\partial_+\hat{\mathcal{J}}^2_{UV}$ and the IR operators since the relation is established at the UV scale and the $\mathcal{L}_{IR}, \mathcal{A}_{IR}$ are merely some basis vectors but not the real IR operators. We have to run down to the IR scale $\rho \to -\infty$[14], then the relation becomes

$$\partial_+ \hat{\mathcal{J}}^2_{UV} = -3i\partial_-\mathcal{L}_{IR}\,, \tag{5.68}$$

we stay at the vicinity of the UV theory. It does not make sense to set $\mu = 0$ in (5.65) since they are relations among UV and IR fields.

[14]In addition, we take $\mu \to \infty$ in the IR. This can be seen from the form of the IR limit (5.45) that μ has to be large in order for the $dx^{\pm}$ term to be non-vanishing.

which can be interpreted as the true relation between the UV and IR operators. Note that we do not see similar runnings in either the bosonic case [86] or the other relations in (5.65) because of the canonical ρ dependence. This ρ dependent way to match the UV and IR operators will be used again in the next section.

5.5.5.2 Relations between operators in AdS$^{(2)}$ and AdS$^{(p)}$

We still want to perturb the RG flow, i.e. the interpolation solution (5.46), by adding all possible fields in the "highest weight" gauge. However, unlike the previous case, the UV part and the IR part do not sit in different components (dx^+ and dx^-) in (5.46). So the simple perturbation method we used in the previous section does not work here.

To deal with this, we only add perturbation terms in the UV vacuum to the interpolation solution (5.46). Solving the equation of motion gives a general ρ dependent perturbed interpolation function between the UV and IR. We then run this interpolation function down to the IR, and compare this running result with the perturbed asymptotic AdS$^{(p)}$ gauge connection in the "highest weight" gauge. This matching gives relations between the fields in the UV and IR. We will demonstrate how this works now.

We perturb around (5.46) as

$$\begin{aligned}\Gamma^{(2p)} &= \left(\frac{1}{3}(4e^{\mu\rho}-e^{e^\rho+\mu\rho})L_1-(e^{\mu\rho}-e^{e^\rho+\mu\rho})K_1\right)dx^+ + (\mu L_0+e^\rho\hat{\hat{L}}_0)d\rho \\ &\quad +(\tilde{\mathcal{L}}'_{UV}\hat{\hat{L}}_{-1}+\sum_{i=1}^{9}\tilde{\mathcal{J}}'^i_{UV}\,\hat{\hat{J}}_i)dx^+\,, \end{aligned} \tag{5.69}$$

where all the fields $\mathcal{O}'_{IR}\,(\mathcal{O}'_{UV})$ depend on $(x^+,\,x^-,\,\rho)$. Solving the equation of motion

gives the following perturbed interpolation solution

$$\begin{aligned}
\Gamma^{(2p)} &= \Big(\frac{1}{3}(4e^{\mu\rho}-e^{e^\rho+\mu\rho})L_1-(e^{\mu\rho}-e^{e^\rho+\mu\rho})K_1\Big)dx^+ + (\mu L_0+e^\rho\hat{\tilde{L}}_0)d\rho \\
&+((C_1e^{-\mu\rho}+\frac{i}{2}C_2e^{\mu\rho}-(e^{-e^\rho-\mu\rho}\tilde{\mathcal{L}}_{UV}+\tilde{\mathcal{J}}^6_{UV}e^{-\mu\rho}))\hat{\tilde{J}}_1 \\
&+i(C_1e^{-\mu\rho}-\frac{i}{2}C_2e^{\mu\rho}-(e^{-e^\rho-\mu\rho}\tilde{\mathcal{L}}_{UV}+\tilde{\mathcal{J}}^6_{UV}e^{-\mu\rho}))\hat{\tilde{J}}_2 \\
&+(C_3-\sqrt{3}C_8)\hat{\tilde{J}}_3+(\tilde{\mathcal{J}}^4_{UV}\cosh(2\mu\rho)+iC_5\sinh(2\mu\rho))\hat{\tilde{J}}_4+\tilde{\mathcal{L}}_{UV}e^{-e^\rho+\mu\rho}\hat{\tilde{L}}_{-1} \\
&+(C_5\cosh(2\mu\rho)-i\tilde{\mathcal{J}}^4_{UV}\sinh(2\mu\rho))\hat{\tilde{J}}_5+(e^{-e^\rho-\mu\rho}\tilde{\mathcal{L}}_{UV}+\tilde{\mathcal{J}}^6_{UV}e^{-\mu\rho}+\frac{i}{2}C_7\,e^{\mu\rho})\hat{\tilde{J}}_6 \\
&+i(e^{-e^\rho-\mu\rho}\tilde{\mathcal{L}}_{UV}+\tilde{\mathcal{J}}^6_{UV}e^{-\mu\rho}-\frac{i}{2}C_7\,e^{\mu\rho})\hat{\tilde{J}}_7+C_8\,\hat{\tilde{J}}_8+\tilde{\mathcal{J}}^9_{UV}\,\hat{\tilde{J}}_9)\,dx^+\,, \qquad (5.70)
\end{aligned}$$

where the $C_1, C_2, C_3, C_5, C_7, C_8$ are integration constant to be determined later. Now we run to the IR theory along the perturbed flow, which is achieved by taking the $\rho \to -\infty$ limit.[15] To compare with the perturbed AdS vacuum in the IR, we further rewrite this expression in the set of bases in the IR theory, which gives

$$\begin{aligned}
\Gamma^{(2p)} &= e^{\mu\rho}L_1dx^+ + \mu L_0 d\rho \\
&+\Big((e^{-\mu\rho}\tilde{\mathcal{L}}_{UV}+\tilde{\mathcal{J}}^6_{UV}e^{-\mu\rho}-\frac{1}{2}C_1\,e^{-\mu\rho})K_{-1}-\frac{C_3}{4}K_0-\frac{i}{8}e^{\rho\mu}(C_7-C_2)K_1 \\
&+(-\frac{1}{3}e^{-\mu\rho}\tilde{\mathcal{L}}_{UV}-\frac{4}{3}\tilde{\mathcal{J}}^6_{UV}e^{-\mu\rho}+\frac{2}{3}C_1\,e^{-\mu\rho})L_{-1}+\frac{C_3}{3}L_0+\frac{i}{6}e^{\rho\mu}(C_7-C_2)L_1 \\
&-\frac{1}{2}e^{-2\rho\mu}(\tilde{\mathcal{J}}^4_{UV}-iC_5)W_{-2}+e^{-\mu\rho}C_1W_{-1}-(\sqrt{3}C_8-\frac{3}{4}C_3)W_0 \\
&-\frac{i}{4}e^{\mu\rho}(C_2+C_7)W_1-\frac{1}{8}e^{2\rho\mu}(\tilde{\mathcal{J}}^4_{UV}+iC_5)W_2+\frac{i}{2\sqrt{3}}\tilde{\mathcal{J}}^9_{UV}\,J\Big)\,dx^+\,. \qquad (5.71)
\end{aligned}$$

This result should be matched with the bosonic part of the perturbed asymptotic AdS connection, which we rewrite here

$$\Gamma = \big(L_1e^\rho+\mathcal{L}_{IR}e^{-\rho}L_{-1}+\mathcal{J}_{IR}J+\mathcal{A}_{IR}e^{-\rho}K_{-1}+\mathcal{W}_{IR}e^{-2\rho}W_{-2}\big)dx^+ + L_0d\rho\,. \quad (5.72)$$

[15] This effectively sets $e^\rho = 0$. But we keep all the $e^{\mu\rho}$ untouched since the unspecific constant μ can be either positive or negative.

By comparing (5.71) and (5.72), we see that the non-highest-weight components, which are the coefficients of the $K_1,\ K_0,\ L_0,\ W_{2,1,0,-1}$ generator, vanish. This fixes all the integration constants in (5.71) as

$$C_1 = C_2 = C_3 = C_7 = C_8 = 0,\ C_5 = i\tilde{\mathcal{J}}^4_{UV}\,. \tag{5.73}$$

Under this parametrization, the perturbed interpolation solution (5.70) reduces to

$$\begin{aligned}\Gamma^{(2p)} &= \left(\frac{1}{3}(4e^{\mu\rho} - e^{e^\rho+\mu\rho})L_1 - (e^{\mu\rho} - e^{e^\rho+\mu\rho})K_1\right)dx^+ + (\mu L_0 + e^\rho\hat{\tilde{L}}_0)d\rho \\ &+\Big((-e^{-e^\rho-\mu\rho}\tilde{\mathcal{L}}_{UV} - \tilde{\mathcal{J}}^6_{UV}e^{-\mu\rho})\hat{\tilde{J}}_1 + i(-e^{-e^\rho-\mu\rho}\tilde{\mathcal{L}}_{UV} - \tilde{\mathcal{J}}^6_{UV}e^{-\mu\rho})\hat{\tilde{J}}_2 \\ &+\tilde{\mathcal{J}}^4_{UV}e^{-2\mu\rho}\hat{\tilde{J}}_4 + \tilde{\mathcal{L}}_{UV}e^{-e^\rho+\mu\rho}\hat{\tilde{L}}_{-1} + (e^{-e^\rho-\mu\rho}\tilde{\mathcal{L}}_{UV} + \tilde{\mathcal{J}}^6_{UV}e^{-\mu\rho})\hat{\tilde{J}}_6 \\ &+i(e^{-e^\rho-\mu\rho}\tilde{\mathcal{L}}_{UV} + \tilde{\mathcal{J}}^6_{UV}e^{-\mu\rho})\hat{\tilde{J}}_7 + i\,\tilde{\mathcal{J}}^4_{UV}e^{-2\mu\rho}\hat{\tilde{J}}_5 + \tilde{\mathcal{J}}^9_{UV}\,\hat{\tilde{J}}_9\Big)\,dx^+\,. \end{aligned} \tag{5.74}$$

The UV limit of this perturbed interpolation is achieved at $\rho \to \infty$, $\mu = 0$

$$\begin{aligned}\Gamma^{(2p)}_{UV} &= \hat{\tilde{L}}_1 e^{e^\rho}dx^+ + e^\rho\hat{\tilde{L}}_0 d\rho + \big(-\tilde{\mathcal{J}}^6_{UV}\hat{\tilde{J}}_1 - i\,\tilde{\mathcal{J}}^6_{UV}\hat{\tilde{J}}_2 + \tilde{\mathcal{J}}^4_{UV}\hat{\tilde{J}}_4 + i\,\tilde{\mathcal{J}}^4_{UV}\hat{\tilde{J}}_5 \\ &+\tilde{\mathcal{J}}^6_{UV}\hat{\tilde{J}}_6 + i\tilde{\mathcal{J}}^6_{UV}\hat{\tilde{J}}_7 + \tilde{\mathcal{J}}^9_{UV}\,\hat{\tilde{J}}_9\big)dx^+\,. \end{aligned} \tag{5.75}$$

And the IR limit of this perturbed interpolation (5.74), which is ran down from the UV connection, reduces to

$$\begin{aligned}\Gamma^{(2p)}_{IR} &= e^{\mu\rho}L_1 dx^+ + \mu L_0 d\rho + \left(e^{-\mu\rho}(\tilde{\mathcal{L}}_{UV} + \tilde{\mathcal{J}}^6_{UV})K_{-1} - \frac{1}{3}e^{-\mu\rho}(\tilde{\mathcal{L}}_{UV} + 4\tilde{\mathcal{J}}^6_{UV})L_{-1}\right. \\ &\left.-e^{-2\rho\mu}\tilde{\mathcal{J}}^4_{UV}W_{-2} + \frac{i}{2\sqrt{3}}\tilde{\mathcal{J}}^9_{UV}\,J\right)dx^+\,. \end{aligned} \tag{5.76}$$

A further field redefinition $\rho \to \tilde{\rho} = \mu\rho$ put it to the conventional form

$$\begin{aligned}\Gamma_{IR}^{(2p)} &= e^{\tilde{\rho}} L_1 dx^+ + L_0 d\tilde{\rho} + \Big(e^{-\tilde{\rho}} (\tilde{\mathcal{L}}_{UV} + \tilde{\mathcal{J}}^6_{UV}) K_{-1} - \frac{1}{3} e^{-\tilde{\rho}} (\tilde{\mathcal{L}}_{UV} + 4\tilde{\mathcal{J}}^6_{UV}) L_{-1} \\ &\quad - e^{-2\tilde{\rho}} \tilde{\mathcal{J}}^4_{UV} W_{-2} + \frac{i}{2\sqrt{3}} \tilde{\mathcal{J}}^9_{UV}\, J \Big) dx^+ \,. \end{aligned} \tag{5.77}$$

Comparing to (5.72), with the trivial identification $\tilde{\rho} = \rho$, we get the relations

$$\mathcal{L}_{IR} = -\frac{1}{3}\tilde{\mathcal{L}}_{UV} - \frac{4}{3}\tilde{\mathcal{J}}^6_{UV} \tag{5.78a}$$

$$\mathcal{A}_{IR} = \tilde{\mathcal{L}}_{UV} + \tilde{\mathcal{J}}^6_{UV} \tag{5.78b}$$

$$\mathcal{W}_{IR} = -\tilde{\mathcal{J}}^4_{UV} \tag{5.78c}$$

$$\mathcal{J}_{IR} = \frac{i}{2\sqrt{3}} \tilde{\mathcal{J}}^9_{UV} \,. \tag{5.78d}$$

Thus we have established relations between the UV operators and the IR operators and the relations do not depend on the parameter μ. The spacetime spin-3 IR current $\mathcal{W}_{IR}$ is locally related to the spacetime spin-1 UV current, and the spacetime spin-2 IR currents $\mathcal{L}_{IR}$, $\mathcal{A}_{IR}$ are related to certain combination of the spacetime spin-2, 1 currents $\tilde{\mathcal{L}}_{UV}$, $\tilde{\mathcal{J}}^6_{UV}$. The R-current $\mathcal{J}_{IR}$ in the IR theory is related to $\tilde{\mathcal{J}}^9_{UV}$. From the CFT point of view, the conformal dimensions of the UV operators $\tilde{\mathcal{L}}_{UV}, \tilde{\mathcal{J}}^4_{UV}, \tilde{\mathcal{J}}^6_{UV}, \tilde{\mathcal{J}}^9_{UV}$ becomes 2, 3, 2, 1 in the IR. The most significant difference between the current case and the previous case (also the bosonic case [86]) is that the spin-2 $\tilde{\mathcal{L}}_{UV}$ field does not acquire anomalous dimension. Instead, the dimension of the spin-1 current $\tilde{\mathcal{J}}^4_{UV}$ jumps by 2. We wish to give a detailed analysis of this interesting phenomena in the future.

5.5.5.3 Dual operators in the two UV theories

As shown in the previous section, we relate the operators in the IR theory with the operators in the UV theories separately. Then the natural question to ask is are

there operators in each of the two UV theories that flow to the same IR operator? If so, we thus find operators in the two different theories dual to each other in the sense that they flow to the same IR operator. This question is easy to answer given the matching result (5.65) and (5.78), we find four pairs of operators that flow to the same IR operators. The result is summarized in Table 5.2. Note that we do not

$\text{AdS}^{(1)}$ operators (UV)		$\text{AdS}^{(2)}$ operators (UV)	$\text{AdS}^{(\text{p})}$ operators (IR)
$\hat{J}^1_{UV} + \hat{J}^4_{UV} + 3\hat{J}^5_{UV},\ \{\ \hat{\mathcal{L}}_{UV}\ \}$	$\sim$	$\tilde{\mathcal{J}}^6_{UV}$	$\mathcal{A}_{IR} + 3\mathcal{L}_{IR}$
$\mathcal{M}_{UV} - \mathcal{N}_{UV}$	$\sim$	$\tilde{\mathcal{J}}^4_{UV}$	$\mathcal{W}_{IR}$
$\{\ \hat{\mathcal{J}}^2_{UV}\ \}$	$\sim$	$\tilde{\mathcal{J}}^6_{UV},\ \tilde{\mathcal{L}}_{UV}$	$\mathcal{L}_{IR}$
$\{\ \hat{\mathcal{J}}^1_{UV} + \hat{\mathcal{J}}^4_{UV}\ \}$	$\sim$	$\tilde{\mathcal{J}}^9_{UV}$	$\mathcal{J}_{IR}$

Table 5.2: This table lists the pairs of UV operators in the two different UV theories. When the UV operators are related to the IR operators through identities with derivatives involved, we put the UV operators in the curly bracket $\{\ \cdots\ \}$.

direct set the UV operators equal to each other, since they are not directly related to each other. Rather, they are related by the same IR operators they flow into. In addition, some UV operators are related to the IR operators through identities with derivatives,[16] these type of UV operators are put in the curly bracket $\{\ \cdots\ \}$. Another observation that is interesting is that for some pairs of the dual operators, their conformal dimension are different. This is not surprising since when run down to the IR theory, many operators acquire anomalous dimensions, as shown in section 5.5.5.1 and 5.5.5.2. This dual relation can be further studied in the content of the dual CFT.

[16]This may be considered as relations between descendent fields.

5.5.6 A remark on the central charge

The general form of the central charge in the bosonic case is shown [67] to be

$$c = 12\, k_{CS}\, \mathrm{Tr}(L_0^2)\,. \tag{5.79}$$

From our computation, we see the general form of the central charge in the supersymmetric case is

$$c = 12\, k_{CS}\, \left|\mathrm{STr}(L_0^2)\right|\,, \tag{5.80}$$

where k_{CS} is the Chern-Simons level. From our explicit computation (or (5.80)), we see that the central charge of the IR theory, corresponding to the principal embedding, is larger than the central charges of the UV theories. This is similar to what happened in the bosonic case [86], and is not a violation of the c-theorem since the UV theories are non-unitary: in both the two non-principal embeddings $\mathrm{AdS}^{(1)}$ and $\mathrm{AdS}^{(2)}$, there are always some spin-1 generators whose commutators have negative central terms. This observation implies that both the two non-principal embeddings are dual to non-unitary CFTs, according to the analysis in [164]. Besides, the argument to circumvent this non-unitarity in [165] may be extended to the supersymmetric case as well.

5.6 Discussion

5.6.1 Relation with the Hamiltonian reductions of the WZW model

A relevant question is how to understand these different embeddings holographically. It has been shown, e.g. in [166], that the resulting theories obtained by classical Hamiltonian reduction of the WZW model based on some supergroup possesses super-W symmetry. In addition, it is shown in [149] that there are three different Hamiltonian reductions of the current algebra associated with the Lie superalgebra

$sl(3|2)$, each containing the usual Virasoro algebra as a subalgebra.[17]

One of the reductions in [149] gives the $\mathcal{N} = 2$ super-W_3 algebra. As discussed in section 5.4.1, the asymptotic symmetry of our principal embedding is precisely the super-W_3 algebra. The second reduction in [149] gives rise to a $u(2|1)$ nonlinear superconformal algebra, which is the same algebra found in [154] . As discussed in section 5.4.2, this algebra matches with the asymptotic symmetry algebra of the non-principal embedding I. The third reduction in [149] gives rise to a $u(3)$ nonlinear superconformal algebra, which is the same algebra found in [155]. As discussed in section 5.4.3, this algebra matches with the asymptotic symmetry algebra of the non-principal embedding II. Thus we see an exact match between

1. the asymptotic symmetry algebras of the higher-spin theories corresponding to the three different embeddings of $osp(1|2)$ into the $sl(3|2)$ superalgebra and

2. the resulting algebra from the three different Hamiltonian reductions of the Lie superalgebra $sl(3|2)$.

The work [149] was done purely algebraically and does not depend on the field theory realization. So it is reasonable to believe that the structure of the three different reductions in [149] should also be present in the Hamiltonian reductions of the WZW model based on the supergroup $sl(3|2)$.

The close relation between the classical Hamiltonian reduction of some Lie (super)algebra and the asymptotic symmetry algebra of the higher-spin theory based on the same Lie (super)algebra has been known in the literature, see e.g. [67, 68, 65, 70]. However, our result contains more information in the sense that we give a physical interpretation to the different Hamiltonian reductions. The above matching relates a certain Hamiltonian reduction to the IR theory and two other Hamiltonian reductions to the UV theories. Since each Hamiltonian reduction is achieved by imposing

[17] There are actually 5 different reductions, but two of them has either constrained stress supercurrent or a spin-0 current, both of which seem unusual and are not considered here [149].

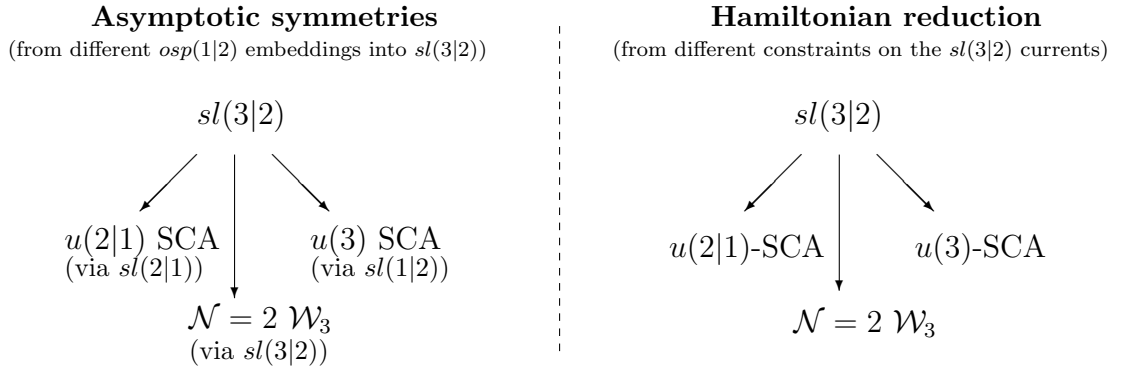

Figure 5.1: This figure shows the similarity between structures of the three different $osp(1|2)$ embeddings into the $sl(3|2)$ (left) and the three different Hamiltonian reductions of the $sl(3|2)$ superalgebra (right). The "SCA" in both figures stands for "superconformal algebra".

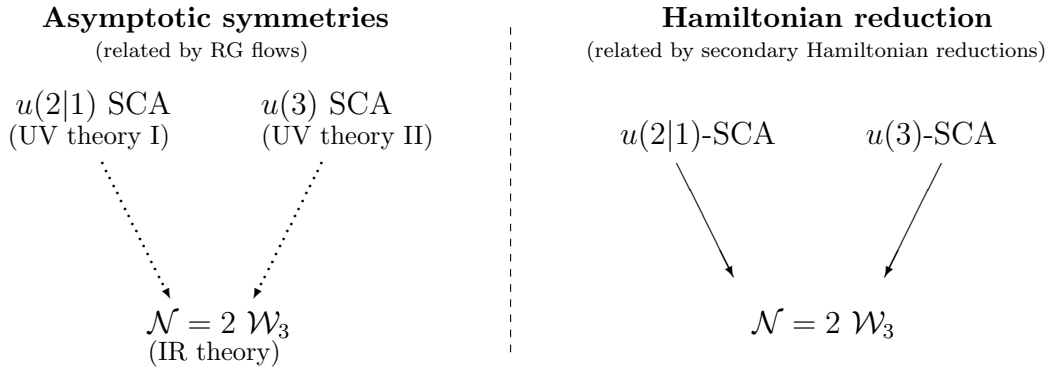

Figure 5.2: The figure on the left shows the physical interpretation of the relations between the three embeddings. The dotted arrows represent RG flows. The figure on the right shows that the $\mathcal{N} = 2$ $\mathcal{W}_3$ algebra can be obtained from secondary Hamiltonian reductions of the $u(3)$-SCA and $u(2|1)$-SCA. The three objects in each diagram are the same as those shown up in Figure 5.1.

a set of constraints on the $sl(3|2)$ current algebra, we further relate different sets of constraints to the WZW model with different higher-spin theories in the UV and in the IR, respectively. It turns out that the constraints corresponding to each U-V theory form a subset of the constraints corresponding to the IR theories. This correspondence can be shown in the Figure 5.1 and Figure 5.2.

We can further establish a close relation between turning on some currents to trigger the RG flow in the higher-spin theory with putting more constraints to induce

a further (secondary) Hamiltonian reduction. It is interesting to understand this correspondence in the future. Concretely, it is interesting to see how do the extra constraints imposed by the secondary Hamiltonian reduction [149] translate into the operators triggering the RG flow? If this translation is understood, can we apply it to the initial constraints put on the $sl(3|2)$?

Another motivation of this comparison between our results and the Hamiltonian reductions is the attempt to find Lagrangian descriptions of the CFT dual to the spin-3 supergravity with different embeddings. For the principal embedding, the dual CFT is proposed to be the $\mathbb{C}\mathrm{P}^n$ minimal models [61, 63, 64] from the Kazama-Suzuki coset construction [128]. For the non-principal embeddings, we identify the symmetry algebras as two different non-linear extended superconformal algebras. But we do not have concrete realizations of these algebras at hand. As known for the bosonic case,[18] even with a special choice of the parameter in a Toda field theory, which can be obtained from the Hamiltonian reduction of a WZW model, such that the Virasoro central charge of the Toda theory agrees with the central charge of a certain W_n-minimal model, the Toda theory is not the Lagrangian description of the W_n-minimal model [150, 151, 146]. The obstruction is the mismatch of the spectrum: the minimal model contains more states than the Toda theory and certain projections are required for the matching. To overcome this difficulty, Mansfield and Spence suggested to consider the conformally extended Toda field theories instead of the original ones [150, 151]. We anticipate that the situation could be similar in our supersymmetric picture and a similar extension may be needed as well. It is interesting to work this out in the future and this may develop our understanding of the higher-spin holography.

[18] We thank Thomas Hartman for pointing this out to the author.

5.6.2 $osp(1|2)$ embedding and $sl(1|2)$ embedding

The $osp(1|2)$ superalgebra can be regarded as the $\mathcal{N}=1$ supersymmetric extension of the bosonic $sl(2)$ algebra, while $sl(2|1)$ is the $\mathcal{N}=2$ supersymmetric extension. Our discussion is in the context of $\mathcal{N}=2$ supersymmetric higher-spin theory. Then a question arises: why do we consider the $osp(1|2)$ embedding instead of the $sl(1|2)$ embedding?

It is shown in [153, 167] that any $sl(1|2)$ embedding provides an $osp(1|2)$ embedding. Furthermore, for the Lie superalgebra $sl(n|n-1)$, the $osp(1|2)$ embedding classifies the $sl(1|2)$ embedding. Therefore considering the $osp(1|2)$ embedding in our case is the same as considering $sl(1|2)$ embedding. We use the $osp(1|2)$ embedding since it is the simplest supersymmetric extension of the $sl(2)$ algebra and we do not need to further group the $\mathcal{N}=1$ multiplets into $\mathcal{N}=2$ multiplets.

5.6.3 Generalizations to arbitrary superalgebra $sl(n+1|n)$

In this chapter, we have given a detailed analysis of the 3 different embeddings of $osp(1|2)$ into $sl(3|2)$. One of them can be interpreted as an IR theory and the other two as UV theories. We find the two UV theories flow to the same IR theory. We can generalize this analysis to higher rank algebras, say $sl(4|3)$, and study the relations between the different embeddings. It is very possible that the principal embedding will again give a theory at IR,[19] then the question left is that do all the different non-principal embeddings flow to this same theory? Are there "cascade" scenarios, namely, are there embeddings corresponding to intermediate scales so that we can construct successive RG flows from some embedding A to some other embedding B then to the IR theory? In the present $sl(3|2)$ case, the structure is that the two non-principal embeddings give two UV theories flowing to the IR respectively. Our analysis

[19] This is because the principal embedding leads to minimal number of primary fields after imposing the boundary conditions and gauge fixing conditions.

in section 5.5.2.3 rules out the possibility of one UV theory being at an intermediate scale and of constructing two successive RG flows. However, the latter case is possible for higher-rank algebras. It is interesting to see what are the structures for general (bosonic or supersymmetric) higher-spin theories. No matter what is the answer, there could be some interesting relations/dualities appear and this construction may provide a playground for further studies.

BIBLIOGRAPHY

BIBLIOGRAPHY

[1] S. Weinberg, "The Quantum theory of fields. Vol. 1: Foundations,". Cambridge, UK: Univ. Pr. (1995) 609 p.

[2] C.-N. Yang and R. L. Mills, "Conservation of Isotopic Spin and Isotopic Gauge Invariance," *Phys.Rev.* **96** (1954) 191–195.

[3] **ATLAS Collaboration** Collaboration, G. Aad *et al.*, "Observation of a new particle in the search for the Standard Model Higgs boson with the ATLAS detector at the LHC," *Phys.Lett.* **B716** (2012) 1–29, arXiv:1207.7214 [hep-ex].

[4] **CMS Collaboration** Collaboration, S. Chatrchyan *et al.*, "Observation of a new boson at a mass of 125 GeV with the CMS experiment at the LHC," *Phys.Lett.* **B716** (2012) 30–61, arXiv:1207.7235 [hep-ex].

[5] S. R. Coleman and J. Mandula, "ALL POSSIBLE SYMMETRIES OF THE S MATRIX," *Phys.Rev.* **159** (1967) 1251–1256.

[6] R. Haag, J. T. Lopuszanski, and M. Sohnius, "All Possible Generators of Supersymmetries of the s Matrix," *Nucl.Phys.* **B88** (1975) 257.

[7] V. Nair, "A CURRENT ALGEBRA FOR SOME GAUGE THEORY AMPLITUDES," *Phys.Lett.* **B214** (1988) 215.

[8] E. Witten, "Perturbative gauge theory as a string theory in twistor space," *Commun.Math.Phys.* **252** (2004) 189–258, arXiv:hep-th/0312171 [hep-th].

[9] M. Bianchi, H. Elvang, and D. Z. Freedman, "Generating Tree Amplitudes in N=4 SYM and N = 8 SG," *JHEP* **0809** (2008) 063, arXiv:0805.0757 [hep-th].

[10] H. Elvang, D. Z. Freedman, and M. Kiermaier, "Recursion Relations, Generating Functions, and Unitarity Sums in N=4 SYM Theory," *JHEP* **0904** (2009) 009, arXiv:0808.1720 [hep-th].

[11] H. Elvang, D. Z. Freedman, and M. Kiermaier, "Proof of the MHV vertex expansion for all tree amplitudes in N=4 SYM theory," *JHEP* **0906** (2009) 068, arXiv:0811.3624 [hep-th].

[12] J. Drummond and J. Henn, "All tree-level amplitudes in N=4 SYM," *JHEP* **0904** (2009) 018, arXiv:0808.2475 [hep-th].

[13] N. Arkani-Hamed, F. Cachazo, and J. Kaplan, "What is the Simplest Quantum Field Theory?," *JHEP* **1009** (2010) 016, arXiv:0808.1446 [hep-th].

[14] N. Arkani-Hamed, F. Cachazo, C. Cheung, and J. Kaplan, "The S-Matrix in Twistor Space," *JHEP* **1003** (2010) 110, arXiv:0903.2110 [hep-th].

[15] N. Arkani-Hamed, F. Cachazo, C. Cheung, and J. Kaplan, "A Duality For The S Matrix," *JHEP* **1003** (2010) 020, arXiv:0907.5418 [hep-th].

[16] N. Arkani-Hamed, J. L. Bourjaily, F. Cachazo, S. Caron-Huot, and J. Trnka, "The All-Loop Integrand For Scattering Amplitudes in Planar N=4 SYM," *JHEP* **1101** (2011) 041, arXiv:1008.2958 [hep-th].

[17] N. Arkani-Hamed, J. L. Bourjaily, F. Cachazo, A. Hodges, and J. Trnka, "A Note on Polytopes for Scattering Amplitudes," *JHEP* **1204** (2012) 081, arXiv:1012.6030 [hep-th].

[18] J. M. Drummond, J. M. Henn, and J. Plefka, "Yangian symmetry of scattering amplitudes in N=4 super Yang-Mills theory," *JHEP* **0905** (2009) 046, arXiv:0902.2987 [hep-th].

[19] L. Mason and D. Skinner, "Scattering Amplitudes and BCFW Recursion in Twistor Space," *JHEP* **1001** (2010) 064, arXiv:0903.2083 [hep-th].

[20] H. Elvang, Y.-t. Huang, and C. Peng, "On-shell superamplitudes in $\mathcal{N} < 4$ SYM," *JHEP* **1109** (2011) 031, arXiv:1102.4843 [hep-th].

[21] L.M. Brown and R.P. Feynman, Phys. Rev. 85 (1952) 231;
G. Passarino and M. Veltman, Nucl. Phys. B160 (1979) 151;
G. 't Hooft and M. Veltman, Nucl. Phys. B153 (1979) 365;
R. G. Stuart, Comp. Phys. Comm. 48:367 (1988);
R. G. Stuart and A. Gongora, Comp. Phys. Comm. 56:337 (1990).

[22] D. B. Melrose, Il Nuovo Cimento 40A:181 (1965);
W. van Neerven and J. A. M. Vermaseren, Phys. Lett. 137B:241 (1984);
G. J. van Oldenborgh and J. A. M. Vermaseren, Z. Phys. C46:425 (1990);
G. J. van Oldenborgh, PhD thesis, University of Amsterdam (1990);
A. Aeppli, PhD thesis, University of Zurich (1992).

[23] L. D. Z. Bern and D. A. Kosower, "Phys. Lett. B302:299 (1993); erratum B318:649 (1993); Nucl. Phys. B412:751 (1994),".

[24] Z. Bern, L. J. Dixon, D. C. Dunbar, and D. A. Kosower, "Fusing gauge theory tree amplitudes into loop amplitudes," *Nucl.Phys.* **B435** (1995) 59–101, arXiv:hep-ph/9409265 [hep-ph].

[25] D. Forde, "Direct extraction of one-loop integral coefficients," *Phys.Rev.* **D75** (2007) 125019, arXiv:0704.1835 [hep-ph].

[26] R. Britto, F. Cachazo, and B. Feng, "New recursion relations for tree amplitudes of gluons," *Nucl.Phys.* **B715** (2005) 499–522, arXiv:hep-th/0412308 [hep-th].

[27] R. Britto, F. Cachazo, B. Feng, and E. Witten, "Direct proof of tree-level recursion relation in Yang-Mills theory," *Phys.Rev.Lett.* **94** (2005) 181602, arXiv:hep-th/0501052 [hep-th].

[28] Y.-t. Huang, D. A. McGady, and C. Peng, "One-loop renormalization and the S-matrix," arXiv:1205.5606 [hep-th].

[29] C. Fronsdal, "Massless Fields with Integer Spin," *Phys.Rev.* **D18** (1978) 3624.

[30] M. A. Vasiliev, "Higher spin gauge theories: Star product and AdS space," arXiv:hep-th/9910096 [hep-th].

[31] I. Klebanov and A. Polyakov, "AdS dual of the critical O(N) vector model," *Phys.Lett.* **B550** (2002) 213–219, arXiv:hep-th/0210114 [hep-th].

[32] E. Sezgin and P. Sundell, "Holography in 4D (super) higher spin theories and a test via cubic scalar couplings," *JHEP* **0507** (2005) 044, arXiv:hep-th/0305040 [hep-th].

[33] J. M. Maldacena, "The Large N limit of superconformal field theories and supergravity," *Adv.Theor.Math.Phys.* **2** (1998) 231–252, arXiv:hep-th/9711200 [hep-th].

[34] E. Witten, "Quantum Field Theory and the Jones Polynomial," *Commun.Math.Phys.* **121** (1989) 351.

[35] E. Fradkin and M. A. Vasiliev, "On the Gravitational Interaction of Massless Higher Spin Fields," *Phys.Lett.* **B189** (1987) 89–95.

[36] M. A. Vasiliev, "HIGHER SPIN ALGEBRAS AND QUANTIZATION ON THE SPHERE AND HYPERBOLOID," *Int.J.Mod.Phys.* **A6** (1991) 1115–1135.

[37] M. A. Vasiliev, "Higher spin gauge theories in four-dimensions, three-dimensions, and two-dimensions," *Int.J.Mod.Phys.* **D5** (1996) 763–797, arXiv:hep-th/9611024 [hep-th].

[38] D. J. Gross, "High-Energy Symmetries of String Theory," *Phys.Rev.Lett.* **60** (1988) 1229.

[39] B. Sundborg, "Stringy gravity, interacting tensionless strings and massless higher spins," *Nucl.Phys.Proc.Suppl.* **102** (2001) 113–119, arXiv:hep-th/0103247 [hep-th].

[40] E. Sezgin and P. Sundell, "Massless higher spins and holography," *Nucl.Phys.* **B644** (2002) 303–370, arXiv:hep-th/0205131 [hep-th].

[41] S. Giombi, S. Minwalla, S. Prakash, S. P. Trivedi, S. R. Wadia, *et al.*, "Chern-Simons Theory with Vector Fermion Matter," *Eur.Phys.J.* **C72** (2012) 2112, arXiv:1110.4386 [hep-th].

[42] C.-M. Chang, S. Minwalla, T. Sharma, and X. Yin, "ABJ Triality: from Higher Spin Fields to Strings," arXiv:1207.4485 [hep-th].

[43] O. Aharony, G. Gur-Ari, and R. Yacoby, "d=3 Bosonic Vector Models Coupled to Chern-Simons Gauge Theories," *JHEP* **1203** (2012) 037, arXiv:1110.4382 [hep-th].

[44] J. Maldacena and A. Zhiboedov, "Constraining Conformal Field Theories with A Higher Spin Symmetry," arXiv:1112.1016 [hep-th].

[45] J. Maldacena and A. Zhiboedov, "Constraining conformal field theories with a slightly broken higher spin symmetry," *Class.Quant.Grav.* **30** (2013) 104003, arXiv:1204.3882 [hep-th].

[46] O. Aharony, G. Gur-Ari, and R. Yacoby, "Correlation Functions of Large N Chern-Simons-Matter Theories and Bosonization in Three Dimensions," *JHEP* **1212** (2012) 028, arXiv:1207.4593 [hep-th].

[47] O. Aharony, S. Giombi, G. Gur-Ari, J. Maldacena, and R. Yacoby, "The Thermal Free Energy in Large N Chern-Simons-Matter Theories," *JHEP* **1303** (2013) 121, arXiv:1211.4843 [hep-th].

[48] S. R. Das and A. Jevicki, "Large N collective fields and holography," *Phys.Rev.* **D68** (2003) 044011, arXiv:hep-th/0304093 [hep-th].

[49] A. Jevicki, K. Jin, and Q. Ye, "Collective Dipole Model of AdS/CFT and Higher Spin Gravity," *J.Phys.* **A44** (2011) 465402, arXiv:1106.3983 [hep-th].

[50] M. R. Douglas, L. Mazzucato, and S. S. Razamat, "Holographic dual of free field theory," *Phys.Rev.* **D83** (2011) 071701, arXiv:1011.4926 [hep-th].

[51] L. A. Pando Zayas and C. Peng, "Toward a Higher-Spin Dual of Interacting Field Theories," arXiv:1303.6641 [hep-th].

[52] M. A. Vasiliev, "Holography, Unfolding and Higher-Spin Theory," arXiv:1203.5554 [hep-th].

[53] D. Anninos, T. Hartman, and A. Strominger, "Higher Spin Realization of the dS/CFT Correspondence," arXiv:1108.5735 [hep-th].

[54] G. S. Ng and A. Strominger, "State/Operator Correspondence in Higher-Spin dS/CFT," *Class.Quant.Grav.* **30** (2013) 104002, arXiv:1204.1057 [hep-th].

[55] D. Das, S. R. Das, A. Jevicki, and Q. Ye, "Bi-local Construction of Sp(2N)/dS Higher Spin Correspondence," *JHEP* **1301** (2013) 107, arXiv:1205.5776 [hep-th].

[56] S. Giombi and X. Yin, "The Higher Spin/Vector Model Duality," arXiv:1208.4036 [hep-th].

[57] M. R. Gaberdiel and R. Gopakumar, "An AdS_3 Dual for Minimal Model CFTs," *Phys.Rev.* **D83** (2011) 066007, arXiv:1011.2986 [hep-th].

[58] M. R. Gaberdiel and R. Gopakumar, "Triality in Minimal Model Holography," *JHEP* **1207** (2012) 127, arXiv:1205.2472 [hep-th].

[59] E. Perlmutter, T. Prochazka, and J. Raeymaekers, "The semiclassical limit of W_N CFTs and Vasiliev theory," *JHEP* **1305** (2013) 007, arXiv:1210.8452 [hep-th].

[60] C. Candu, M. R. Gaberdiel, M. Kelm, and C. Vollenweider, "Even spin minimal model holography," *JHEP* **1301** (2013) 185, arXiv:1211.3113 [hep-th].

[61] T. Creutzig, Y. Hikida, and P. B. Ronne, "Higher spin AdS_3 supergravity and its dual CFT," *JHEP* **1202** (2012) 109, arXiv:1111.2139 [hep-th].

[62] T. Creutzig, Y. Hikida, and P. B. Ronne, "N=1 supersymmetric higher spin holography on AdS_3," *JHEP* **1302** (2013) 019, arXiv:1209.5404 [hep-th].

[63] C. Candu and M. R. Gaberdiel, "Supersymmetric holography on AdS_3," arXiv:1203.1939 [hep-th].

[64] C. Candu and M. R. Gaberdiel, "Duality in N=2 Minimal Model Holography," *JHEP* **1302** (2013) 070, arXiv:1207.6646 [hep-th].

[65] M. R. Gaberdiel, R. Gopakumar, T. Hartman, and S. Raju, "Partition Functions of Holographic Minimal Models," *JHEP* **1108** (2011) 077, arXiv:1106.1897 [hep-th].

[66] M. Henneaux and S.-J. Rey, "Nonlinear $W_{infinity}$ as Asymptotic Symmetry of Three-Dimensional Higher Spin Anti-de Sitter Gravity," *JHEP* **1012** (2010) 007, arXiv:1008.4579 [hep-th].

[67] A. Campoleoni, S. Fredenhagen, S. Pfenninger, and S. Theisen, "Asymptotic symmetries of three-dimensional gravity coupled to higher-spin fields," *JHEP* **1011** (2010) 007, arXiv:1008.4744 [hep-th].

[68] M. R. Gaberdiel and T. Hartman, "Symmetries of Holographic Minimal Models," *JHEP* **1105** (2011) 031, arXiv:1101.2910 [hep-th].

[69] M. Henneaux, G. Lucena Gomez, J. Park, and S.-J. Rey, "Super- W(infinity) Asymptotic Symmetry of Higher-Spin AdS_3 Supergravity," *JHEP* **1206** (2012) 037, arXiv:1203.5152 [hep-th].

[70] K. Hanaki and C. Peng, "Symmetries of Holographic Super-Minimal Models," arXiv:1203.5768 [hep-th].

[71] C. Ahn, "The Large N 't Hooft Limit of Kazama-Suzuki Model," *JHEP* **1208** (2012) 047, arXiv:1206.0054 [hep-th].

[72] C. Ahn, "The Operator Product Expansion of the Lowest Higher Spin Current at Finite N," *JHEP* **1301** (2013) 041, arXiv:1208.0058 [hep-th].

[73] T. Creutzig, Y. Hikida, and P. B. Ronne, "Three point functions in higher spin AdS_3 supergravity," *JHEP* **1301** (2013) 171, arXiv:1211.2237 [hep-th].

[74] H. Moradi and K. Zoubos, "Three-Point Functions in $N = 2$ Higher-Spin Holography," *JHEP* **1304** (2013) 018, arXiv:1211.2239 [hep-th].

[75] A. Castro, E. Hijano, A. Lepage-Jutier, and A. Maloney, "Black Holes and Singularity Resolution in Higher Spin Gravity," *JHEP* **1201** (2012) 031, arXiv:1110.4117 [hep-th].

[76] A. Castro, R. Gopakumar, M. Gutperle, and J. Raeymaekers, "Conical Defects in Higher Spin Theories," *JHEP* **1202** (2012) 096, arXiv:1111.3381 [hep-th].

[77] M. Gutperle and P. Kraus, "Higher Spin Black Holes," *JHEP* **1105** (2011) 022, arXiv:1103.4304 [hep-th].

[78] H.-S. Tan, "Aspects of Three-dimensional Spin-4 Gravity," *JHEP* **1202** (2012) 035, arXiv:1111.2834 [hep-th].

[79] M. R. Gaberdiel, T. Hartman, and K. Jin, "Higher Spin Black Holes from CFT," *JHEP* **1204** (2012) 103, arXiv:1203.0015 [hep-th].

[80] H. Tan, "Exploring Three-dimensional Higher-Spin Supergravity based on sl(N —N - 1) Chern-Simons theories," *JHEP* **1211** (2012) 063, arXiv:1208.2277 [hep-th].

[81] S. Datta and J. R. David, "Supersymmetry of classical solutions in Chern-Simons higher spin supergravity," *JHEP* **1301** (2013) 146, arXiv:1208.3921 [hep-th].

[82] B. Chen, J. Long, and Y.-n. Wang, "Black holes in Truncated Higher Spin AdS_3 Gravity," *JHEP* **1212** (2012) 052, arXiv:1209.6185 [hep-th].

[83] M. R. Gaberdiel and R. Gopakumar, "Large N=4 Holography," arXiv:1305.4181 [hep-th].

[84] M. R. Gaberdiel and R. Gopakumar, "Minimal Model Holography," arXiv:1207.6697 [hep-th].

[85] M. Ammon, M. Gutperle, P. Kraus, and E. Perlmutter, "Black holes in three dimensional higher spin gravity: A review," arXiv:1208.5182 [hep-th].

[86] M. Ammon, M. Gutperle, P. Kraus, and E. Perlmutter, "Spacetime Geometry in Higher Spin Gravity," *JHEP* **1110** (2011) 053, arXiv:1106.4788 [hep-th].

[87] J. R. David, M. Ferlaino, and S. P. Kumar, "Thermodynamics of higher spin black holes in 3D," *JHEP* **1211** (2012) 135, arXiv:1210.0284 [hep-th].

[88] C. Peng, "Dualities from higher-spin supergravity," *JHEP* **1303** (2013) 054, arXiv:1211.6748 [hep-th].

[89] A. Ferber, "Supertwistors and Conformal Supersymmetry," *Nucl.Phys.* **B132** (1978) 55.

[90] G. Georgiou and V. V. Khoze, "Tree amplitudes in gauge theory as scalar MHV diagrams," *JHEP* **0405** (2004) 070, arXiv:hep-th/0404072 [hep-th].

[91] A. Brandhuber, B. J. Spence, and G. Travaglini, "One-loop gauge theory amplitudes in N=4 super Yang-Mills from MHV vertices," *Nucl.Phys.* **B706** (2005) 150–180, arXiv:hep-th/0407214 [hep-th].

[92] J. Drummond, J. Henn, G. Korchemsky, and E. Sokatchev, "Dual superconformal symmetry of scattering amplitudes in N=4 super-Yang-Mills theory," *Nucl.Phys.* **B828** (2010) 317–374, arXiv:0807.1095 [hep-th].

[93] Z. Bern, J. Carrasco, H. Ita, H. Johansson, and R. Roiban, "On the Structure of Supersymmetric Sums in Multi-Loop Unitarity Cuts," *Phys.Rev.* **D80** (2009) 065029, arXiv:0903.5348 [hep-th].

[94] L. J. Dixon, J. M. Henn, J. Plefka, and T. Schuster, "All tree-level amplitudes in massless QCD," *JHEP* **1101** (2011) 035, arXiv:1010.3991 [hep-ph].

[95] J. L. Bourjaily, "Efficient Tree-Amplitudes in N=4: Automatic BCFW Recursion in Mathematica," arXiv:1011.2447 [hep-ph].

[96] S. Lal and S. Raju, "The Next-to-Simplest Quantum Field Theories," *Phys.Rev.* **D81** (2010) 105002, arXiv:0910.0930 [hep-th].

[97] M. T. Grisaru and H. Pendleton, "Some Properties of Scattering Amplitudes in Supersymmetric Theories," *Nucl.Phys.* **B124** (1977) 81.

[98] J. Broedel and L. J. Dixon, "R**4 counterterm and E(7)(7) symmetry in maximal supergravity," *JHEP* **1005** (2010) 003, arXiv:0911.5704 [hep-th].

[99] T. Cohen, H. Elvang, and M. Kiermaier, "On-shell constructibility of tree amplitudes in general field theories," *JHEP* **1104** (2011) 053, arXiv:1010.0257 [hep-th].

[100] A. Brandhuber, P. Heslop, and G. Travaglini, "A Note on dual superconformal symmetry of the N=4 super Yang-Mills S-matrix," *Phys.Rev.* **D78** (2008) 125005, arXiv:0807.4097 [hep-th].

[101] M. Kiermaier and S. G. Naculich, "A Super MHV vertex expansion for N=4 SYM theory," *JHEP* **0905** (2009) 072, arXiv:0903.0377 [hep-th].

[102] H. Elvang, D. Z. Freedman, and M. Kiermaier, "Solution to the Ward Identities for Superamplitudes," *JHEP* **1010** (2010) 103, arXiv:0911.3169 [hep-th].

[103] H. Elvang, D. Z. Freedman, and M. Kiermaier, "SUSY Ward identities, Superamplitudes, and Counterterms," *J.Phys.* **A44** (2011) 454009, arXiv:1012.3401 [hep-th].

[104] Z. Kunszt and D. E. Soper, "Calculation of jet cross-sections in hadron collisions at order alpha-s**3," *Phys.Rev.* **D46** (1992) 192–221.

[105] W. Giele and E. N. Glover, "Higher order corrections to jet cross-sections in e+ e- annihilation," *Phys.Rev.* **D46** (1992) 1980–2010.

[106] W. Giele, E. N. Glover, and D. A. Kosower, "Higher order corrections to jet cross-sections in hadron colliders," *Nucl.Phys.* **B403** (1993) 633–670, arXiv:hep-ph/9302225 [hep-ph].

[107] Z. Kunszt, A. Signer, and Z. Trocsanyi, "Singular terms of helicity amplitudes at one loop in QCD and the soft limit of the cross-sections of multiparton processes," *Nucl.Phys.* **B420** (1994) 550–564, arXiv:hep-ph/9401294 [hep-ph].

[108] L. Dixon, "Notes on the one-loop qcd β-function without ghosts, private communication,".

[109] F. Cachazo, P. Svrcek, and E. Witten, "MHV vertices and tree amplitudes in gauge theory," *JHEP* **0409** (2004) 006, arXiv:hep-th/0403047 [hep-th].

[110] B. Feng, J. Wang, Y. Wang, and Z. Zhang, "BCFW Recursion Relation with Nonzero Boundary Contribution," *JHEP* **1001** (2010) 019, arXiv:0911.0301 [hep-th].

[111] S. J. Parke and T. Taylor, "An Amplitude for n Gluon Scattering," *Phys.Rev.Lett.* **56** (1986) 2459.

[112] N. Arkani-Hamed and J. Kaplan, "On Tree Amplitudes in Gauge Theory and Gravity," *JHEP* **0804** (2008) 076, arXiv:0801.2385 [hep-th].

[113] L. J. Dixon, "Calculating scattering amplitudes efficiently," arXiv:hep-ph/9601359 [hep-ph].

[114] G. 't Hooft and M. Veltman, "One loop divergencies in the theory of gravitation," *Annales Poincare Phys.Theor.* **A20** (1974) 69–94.

[115] A. Maloney and E. Witten, "Quantum Gravity Partition Functions in Three Dimensions," *JHEP* **1002** (2010) 029, arXiv:0712.0155 [hep-th].

[116] M. A. Vasiliev, "Consistent equation for interacting gauge fields of all spins in (3+1)-dimensions," *Phys.Lett.* **B243** (1990) 378–382.

[117] M. Vasiliev, "Nonlinear equations for symmetric massless higher spin fields in (A)dS(d)," *Phys.Lett.* **B567** (2003) 139–151, arXiv:hep-th/0304049 [hep-th].

[118] A. Campoleoni, S. Fredenhagen, and S. Pfenninger, "Asymptotic W-symmetries in three-dimensional higher-spin gauge theories," *JHEP* **1109** (2011) 113, arXiv:1107.0290 [hep-th].

[119] K. Papadodimas and S. Raju, "Correlation Functions in Holographic Minimal Models," *Nucl.Phys.* **B856** (2012) 607–646, arXiv:1108.3077 [hep-th].

[120] M. Ammon, P. Kraus, and E. Perlmutter, "Scalar fields and three-point functions in D=3 higher spin gravity," *JHEP* **1207** (2012) 113, arXiv:1111.3926 [hep-th].

[121] A. Castro, A. Lepage-Jutier, and A. Maloney, "Higher Spin Theories in AdS_3 and a Gravitational Exclusion Principle," *JHEP* **1101** (2011) 142, arXiv:1012.0598 [hep-th].

[122] C.-M. Chang and X. Yin, "Higher Spin Gravity with Matter in AdS_3 and Its CFT Dual," *JHEP* **1210** (2012) 024, arXiv:1106.2580 [hep-th].

[123] C. Ahn, "The Large N 't Hooft Limit of Coset Minimal Models," *JHEP* **1110** (2011) 125, arXiv:1106.0351 [hep-th].

[124] M. R. Gaberdiel and C. Vollenweider, "Minimal Model Holography for SO(2N)," *JHEP* **1108** (2011) 104, arXiv:1106.2634 [hep-th].

[125] M. R. Gaberdiel, T. Hartman, and K. Jin, "Higher Spin Black Holes from CFT," *JHEP* **1204** (2012) 103, arXiv:1203.0015 [hep-th].

[126] E. Bergshoeff, M. A. Vasiliev, and B. de Wit, "The SuperW(infinity) (lambda) algebra," *Phys.Lett.* **B256** (1991) 199–205.

[127] E. Bergshoeff, B. de Wit, and M. A. Vasiliev, "The Structure of the superW(infinity) (lambda) algebra," *Nucl.Phys.* **B366** (1991) 315–346.

[128] Y. Kazama and H. Suzuki, "New N=2 Superconformal Field Theories and Superstring Compactification," *Nucl.Phys.* **B321** (1989) 232.

[129] A. Achucarro and P. Townsend, "A Chern-Simons Action for Three-Dimensional anti-De Sitter Supergravity Theories," *Phys.Lett.* **B180** (1986) 89.

[130] E. Witten, "(2+1)-Dimensional Gravity as an Exactly Soluble System," *Nucl.Phys.* **B311** (1988) 46.

[131] M. Blencowe, "A CONSISTENT INTERACTING MASSLESS HIGHER SPIN FIELD THEORY IN D = (2+1)," *Class.Quant.Grav.* **6** (1989) 443.

[132] E. Fradkin and M. A. Vasiliev, "SUPERALGEBRA OF HIGHER SPINS AND AUXILIARY FIELDS," *Int.J.Mod.Phys.* **A3** (1988) 2983.

[133] T. Regge and C. Teitelboim, "Role of Surface Integrals in the Hamiltonian Formulation of General Relativity," *Annals Phys.* **88** (1974) 286.

[134] R. Benguria, P. Cordero, and C. Teitelboim, "Aspects of the Hamiltonian Dynamics of Interacting Gravitational Gauge and Higgs Fields with Applications to Spherical Symmetry," *Nucl.Phys.* **B122** (1977) 61.

[135] M. Banados, "Three-dimensional quantum geometry and black holes," arXiv:hep-th/9901148 [hep-th].

[136] M. Henneaux, L. Maoz, and A. Schwimmer, "Asymptotic dynamics and asymptotic symmetries of three-dimensional extended AdS supergravity," *Annals Phys.* **282** (2000) 31–66, arXiv:hep-th/9910013 [hep-th].

[137] J. D. Brown and M. Henneaux, "Central Charges in the Canonical Realization of Asymptotic Symmetries: An Example from Three-Dimensional Gravity," *Commun.Math.Phys.* **104** (1986) 207–226.

[138] M. Banados, "Global charges in Chern-Simons field theory and the (2+1) black hole," *Phys.Rev.* **D52** (1996) 5816, arXiv:hep-th/9405171 [hep-th].

[139] M. Banados, K. Bautier, O. Coussaert, M. Henneaux, and M. Ortiz, "Anti-de Sitter / CFT correspondence in three-dimensional supergravity," *Phys.Rev.* **D58** (1998) 085020, arXiv:hep-th/9805165 [hep-th].

[140] P. Bowcock and G. Watts, "On the classification of quantum W algebras," *Nucl.Phys.* **B379** (1992) 63–95, arXiv:hep-th/9111062 [hep-th].

[141] V. Kac, "Lie Superalgebras," *Adv.Math.* **26** (1977) 8–96.

[142] V. Dobrev and V. Petkova, "GROUP THEORETICAL APPROACH TO EXTENDED CONFORMAL SUPERSYMMETRY: FUNCTION SPACE REALIZATIONS AND INVARIANT DIFFERENTIAL OPERATORS," *Fortsch.Phys.* **35** (1987) 537.

[143] K. Ito, "Quantum Hamiltonian reduction and N=2 coset models," *Phys.Lett.* **B259** (1991) 73–78.

[144] K. Ito, "N=2 superconformal CP(n) model," *Nucl.Phys.* **B370** (1992) 123–142.

[145] K. Ito, "Free field realization of N=2 superW(3) algebra," *Phys.Lett.* **B304** (1993) 271–277, arXiv:hep-th/9302039 [hep-th].

[146] P. Bouwknegt and K. Schoutens, "W symmetry in conformal field theory," *Phys.Rept.* **223** (1993) 183–276, arXiv:hep-th/9210010 [hep-th].

[147] E. Fradkin and V. Y. Linetsky, "Supersymmetric Racah basis, family of infinite dimensional superalgebras, SU(infinity + 1—infinity) and related 2-D models," *Mod.Phys.Lett.* **A6** (1991) 617–633.

[148] C. Candu and M. R. Gaberdiel, "Supersymmetric holography on AdS_3," arXiv:1203.1939 [hep-th].

[149] C.-h. Ahn, E. Ivanov, and A. S. Sorin, "N=2 affine superalgebras and Hamiltonian reduction in N=2 superspace," *Commun.Math.Phys.* **183** (1997) 205–252, arXiv:hep-th/9508005 [hep-th].

[150] P. Mansfield, "Conformally extended Toda theories," *Phys.Lett.* **B242** (1990) 387–397.

[151] P. Mansfield and B. J. Spence, "Toda theories, the geometry of W algebras and minimal models," *Nucl.Phys.* **B362** (1991) 294–328.

[152] L. Frappat, P. Sorba, and A. Sciarrino, "Dictionary on Lie superalgebras," arXiv:hep-th/9607161 [hep-th].

[153] L. Frappat, E. Ragoucy, and P. Sorba, "W algebras and superalgebras from constrained WZW models: A Group theoretical classification," *Commun.Math.Phys.* **157** (1993) 499–548, arXiv:hep-th/9207102 [hep-th].

[154] F. Defever, W. Troost, and Z. Hasiewicz, "Superconformal algebras with quadratic nonlinearity," *Phys.Lett.* **B273** (1991) 51–55.

[155] M. Bershadsky, "SUPERCONFORMAL ALGEBRAS IN TWO-DIMENSIONS WITH ARBITRARY N," *Phys.Lett.* **B174** (1986) 285–288.

[156] P. Mathieu, "REPRESENTATION OF THE SO(N) AND U(N) SUPERCONFORMAL ALGEBRAS VIA MIURA TRANSFORMATIONS," *Phys.Lett.* **B218** (1989) 185.

[157] V. Knizhnik, "SUPERCONFORMAL ALGEBRAS IN TWO-DIMENSIONS," *Theor.Math.Phys.* **66** (1986) 68–72.

[158] H. Lu, C. Pope, L. Romans, X. Shen, and X. Wang, "Polyakov construction of the N=2 superW(3) algebra," *Phys.Lett.* **B264** (1991) 91–100.

[159] E. Ivanov and S. Krivonos, "Superfield realizations of N=2 superW(3)," *Phys.Lett.* **B291** (1992) 63–70, arXiv:hep-th/9204023 [hep-th].

[160] C.-h. Ahn, "Free superfield realization of N=2 quantum superW(3) algebra," *Mod.Phys.Lett.* **A9** (1994) 271–278, arXiv:hep-th/9304038 [hep-th].

[161] J.-F. Fortin, B. Grinstein, and A. Stergiou, "Limit Cycles in Four Dimensions," *JHEP* **1212** (2012) 112, arXiv:1206.2921 [hep-th].

[162] J.-F. Fortin, B. Grinstein, and A. Stergiou, "Limit Cycles and Conformal Invariance," *JHEP* **1301** (2013) 184, arXiv:1208.3674 [hep-th].

[163] M. A. Luty, J. Polchinski, and R. Rattazzi, "The a-theorem and the Asymptotics of 4D Quantum Field Theory," *JHEP* **1301** (2013) 152, arXiv:1204.5221 [hep-th].

[164] A. Castro, E. Hijano, and A. Lepage-Jutier, "Unitarity Bounds in AdS_3 Higher Spin Gravity," *JHEP* **1206** (2012) 001, arXiv:1202.4467 [hep-th].

[165] H. Afshar, M. Gary, D. Grumiller, R. Rashkov, and M. Riegler, "Semi-classical unitarity in 3-dimensional higher-spin gravity for non-principal embeddings," *Class.Quant.Grav.* **30** (2013) 104004, arXiv:1211.4454 [hep-th].

[166] F. Delduc, E. Ragoucy, and P. Sorba, "SuperToda theories and W algebras from superspace Wess-Zumino-Witten models," *Commun.Math.Phys.* **146** (1992) 403–426.

[167] E. Ragoucy, A. Sevrin, and P. Sorba, "Strings from N=2 gauged Wess-Zumino-Witten models," *Commun.Math.Phys.* **181** (1996) 91–130, arXiv:hep-th/9511049 [hep-th].